Asia-Pacific asa
science. services. solutions.

Mangles Bay Marina

Marine Modelling Study

Revision 0 – 15/09/2011

Prepared for:
Cedar Woods Properties Limited

Document control form:

Revision	*Originated*	*Edit & review*	*Authorised*	*Date*
Rev A - Issued for internal review	*M Burling* *H Strikwerda* *N Page*	*M Burling*	*N/A*	*14/09/11*
Rev B – Internal review		*S Langtry*	*N/A*	*15/09/11*
Rev 0 – Issued as 1st client draft		*M. Burling* *S. Langtry*	*M. Burling* *S. Langtry*	*16/09/11*

Document name: J0105 Cedar Woods Marine Modelling Study - Rev 0

APASA Project Number: J0105

APASA Project Manager: Murray Burling

Contact Details:

Asia-Pacific Applied Science Associates

Physical Address: Suite 6, 1050 Hay Street
Perth WA 6005

Postal Address: PO Box 7650
Cloisters Square WA 6850

Telephone: 9226 2911

Facsimile: 9226 2411

Contents

Figures

Tables

EXECUTIVE SUMMARY

Asia-Pacific ASA Pty Ltd (APASA) was commissioned by Cedar Woods Properties Limited (Cedar Woods) to undertake a marine modelling study in order to inform the environmental impact assessment process related to a proposed marina development in Mangles Bay, located at the southern end of Cockburn Sound. The development would involve dredging a short approach channel, main basin and three internal canals extending off a central marina in the easterly, southerly and south-westerly direction.

The study has considered the likely hydrodynamic and flushing performance of the development, the likely dispersion of nutrients that influx from the ground water, as well as the potential effect of the proposed dredging on local suspended sediment concentrations. The modelling scope has included the preparation and validation of a three-dimensional, baroclinic (density, tide and wind-forced), hydrodynamic model of the area, a regional-scale wave model and a three-dimensional sediment fate model. Validation data for the hydrodynamic model was collected during the study, which included measurement of wind and currents, at fixed locations, and of water trajectories over space around the proposed marina site.

The following main forecasts have been made relating to the flushing, nutrient and sediment modelling components of the project:

FLUSHING PERFORMANCE

- Flushing will rely primarily on tidal exchange and wind-induced circulation. Due to the relatively small tidal range and the design of the proposed marina, having smaller canals branching off a main canal that will have one entrance channel, only incomplete flushing will occur over any tidal cycle. Increased flushing would be expected when strong winds are aligned with the proposed canal system;
- Flushing will be fastest near the entrance to the main channel and decrease with distance from the entrance. Minimum flushing times near the entrance in any simulation was 1.9 days. Maximum flushing times calculated for the back end of the longest secondary canal (the western canal) was 12.7 days;
- A wide range of flushing times can be expected for any given location, depending upon the prevailing tide and wind conditions. The range of maximum flushing rates, calculated at the back of the canals in the simulations, varied from 4 days to 13 days;
- Average maximum flushing times calculated at the back end of the canals were statistically similar for simulations using example wind conditions for summer (8.36 $\pm$ 2.21 days), autumn (9.91 $\pm$ 2.14) and winter (8.30 $\pm$ 2.30);
- The median flushing time for all locations throughout the canals, for all seasons, is estimated at 6.8 days and 83% of the flushing time predictions were 10 days or less, while 55% of predictions were less than 7 days;
- Only small differences in flushing times should occur between the surface and the bottom waters at a given location, with the surface waters flushing slowest.

NUTRIENT MODELLING

- Dissolved Inorganic Nitrogen (DIN) concentrations within the development are expected to be highest during winter when the loading is highest, with concentrations generally being up to 4 times the background concentrations expected outside of the canals development;
- During autumn and summer, the DIN concentration is expected to be generally less than twice the background concentration, based on the values applied in this study;
- Flushing is expected to be sufficiently effective to prevent the gradual build-up of nutrient concentrations over time within the canal development, based on the assumptions made and the input data provided for this study. This suggests that the risk of adverse escalation of nutrient concentrations is relatively low.

SEDIMENT FATE MODELLING

- The region where a visible plume is expected to occur will generally be restricted to within the vicinity of the dredging channel.
- A significant TSSC plume is not expected to persist for long periods of time (<5% of the time) over the majority of the dredging area. Some persistence of the plume is predicted at the southern end of the access channel where the dredging is most intense. However, the persistent TSSC are predicted to be less than 10 mg/l.

1 INTRODUCTION

1.1 Project Description

Cedar Woods, on behalf of Landcorp, are developing a proposal for a marina precinct to be constructed in Mangles Bay, at the southern end of Cockburn Sound. The development would consist of a 550 m long approach-channel that would be dredged, leading to main marina canal that would be excavated from the existing land (Table 1-1; Figure 1-1). Three major canals would be excavated to extend off the central marina basin and orientated towards the east, south and south-west of the marina canal. The marina approach would be flanked by two breakwaters extending up to 290 m from the existing shore The entrance channel and main basin depths are proposed at 4.0 m below AHD (approximately MSL), with the canals being no deeper. The dimensions of the major project components are summarised in Table 1-1.

APASA was commissioned by Cedar Woods to undertake a marine modelling study in order to inform the environmental impact assessment process. The work was completed with detailed inputs provided by Oceanica Consulting Pty Ltd (Oceanica), Strategen and ERM.

The study has considered the likely hydrodynamic and flushing performance of the development, as well as the potential effect of the proposed dredging on local suspended sediment concentrations. The modelling scope has included the preparation and validation of a three-dimensional, baroclinic, hydrodynamic model of the area, a regional scale wave model and a three-dimensional sediment fate model. Validation data for the hydrodynamic model was collected during the study and included measured wind and, currents, at nearby locations, and water trajectories at nearby locations.

This report provides a description of the background, methods and outcomes of the study, with components of the work subsequently included in the PER submission.

Figure 1-1 Project layout drawing showing proposed entrance channel (blue), breakwaters (red) and marina layout (yellow). Drawing provided by Cedar Woods.

Table 1-1: Summary of major project components (provided by Strategen)

Project detail	Characteristics
Main activities	Construction activities to include clearing, dewatering and excavation of the marina and dredging of the access channel. Operational activities include marina operation and maintenance dredging.
Proposal area (Refer to Figure 2).	Proposal area up to 77 ha Total land development area up to 47.1 ha Total vegetation clearing up to 38 ha Total marine disturbance (below current high water mark): 6 ha
Marina	Total water area of marina up to 12 ha Deepest depth in marina up to -4.0 mAHD Excavation for marina up to 1 000 000 m^3
Dewatering requirements	Dewatering required for up to 18 months during construction Dewater returned to the local groundwater system via infiltration ponds within Proposal area. Total dewatering requirements will be further defined as hydrogeological information from pump testing becomes available.
Channel construction	Total channel length up to 550 m Total channel width up to 30 m Total channel area up to 3.4 ha (includes the footprint of 1:5 batters) Total channel depth up to -4.0 mAHD Total channel dredging of up to 50 000 m^3 Dredged material will be piped to the Proposal area, where it will be settled and then the water infiltrated and solid material treated and disposed of offsite.
Reclamation	Total reclamation area up to 1 ha Total breakwater length up to 290 m Total breakwater width up to 40 m includes breakwater batters of 1:5 Total breakwater area up to 1.1 ha
Area west of Garden Island causeway	Improvement works potentially including an upgrade to the car park, boat ramp and jetty platforms
Seagrass loss	Total seagrass removal up to 5 ha (includes breakwaters, reclamation areas, channel and batters) Total indirect loss of seagrass (due to halo effects around infrastructure of approximately 15 m) up to 1 ha. Total marine footprint up to 6 ha
Water Corporation asset	Relocation of Water Corporation pipeline
Outfall	Relocation of Mangles Bay ocean outfall pipe to Hymus Street.

1.2 Study Datums and Conventions

All locations referenced in geographical coordinates (latitude and longitude) are to the WGS 84 datum unless otherwise specified. All locations referenced in UTM coordinates are to Map Grid of Australia (MGA) Zone 50, to GDA 94.

All current directions are reported as “Direction Towards”, in accordance with standard conventions.

All wind and wave directions are reported as “Direction From”, in accordance with standard conventions.

2 METOCEAN CHARACTERISTICS OF THE SITE

2.1 General

An understanding of the broad-scale circulation processes in southern Cockburn Sound and Mangles Bay is essential to determining the anticipated level of impact of the marina on adjacent waters. The hydrodynamic processes of Cockburn Sound have been the subject of many studies and comprehensive reviews of the studies are contained in Hearn (1991), D'Adamo (1992) and DEP (1996). This section presents a brief review of the relevant literature related to circulation and mixing within southern Cockburn Sound.

The circulation and exchange processes within Cockburn Sound are very complex. These processes are driven at time-scales ranging from diurnal to annual by astronomical tides, winds (including storm events), buoyant coastal currents and estuarine discharges, differential heating and cooling and to a lesser extent by submarine groundwater discharge (DEP, 1996). The interplay between these processes governs the rates of circulation and exchange within the local area.

As a result of the protected nature of the Sound, the three main processes that control the hydrodynamics include:

1. Wind
2. Horizontal pressure gradients due to differences in water level (from wind, tides, waves, atmospheric pressure and continental shelf waves)
3. Horizontal pressure gradients due to differences in density

At different times and locations, each of these mechanisms may dominate the local circulation. The circulation in Mangles Bay is also strongly influenced by the presence of the Garden Island Causeway, which has openings at the southern and northern ends allowing exchange between Mangles Bay and the ocean.

2.2 Wind Climate

The wind climate of Garden Island is controlled at a regional level by annual movements of the anti-cyclonic belt. At a local level, the diurnal land/ sea breeze cycle results in strong sea breezes during summer, and weaker breezes throughout the year.

Winds have been measured at Garden Island since November 2001 by the Bureau of Meteorology (BOM). The mean annual wind speed for this data set is 6.5 m/s, which is similar to the mean annual wind speed of 7 m/s quoted in the Perth Coastal Waters study. There is a strong seasonality to the wind record, as indicated in Figure 2-1. Summer winds are more persistent, with a higher wind speed of 7.2 m/s. In winter and spring, calms are more likely, although the incidence of storm winds keeps the mean wind speed approximately the same as the annual mean. In autumn, calmer winds dominate the wind record, with few storm events, and the mean wind speed is the lowest of the seasonal averages (5.4 m/s).

The dominant wind direction is from the south-southwest sector, particularly during summer. During winter and autumn there is greater variability in the wind direction. In winter there are more frequent northerly wind events and the prevailing winds shift towards the west.

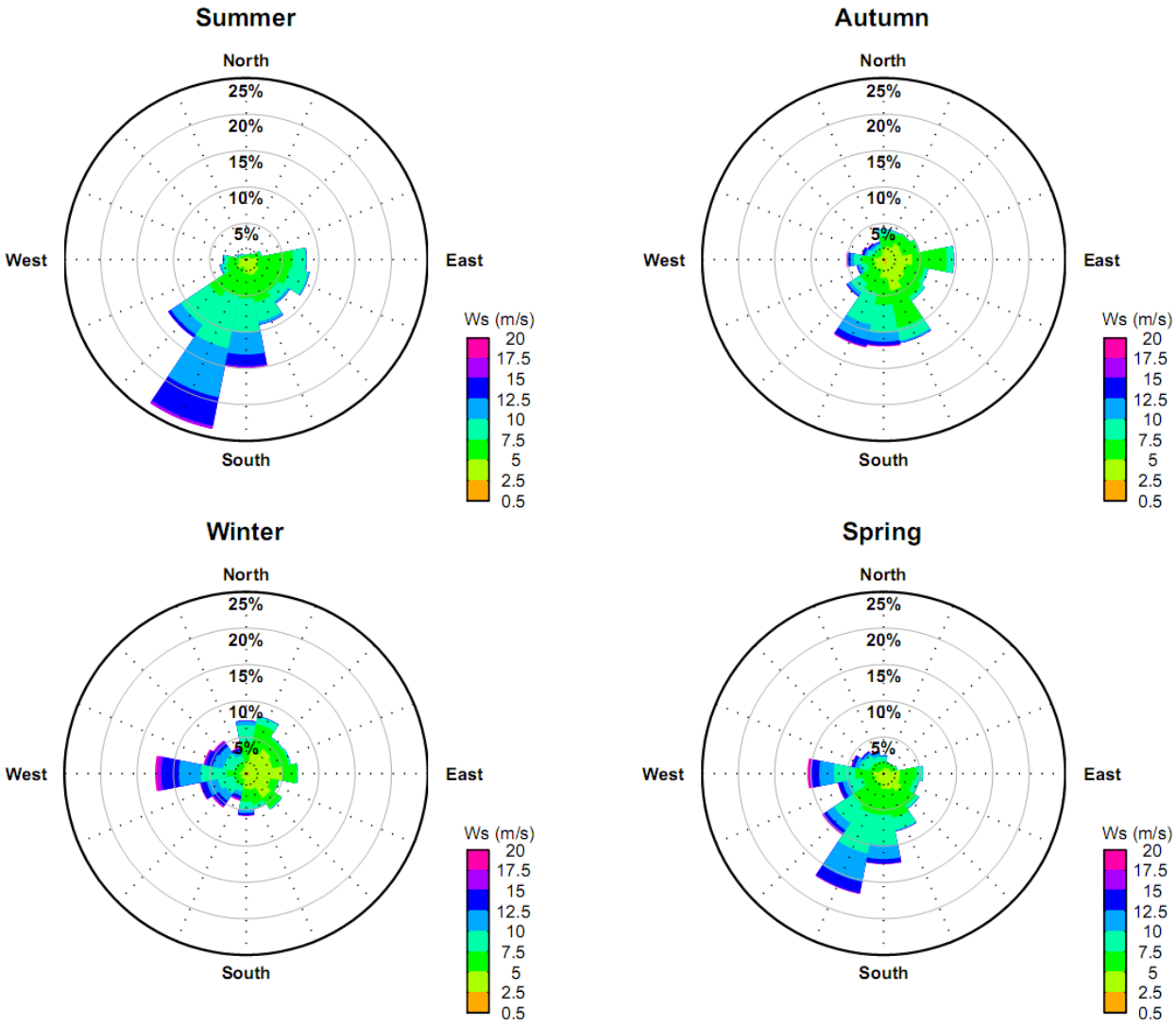

Figure 2-1 Seasonal wind roses (direction from) for Garden Island from November 2001 to September 2008.

2.3 Water Level Variations

The magnitude of tidal variations in the region is small, due to the presence of an amphidromic point off the southwest coast of Western Australia. The tidal range is typically around 0.5 m, and ranges between 0.1 m and 0.9 m. The tides are predominantly diurnal, with the major diurnal constituents (K1 and O1) having 2 – 3 times the amplitude of the semi-diurnal M2 and S2 constituents. These weak tides drive very small currents, with the exception at times of peak ebb and flood flow through the gaps in the Garden Island Causeway.

Sea level is also influenced by the passage of pressure systems and associated storm surges (typically 0.3 m up to 0.9 m) and other long period forcing, such as coastally trapped waves (DEP, 1996). Seiches also contribute to significant water level variation within Mangles Bay and Cockburn Sound, with a dominant period of around 3 hours observed (Molloy, 2001; Ilich, 2006). Seiches appear to be commonly generated due the abrupt change in wind direction, and possibly wind speed (Molloy, 2001).

Given the relatively low tidal range, the above factors have the capacity to dominate over tidal influences.

2.4 Density Gradients

The circulation of greater Cockburn Sound is strongly influenced by baroclinic (density-induced) effects. The Leeuwin current and the coastal estuaries are sources of buoyancy that peak in winter and have a significant influence over the water properties in the coastal region. Within the shallow region of Mangles Bay, particularly to the south and east, baroclinic processes are expected to be less important for circulation due to the likely dominance of exchange through the Causeway due to wind transport and height differences between the sound and the offshore waters (Pattiaratchi, 2002).

However, as baroclinic exchange is typically an important flushing mechanism within semi-enclosed marinas, the effect of density gradients on exchange must be included in this study.

2.5 Hydrodynamic Regimes

Three distinct hydrodynamic regimes have been identified in Cockburn Sound based on the relative importance of wind and pressure gradients in determining circulation patterns and flushing. These regimes are “winter-spring”, “summer” and “autumn” (DEP, 1996). A description of each of these regimes follows, and these regimes have been used to define periods for the assessment of flushing and water quality outcomes.

2.5.1 Summer

During summer, wind dominates the circulation within Cockburn Sound. Sea breezes are both strong and persistent during this time and act to maintain vertically-mixed conditions most of the time. Given the dominant south-west direction of the sea breezes, net transport northward can be expected.

2.5.2 Autumn

During the autumn period, vertical mixing in the deep waters is less frequent than in summer, due to a reduced energy input from both wind and surface cooling. The waters of Cockburn Sound are typically denser than the adjacent coastal waters, and are confined by the presence of bathymetric barriers. The exchange time-scale for the whole of Cockburn Sound is expected to be greatest at this time (DEP, 1996) and it would be expected that, overall, mixing of the water column would be least efficient during this period.

2.5.3 Winter-Spring

During the winter-spring period, the dynamics of the Sound are strongly influenced by the passage of storm systems at 7 – 10 day intervals. Wind magnitudes during the winter storm events are sufficient to fully mix the water column within Cockburn Sound and Mangles Bay.

Between storm events, lighter, and generally southerly winds act in combination with baroclinic forces to promote renewal of both surface and bottom waters in Cockburn Sound. Greater variability in current magnitude and direction would be expected during this period.

2.6 Water Currents

Pattiaratchi (2002) conducted a current measurement program during summer of 2001 as part of a study for the Cockburn Sound Management Council. Current meters were deployed at two locations, one to the west of the northern Causeway entrance, and one to the east within central Mangles Bay. Earlier, Rose (2001) had analysed some measurements made in late autumn/early winter of 2001 at a similar location to the western location reported in Pattiaratchi (2002).

Both of the measurement programs revealed that the flow through the Causeway is not dominated by the ebb and flow of the tide. In fact, it was found that the tidal component of the currents was only around 50% of the strength of the wind, seiche and low frequency driven components (Pattiaratchi, 2002). In particular, the correlation of the current magnitudes to the incidence of long-period (several days) mean sea level variations was strong.

It was observed that, in general, the flow would be directed out of Cockburn Sound as the mean water level was rising, and into the Sound as the mean water level was falling. This behaviour is consistent with response to a travelling wave (such as a coastally trapped wave) and suggests that large scale-flows are generated by gradients in water level between the northern and southern extents of the Sound.

During the measurement periods of Rose (2001) and Pattiaratchi (2002), current speeds near the northern Causeway opening reached up to 0.5 m/s, and up to around 0.3 m/s in Mangles Bay. The currents near the Causeway openings were observed to be strongly correlated with the wind, exhibiting a near instantaneous response to variations in the wind. Currents within Mangles Bay itself were observed to be primarily wind-dominated, with the water currents exhibiting a lag of 2 to 6 hours to changes in the wind climate.

3 FIELD MEASUREMENTS

3.1 Fixed Point ADCP Measurements

An ADCP was deployed on 10th February 2011 at coordinates -32.2714, 115.7123, (Location 1, Figure 3-1). During an inspection at the time of a subsequent drogue release run, the ADCP was found to have been dragged onto its side. It was retrieved and re-deployed slightly to the south-east (Location 2, Figure 3-1, about 25 m away) and then re-anchored. This deployment period continued through to the 11th of March when data retrieval and relocation of the instrument occurred. This period is referred to as Deployment 1 and the data is considered to be representative of a single location.

On the 11th of March the ADCP was re-deployed to a location adjacent to the southern opening in the Garden Island Causeway (Location 3, Figure 3-1). The instrument was retrieved on 7th April 2011.

Each of these locations and deployments are summarised in Table 3-1 and the data is presented in the following sections.

Figure 3-1: The three ADCP locations spanning the two deployment periods.

Table 3-1: ADCP deployments summary.

Deployment #	Location	Dates	Coordinates (Lat., Long.)	Water Depth (rel MSL)
1	1	10/02 – 25/02	-32.2714, 115.7123	3.36
	2	25/02 – 11/03	-32.2716, 115.7124	3.36
2	3	11/03 – 07/04	-32.2679, 115.7002	3.86

3.1.1 Deployment 1 – Mangles Bay

The data set obtained during Deployment 1 is presented in Figure 3-2. During this period, the wind was unusually persistent from the east, with a mild sea-breeze pattern occurring towards the latter part of the period. The effect of the persistent easterly winds was to drive a persistent west-north-westerly flow over this site in Mangles Bay for the majority of the period. Currents reached around 0.25 m/s at the peak, with a median current speed of 0.05 m/s. Current speeds were less than 0.1 m/s for most of the record.

3.1.2 Deployment 2 – Southern Causeway entrance

The ADCP was relocated near to the southern entrance of the Garden Island Causeway in order to characterise the flow regime between the open ocean and Mangles Bay. The instrument was deployed as near as practical to the centre of the opening with the aim of sampling the peak flows through the gap.

The measured current speeds and directions are presented in Figure 3-3. The data exhibited a range up to 0.54 m/s (approximately 1 knot) with a median current speed of 0.15 m/s. The currents were typically aligned along a west-northwest or east-southeastly axis, reflecting the local alignment of the causeway opening.

The record shows periods of time where flow either into or out of Cockburn Sound persists for several days at a time, suggesting that the flow is not totally governed by the local flood and ebb of the tide. This phenomenon may be due to larger scale gradients in water level. There was no clear relationship to prevailing wind conditions during this period, and overall the current record at this site suggests an extremely complex exchange regime between Mangles Bay and the ocean waters to the west.

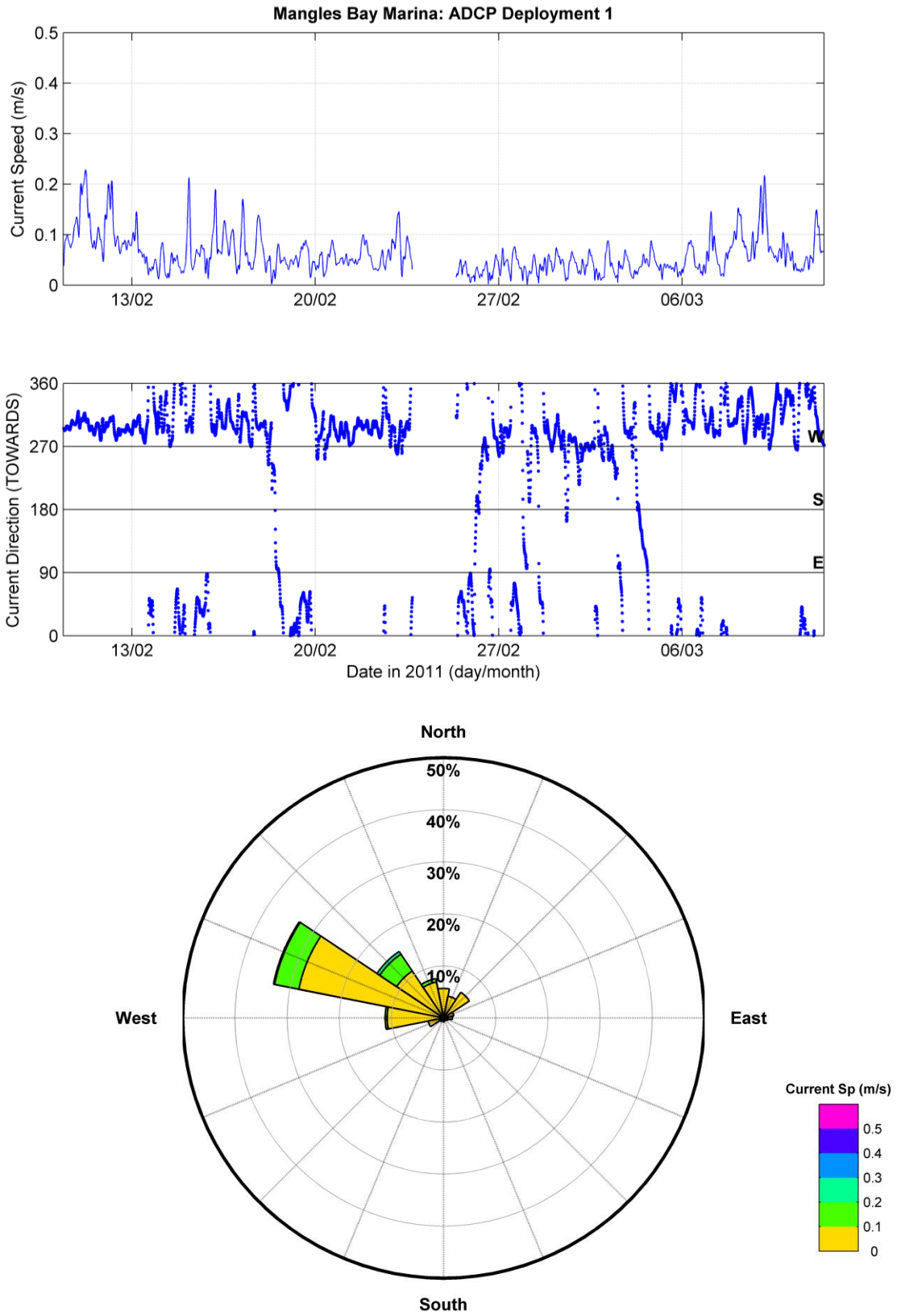

Figure 3-2 Time-series of current speed and direction (top) and current rose derived from data measured at mid-depth during Deployment 1 (February 10 to March 11, 2011).

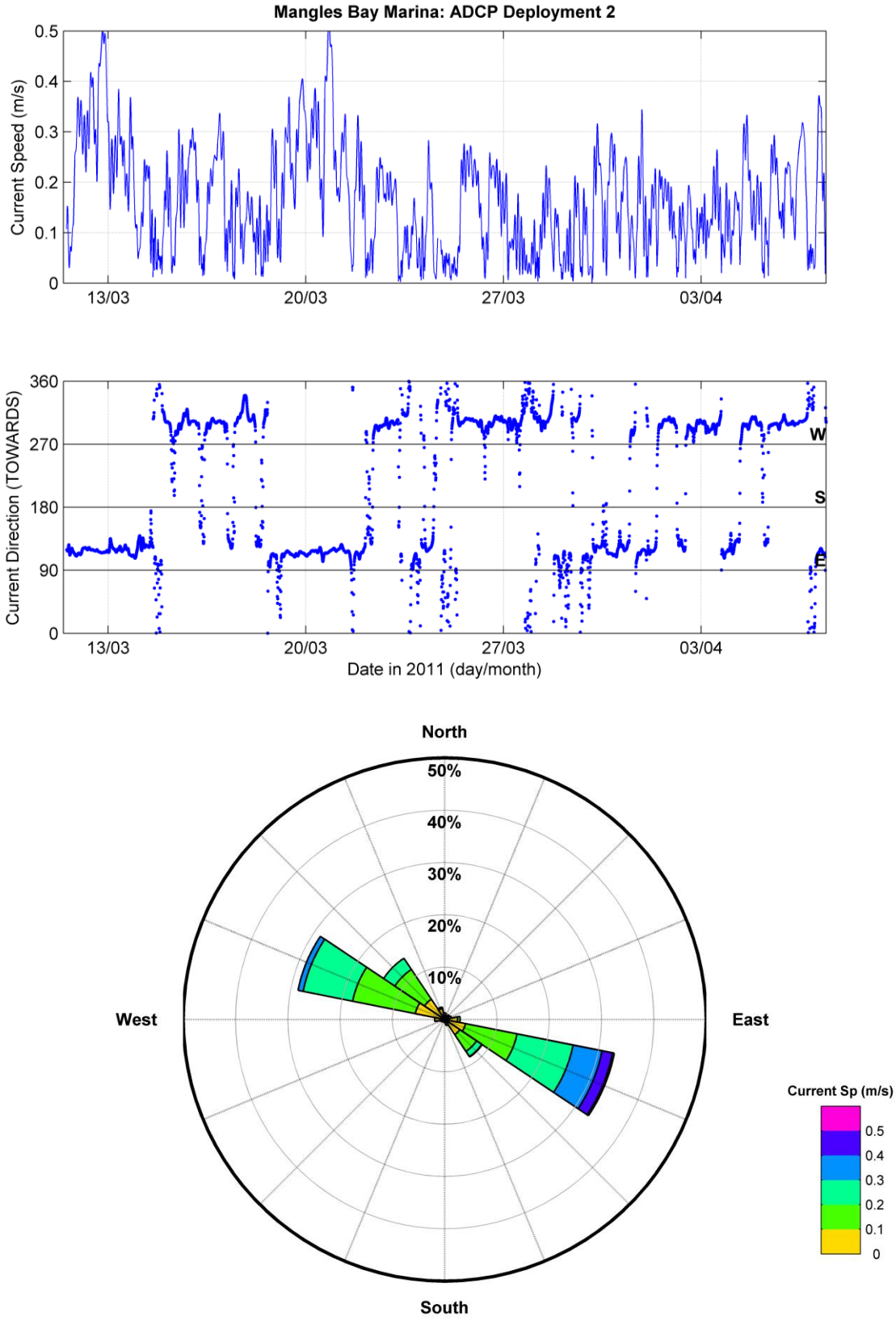

Figure 3-3 Time-series of current speed and direction (top) and current rose derived from data measured at mid-depth during Deployment 2 (March 11 to April 7, 2011).

3.2 Drogue Measurements

3.2.1 Background

Drogue measurements were undertaken on four separate days (Table 3-2) to provide a means of assessing the currents in Mangles Bay over wider spatial and longer time-scales. Drogues were constructed of a flat foam disk from which a weighted cylindrical stiff tube (0.4 m high x 0.3 m diameter) was suspended by a rope bridle to sample the current over a the upper metre. Small GPS units were inserted into a compartment within the foam disk to record the track of the drogue over time. These measurements form a complimentary set to the fixed point measurements described above and allow for an alternative validation of the hydrodynamic model developed for the study.

Table 3-2: Summary of drogue deployments during February to April, 2011

Measurement Date	# of Deployments	Tide Conditions	Winds
10 February 2011	4	0.54 – 0.91 m, rising	Easterly, 15 – 18 knots easing
25 March 2011	4	0.45 – 0.98 m, rising	Light southwest
11 March 2011	3	0.58 – 1.00m, rising	Seabreeze – morning SSE, shifting SSW
7 April 2011	3	~ 1.0 m, high tide	Moderate to Strong SSW to SW

The observations from each of the deployment days are summarised below.

3.2.2 Day 1 10th February 2011

On 10h February 2011, low tide at Fremantle was 0.54 m at 05:14 am and high tide was 0.91 m at 02:34 pm. Wind was from the east at 15-18 knots during deployment 1, easing to below 10 knots from the east during each of the other deployments. Multiple drogues were deployed from a given location on four separate occasions, as summarised in Table 3-3, to measure the prevailing current flow and horizontal dispersion rates.

The drogue tracks consistently showed currents flowing towards the west on the flood tide, indicating that circulation through the southern Causeway entrance may not always be consistent with the expected tidal direction or that the phase of the currents at this location is offset with respect to the surface elevation. Strongest speeds were recorded in the afternoon through the southern Causeway entrance (Figure 3-4), when current speeds were 0.2 to 0.3 m/s. Tracks of drogues co-deployed showed small divergence, indicating low levels of horizontal dispersion.

Table 3-3: Drogue tracking summary for Day 1, 10th February 2011

Deployment # (track colour)	Time	Average Speed (m/s)	Average Direction (° from N, towards)
1 (red)	10:02 – 10:53	0.13	280
1 (green)	10:02 – 10:53	0.14	283
1 (blue)	10:02 – 10:53	0.15	280
1 (purple)	10:02 – 10:53	0.14	278
2 (red)	11:00 – 12:10	0.10	286
2 (green)	11:00 – 12:10	0.10	289
2 (blue)	11:00 – 12:10	0.13	302
2 (purple)	11:00 – 12:10	0.13	299
3 (red)	12:15 – 13:11	0.15	272
3 (green)	12:15 – 13:11	0.15	278
3 (blue)	12:15 – 13:11	0.23	283
3 (purple)	12:15 – 13:11	0.23	281
4 (red)	13:15 – 14:00	0.31	318
4 (green)	13:15 – 14:00	0.28	314

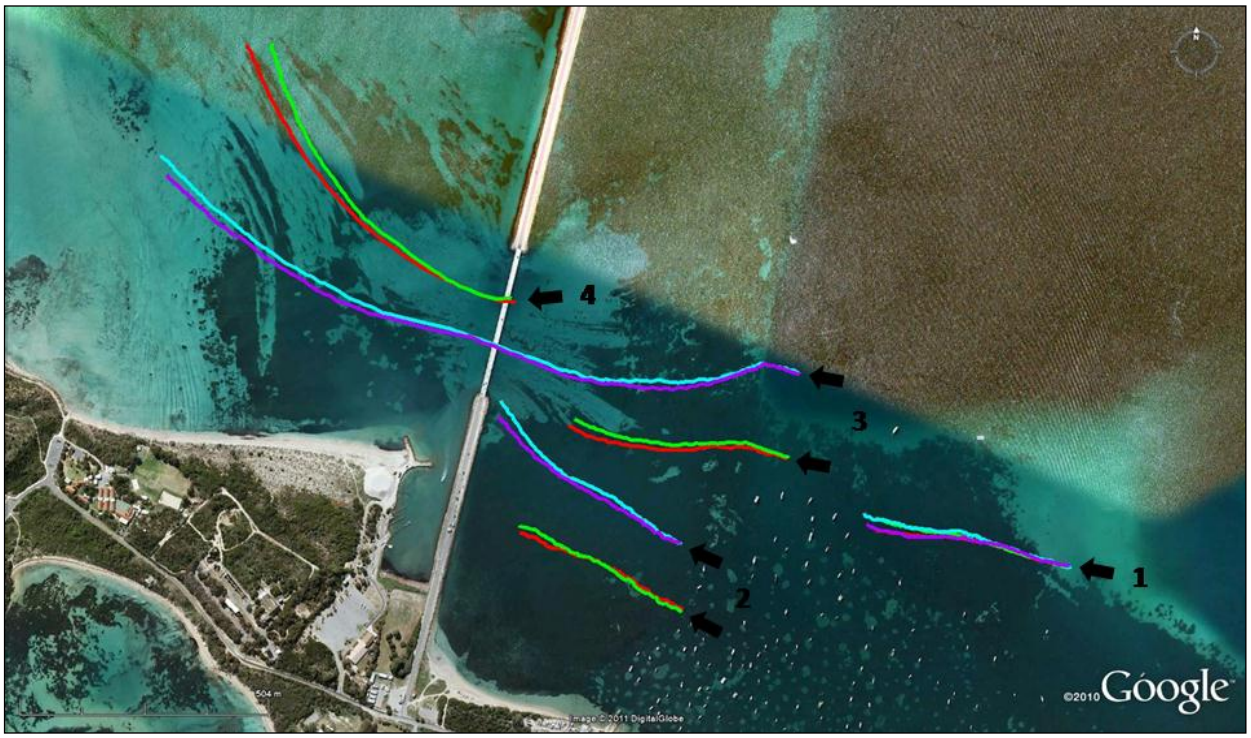

Figure 3-4: Recorded drogue tracks on the flood tide on 10th February 2011. The extent of the southern causeway opening is indicated by the narrowest section of the causeway.

3.2.3 Day 2 25th February 2011

On 25th February 2011, low tide at Fremantle was 0.45 m at 02:13 am and high tide was 0.98 m at 03:21 pm. Winds were light and from the southwest all day, gradually increasing from 5 knots during deployment 1 to 10-12 knots during deployment 4. Drogues were deployed on four occasions, as summarised in Table 3-4.

Drogue tracks on this day indicated a net flow into Cockburn Sound through the causeway entrances. Recorded tracks from deployments 1 and 2 show drogues drifting generally towards the east, although drogues released close to the rock groin on the south side of the southern causeway entrance drifted northward parallel with the groin before diverting eastward parallel with the entrance (Figure 3-5). Strongest current magnitudes were recorded through the northern Causeway entrance as drogues drifted to the east and northeast (Figure 3-6), with the observed current speed up to 0.30 m/s. Multiple drogue tracks for all deployments were consistent.

Table 3-4: Drogue tracking summary for Day 2, 25th February 2011

Deployment # (track colour)	Time	Average Speed (m/s)	Average Direction (° from N, towards)
1 (red)	09:40 – 10:40	0.03	158
1 (green)	09:40 – 10:40	0.04	174
1 (blue)	09:40 – 10:40	0.05	139
1 (purple)	09:40 – 10:40	0.05	138
2 (red)	10:50 – 11:50	0.09	99
2 (green)	10:50 – 11:50	0.10	99
2 (blue)	10:50 – 11:50	0.10	82
2 (purple)	10:50 – 11:50	0.10	79
3 (red)	12:00 – 13:00	0.06	179
3 (green)	12:00 – 13:00	0.07	159
3 (blue)	12:00 – 13:00	0.10	226
3 (purple)	12:00 – 13:00	0.10	237
4 (red)	13:10 – 14:00	0.17	81
4 (green)	13:10 – 14:00	0.20	79
4 (blue)	13:10 – 14:00	0.28	56
4 (purple)	13:10 – 14:00	0.29	54

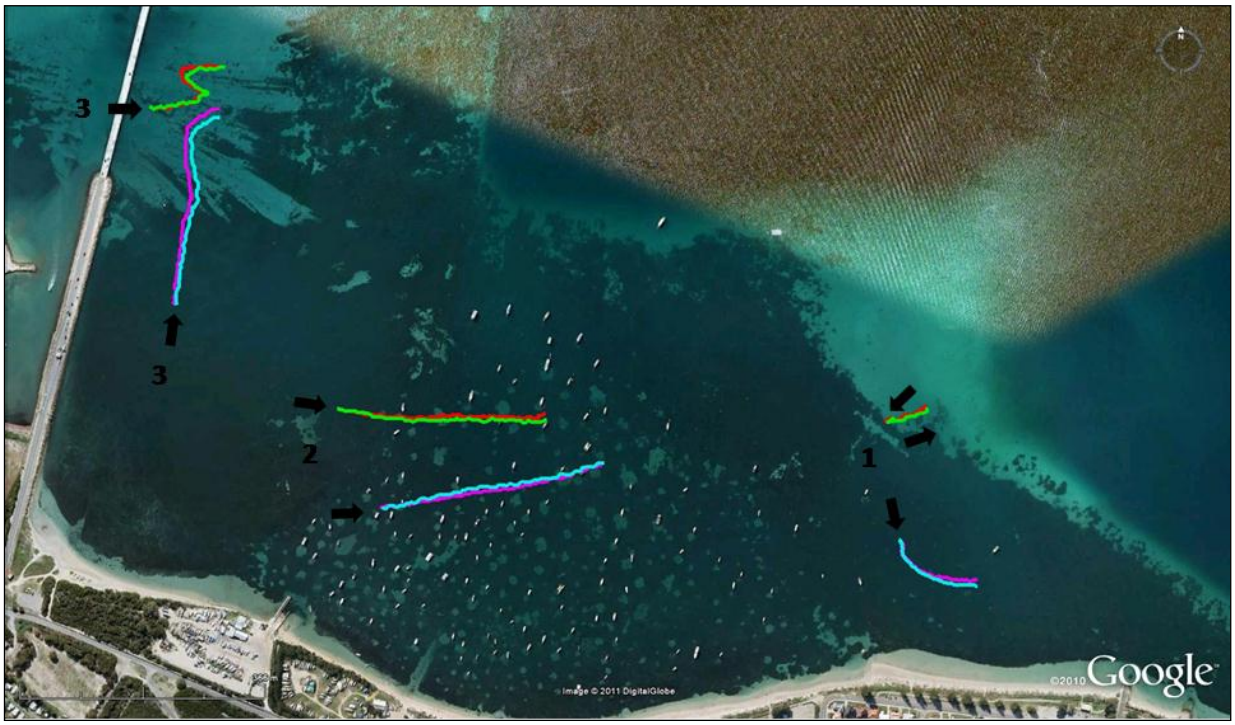

Figure 3-5: Recorded drogue tracks in the morning on the flood tide on 25th February 2011, near the southern causeway entrance.

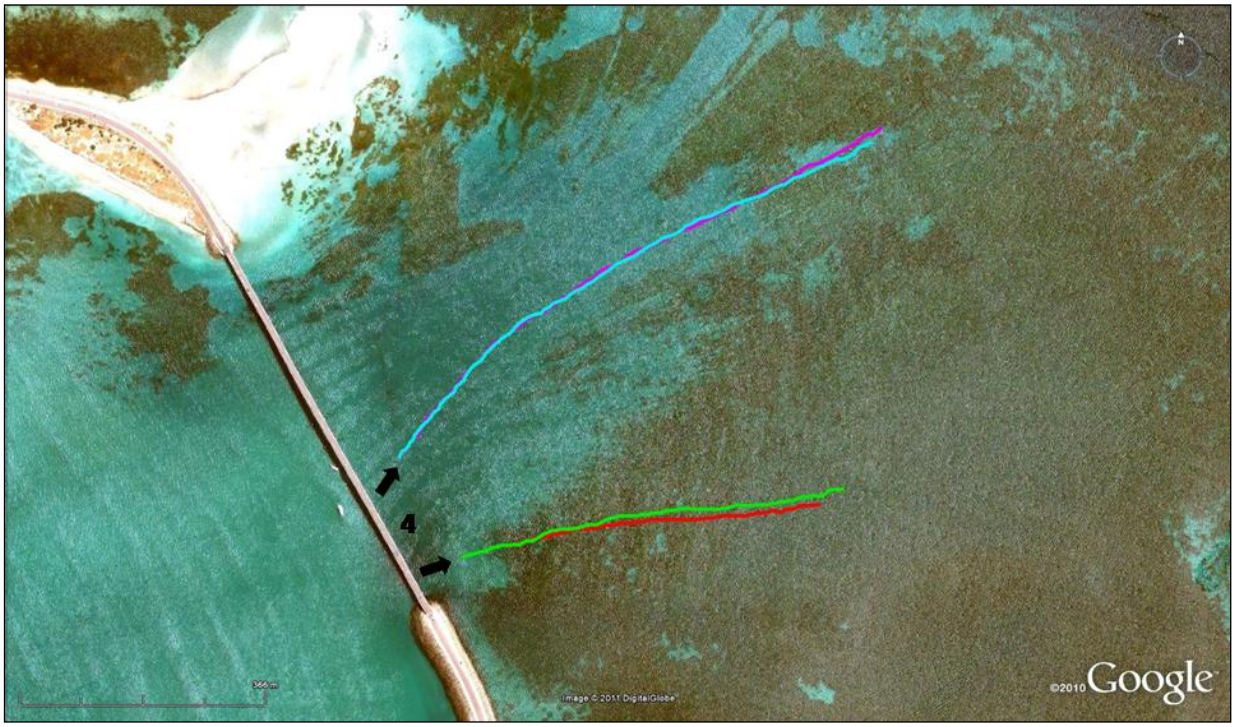

Figure 3-6: Recorded drogue tracks in the afternoon on the flood tide on 25th February 2011, near the northern causeway entrance.

3.2.4 Day 3 11th March 2011

On 11th March 2011, low tide at Fremantle was 0.58 m at 3:56 am and high tide was 1.00 m at 12:31 pm. Wind at 08:30 am in Mangles Bay was 5 knots out of the south-southeast, increasing to 10-15 knots by 10:30 am from the same direction. By 11:00 am, moderate (15-18 knot) south-south-westerly winds were blowing and wind conditions remained this way for the remainder of the drogue deployments. Drogues were deployed on three occasions, as summarised in Table 3-5.

Drogue tracks indicated a net flow eastward through the causeway entrance. During deployment 1, all drogues drifted to the north-west until they reached deeper water and then drifted north-east (Figure 3-7). Recorded drogue tracks during deployment 2 show currents flowing towards the east and tracks recorded during deployment 3 indicate north-east flowing currents through the northern Causeway entrance (Figure 3-8) with a current speed approaching 0.2 m/s. Tracks of drogues deployed together showed little variance, indicating low horizontal dispersive forces.

Table 3-5: Drogue tracking summary for day 3, 11th March 2011

Deployment # (track colour)	Time	Average Speed (m/s)	Average Direction (° from N, towards)
1 (red)	08:18 – 10:35	0.12	191
1 (green)	08:18 – 10:35	0.12	196
1 (blue)	08:18 – 10:35	0.14	203
1 (purple)	08:18 – 10:35	0.13	204
2 (red)	10:40 – 11:37	0.17	88
2 (green)	10:40 – 11:37	0.17	89
2 (blue)	10:40 – 11:37	0.11	148
2 (purple)	10:40 – 11:37	0.07	149
3 (red)	11:46 – 13:00	0.08	61
3 (green)	11:46 – 13:00	0.09	62
3 (blue)	11:46 – 13:00	0.17	67
3 (purple)	11:46 – 13:00	0.17	70

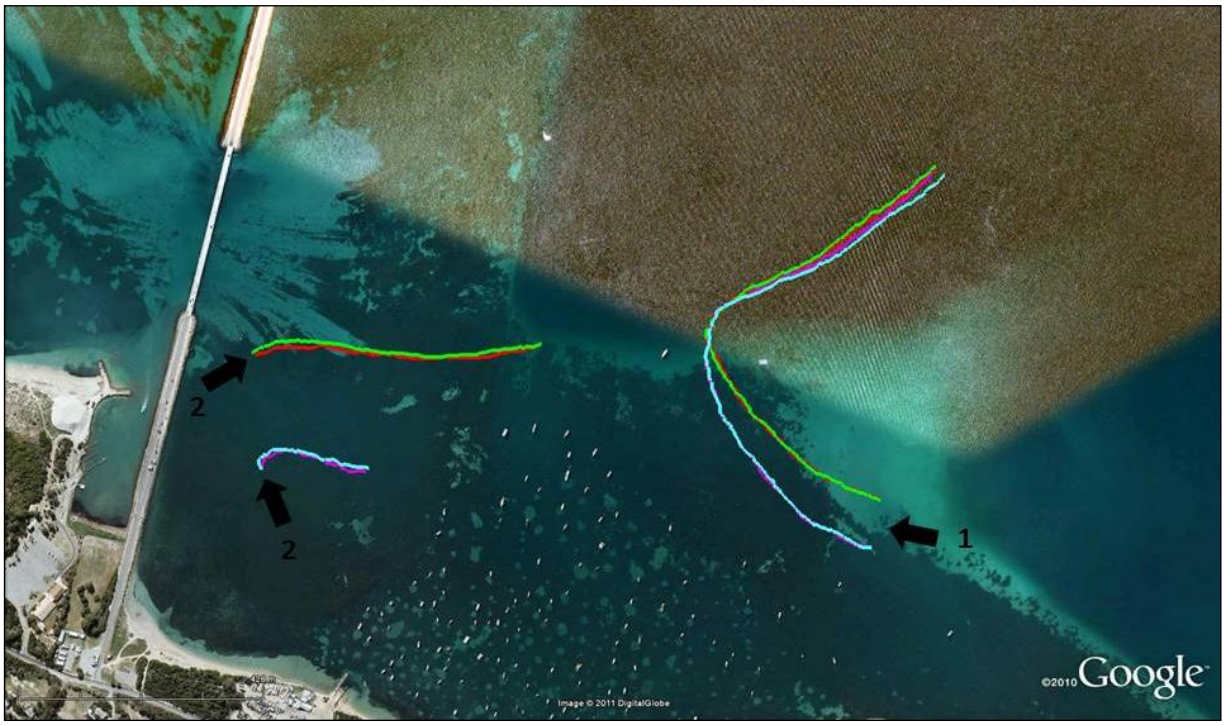

Figure 3-7: Recorded drogue tracks in the morning on the flood tide on 11th March 2011.

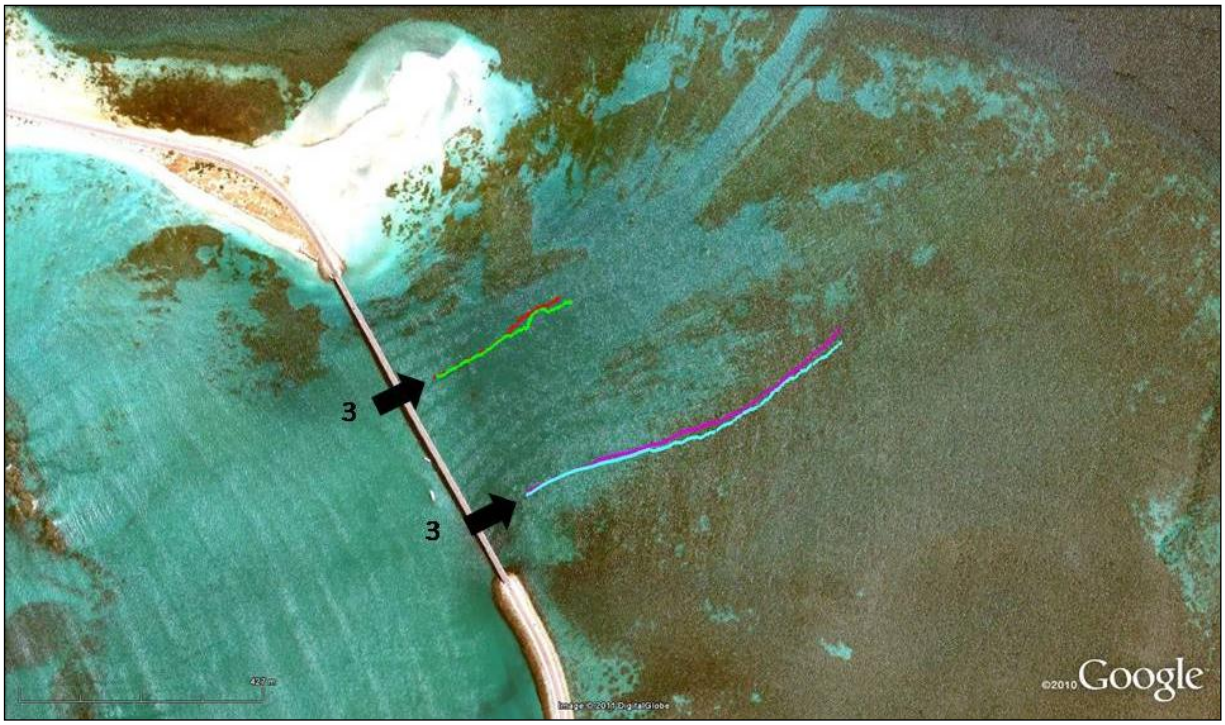

Figure 3-8: Recorded drogue tracks around midday either side of the flood tide on 11th March 2011.

3.2.5 Day 4 7th April 2011

On 7th April 2011, high tide at Fremantle was 1.10 m at 11:00 am. Low tide on 6th April was 0.64 m at 6:31 pm and low tide on 8th April was 0.66 m at 12:11 pm. Wind speeds on this day were generally moderate to strong, creating choppy seas. At 09:00 am wind was from the southwest at 15-18 knots and by 10:00 am speeds had increased to 20-25 knots. Winds eased slightly to 12-18 knots and swung to the south-southwest at 10:45 am before increasing again up to 25 knots by 01:30 pm. Drogues were deployed on three occasions, as summarised in Table 3-6.

During the morning, drogues were first deployed at the ADCP location, and were observed to drift towards the northeast at average speeds of around 0.13 m/s. During deployment 2, near the southern Causeway entrance, currents were observed to be flowing to the north along the causeway and the northwest on the flood tide, before changing to the east on the ebb tide (Figure 3-9). Drogues deployed at the northern Causeway entrance,, during the afternoon, drifted northeast at average speeds of around 0.22 m/s. It should be noted that whitecaps from the choppy seas were breaking over the drogues during this deployment (Figure 3-10) and it is likely that this may have affected the recorded speed and directions of the drogues.

Table 3-6: Drogue tracking summary for Day 4, 7th April 2011

Deployment # (track colour)	Time	Average Speed (m/s)	Average Direction (° from N, towards)
1 (red)	09:09 – 10:25	0.13	83
1 (green)	09:09 – 10:25	0.13	66
1 (blue)	09:09 – 10:25	0.14	65
2 (red)	10:35 – 12:36	0.12	221
2 (green)	10:35 – 12:36	0.12	211
2 (blue)	10:35 – 12:36	0.12	217
3 (red)	12:43 – 13:30	0.20	66
3 (green)	12:43 – 13:30	0.22	70
3 (blue)	12:43 – 13:30	0.23	63

Figure 3-9: Recorded drogue tracks on the flood tide (1) and on either side of the flood tide (2) on 7th April 2011.

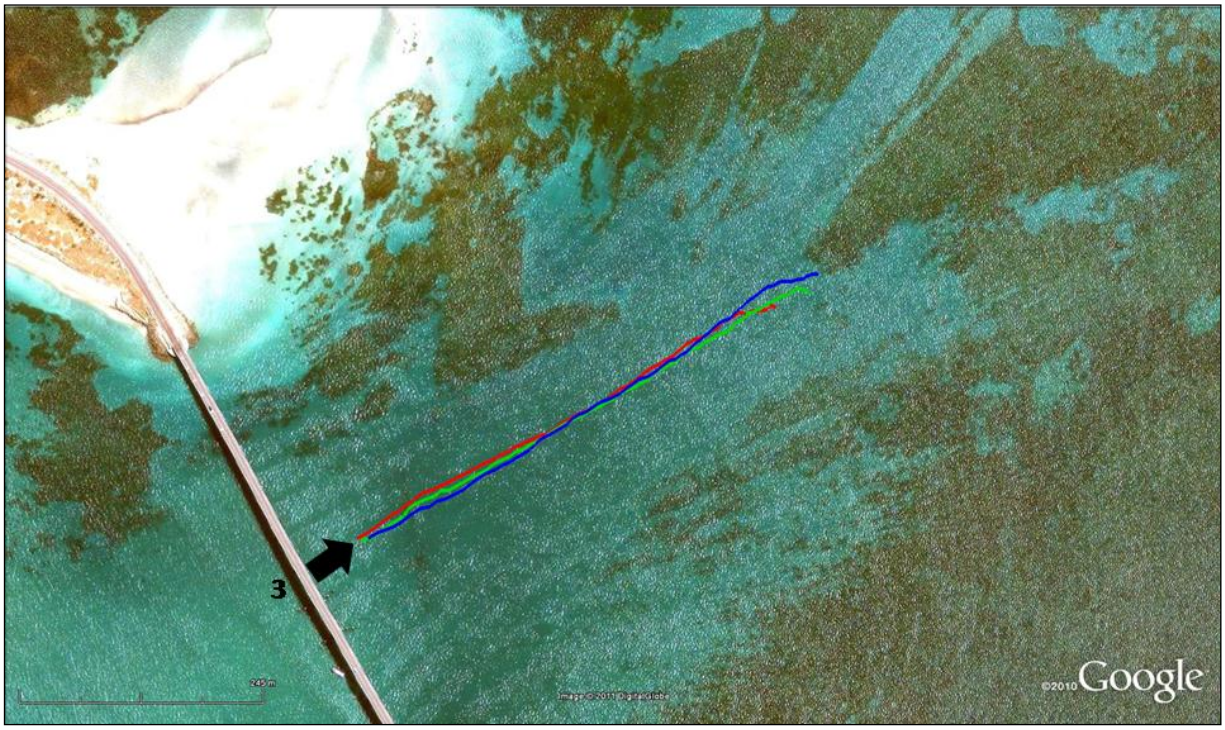

Figure 3-10: Recorded drogue tracks in the afternoon on the ebb tide on 7th April 2011.

3.2.6 Summary

The drogue measurements generally showed that current speeds through the causeway openings were on average 0.3 m/s, with lower current speeds in Mangles Bay (typically around 0.05 to 0.1 m/s). Some evidence was seen of consistency with tidal and wind driven flows, however at times the drogues were observed to move through the causeway openings counter to the expected tidal flow direction. Such behaviour is consistent with the fixed point ADCP measurements during Deployment 2, when persistent in or out-flow was observed, with little variation despite the tidal state.

3.3 Wind Measurements

To determine whether wind measurements at the Bureau of Meteorology (BOM) weather station on the northern end of the Garden Island Causeway could be appropriately applied to represent winds at Mangles Bay, APASA conducted a short measurement program for wind at a site in Mangles Bay. The BOM weather station is in a relatively exposed location. Given the location of Mangles Bay in the southern end of Cockburn Sound, and the shape of the coastline in this area, Mangles Bay is generally more sheltered from winds from the east and south-westerly sectors than the BOM station..

Wind speed and direction were measured using a recording anemometer mounted on a pole that was located on the southern end of the Garden Island Causeway, near Mangles Bay (see Figure 3-11) from 4th-14th February 2011 and compared with measurements from the same period at the BOM wind station at Garden Island. A longer deployment was intended however the wind station experienced a data recording problem after the 14th of February. Following retrieval, the location of the deployment (within secure Royal Australian Navy land) was no longer available to APASA.

Figure 3-12 shows a comparison of the measurements at the Mangles Bay site and at the Garden Island weather station. Wind speeds given are 10 minute means converted to 10 m height, and wind direction is direction the wind is coming from, in degrees clockwise from North.

Figure 3-11: Location of the wind station used for comparison to the Garden Island weather station at the northern end of the causeway.

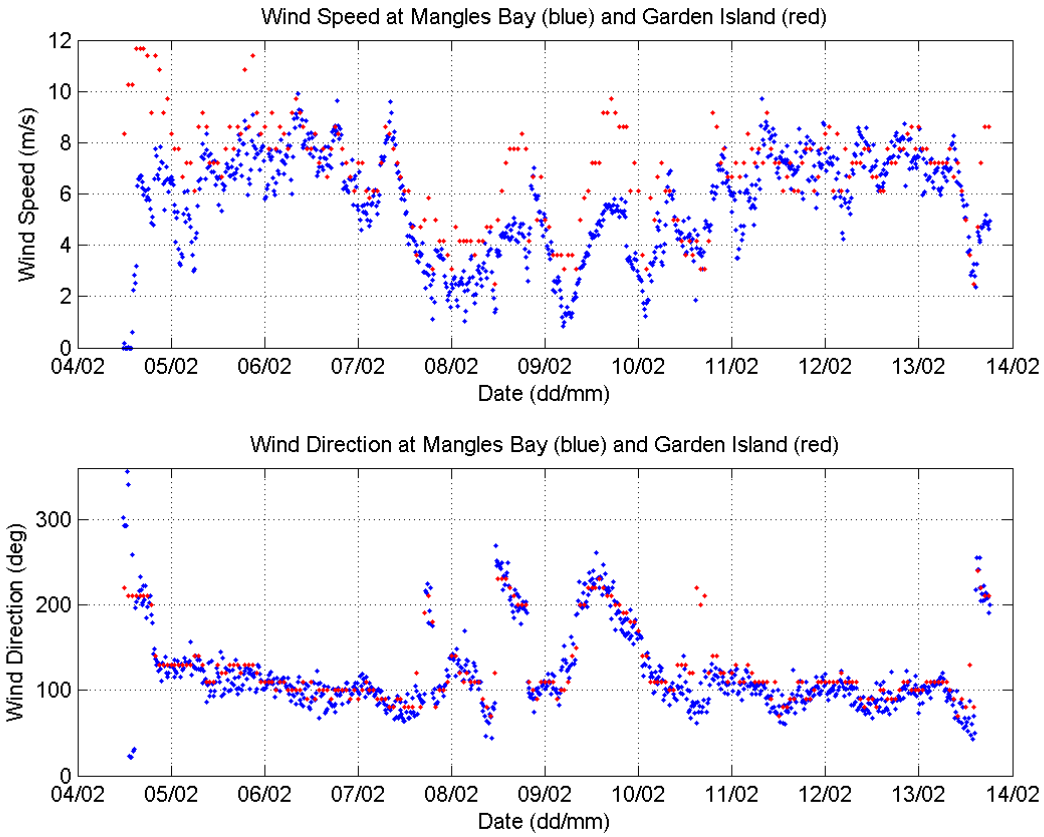

Figure 3-12 Measurements of wind speed and direction at Mangles Bay (blue) and Garden Island (red) in February 2011

This comparison reveals that, as expected, wind speeds at Garden Island are consistently higher for wind directions from the SW quadrant (180-270°) and from the East (45-135°). In general, the speeds at the Mangles Bay location were typically about 65% of those at Garden Island for south-westerly, and 75% for easterly winds. The direction at the two locations was generally very similar, as were the recorded wind speeds when the wind was from other directions.

This comparison suggests that winds in Mangles Bay will be slightly weaker from sheltered sectors than indicated in the long run records at the more exposed Garden Island location, and that this should be considered in the application of the wind data in the modelling.

4 MODELLING METHODOLOGY

In order to develop a robust modelling framework to predict the likely flushing performance of the proposed marina, it was necessary to prepare a model that included the major forcing mechanisms, appropriate spatial scales and an adequate sampling of the expected conditions. In order to achieve this, it was necessary to develop a model that included the wider Cockburn Sound area so that the dynamics of the exchange between the marina, Mangles Bay and Garden Island Causeway entrances could be represented.

It was not the intention of this study to develop a fully calibrated model of Cockburn Sound, as such a task was outside the scope of this project, and largely unnecessary with respect to achieving the aims of this work. However, the spatial and time scales that were employed in the model do allow for the influence of the broader hydrodynamics of Cockburn Sound to play their part in local circulation and exchange.

4.1 Simulation Scenarios

Simulations were conducted to represent the three identified hydrodynamic regimes in Cockburn Sound; summer, autumn and winter-spring (winter). In this way, a wide range of typical environmental conditions at the site were covered. The selection of typical or representative conditions for each regime involved an analysis of 7 years of wind data at Garden Island, in the knowledge that the wind was identified as the major driver of water currents within Mangles Bay (Pattiaratchi, 2002).

The representative periods were chosen based on a statistical assessment of the wind magnitudes of selected years consistent with mean conditions. The selected periods were also defined based on achieving a good match with the overall directional roses for that season. A summary of the selected periods is provided in Table 4-1.

Table 4-1: Summary of selected representative periods and the wind statistics for these periods. Bracketed values represent the statistics for that season for all years in the dataset.

Season/ regime	Selected Period	Mean Wind Speed (m/s)	75th percentile Wind Speed (m/s)	95th percentile Wind Speed (m/s)
Summer	1/12/05 - 28/02/06	7.2 (7.2)	9.3 (9.3)	12.5 (12.5)
Autumn	1/03/04 – 29/05/04	5.4 (5.4)	8.4 (7.8)	12.3 (11.7)
Winter	1/06/03 – 29/08/03	6.6 (6.3)	9.9 (9.3)	14.3 (13.7)

The roses shown in Figure 4-1 (summer), Figure 4-2 (autumn) and Figure 4-3 (winter) illustrate that the directional and speed distribution of the modelled periods match the longer term records very well. Consequently, all of the modelled periods were considered suitable for representing the expected behaviour during the assessed seasons.

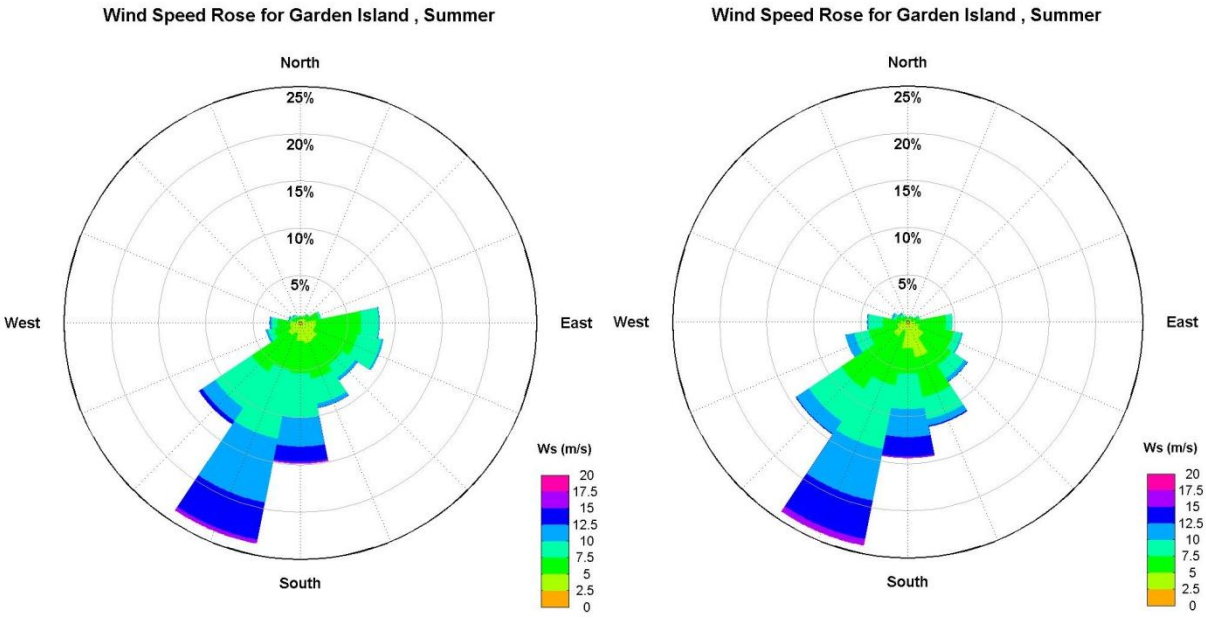

Figure 4-1 Wind roses (direction from) for Garden Island Nov 2001 to Sept 2008 - summer (left) and Dec 2005 to Feb 2006 summer (right).

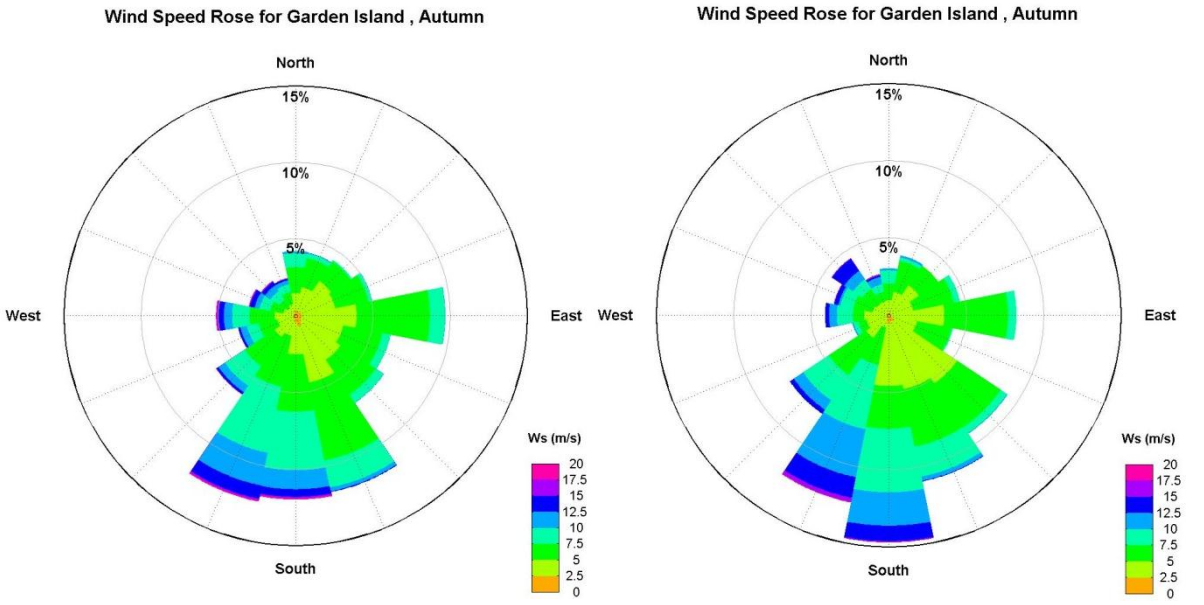

Figure 4-2 Wind roses (direction from) for Garden Island Nov 2001 to Sept 2008 - autumn (left) and Mar 2004 to May 2004 autumn (right).

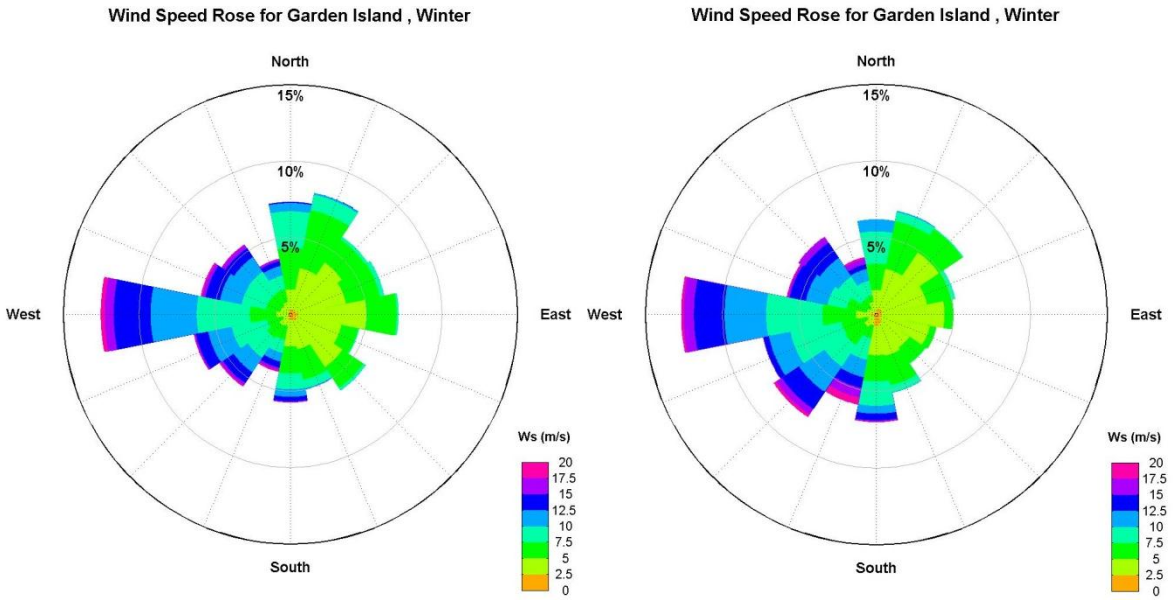

Figure 4-3 Wind roses (direction from) for Garden Island Nov 2001 to Sept 2008 - winter (left) and Jun 2003 to Aug 2003 winter (right).

5 HYDRODYNAMIC MODELLING

5.1 Model Description

Due to the necessity to accurately simulate both baroclinic flows and wind, tide and groundwater inputs, the EFDC (Environmental Fluid Dynamics Code) model was applied within ASA's WQMAP framework. EFDC has been widely used around the world for environmental assessments, and has also been applied in numerous studies in Australia.

The EFDC model was originally developed in the early 1990's, with development continuing to the present day (Hamrick 1992, 1992b; Hamrick *et al* 1995; Hamrick and Wu 1997). EFDC is based on a curvilinear orthogonal system in the horizontal, which allows a continuous representation of features such as channels, coastlines and bottom contours. The model is three dimensional in space, using a sigma, or stretched, grid in the vertical that allows a constant proportionate resolution throughout the domain.

Vertical turbulence is represented using the Galperin *et al* (1988) revision of the Mellor and Yamada (1982) 2.5 level scheme. This scheme accounts for the contribution of shear and buoyancy forces in regulating the exchange of momentum through the water column. The effect of wind drag on the surface is modelled using the variable drag coefficient formulation of Wu (1980). .

EFDC has been applied previously by APASA and its personnel for analysis of the hydrodynamics and discharge fate within Cockburn Sound, Perth Coastal Waters, the Peel Inlet, Mermaid Sound, Port Hedland Harbour, Darwin Harbour, Hawkes Bay in New Zealand and Caution Bay in Papua New Guinea. Most of these studies involved rigorous validation of the hydrodynamic model performance. Hence, the model algorithms were considered robust and fit for the purposes of this study.

5.2 Model Application

5.2.1 Model domain and computational grid

The model domain and computational grid developed for this study are shown in Figure 5-1 and Figure 5-2. The model domain measures 25km north/south along the coast by 17km east/west, encompassing Cockburn Sound and extending offshore to approximately 35m water depth. The computational grid includes more than 27,000 horizontal cells, with 6 vertical layers. The middle layers were specified as 20% of the local water depth. The top and bottom layers were specified as 10% of the local water depth to provide better resolution near the seabed and the water surface. The horizontal model resolution varies from 8-10 m within the marina, to 450 m at the outer edges of the domain.

The model bathymetry was developed based on data digitised from Australian hydrographic charts AUS117 and AUS334 extracted from the CMAP database and supplemented with data provided by the project team.

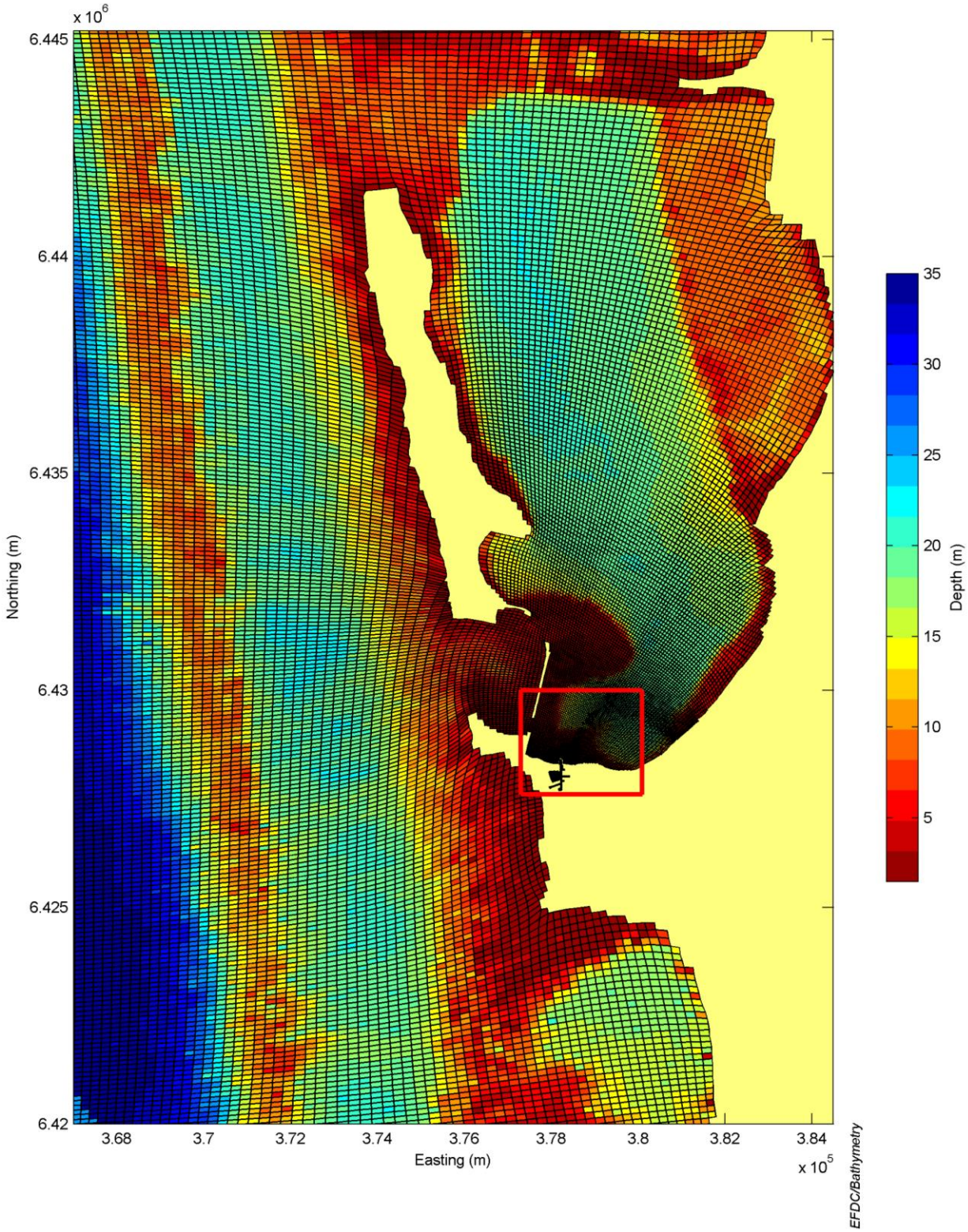

Figure 5-1 Model domain, computational grid and bathymetry. Red area is shown in more detail in Figure 5-2.

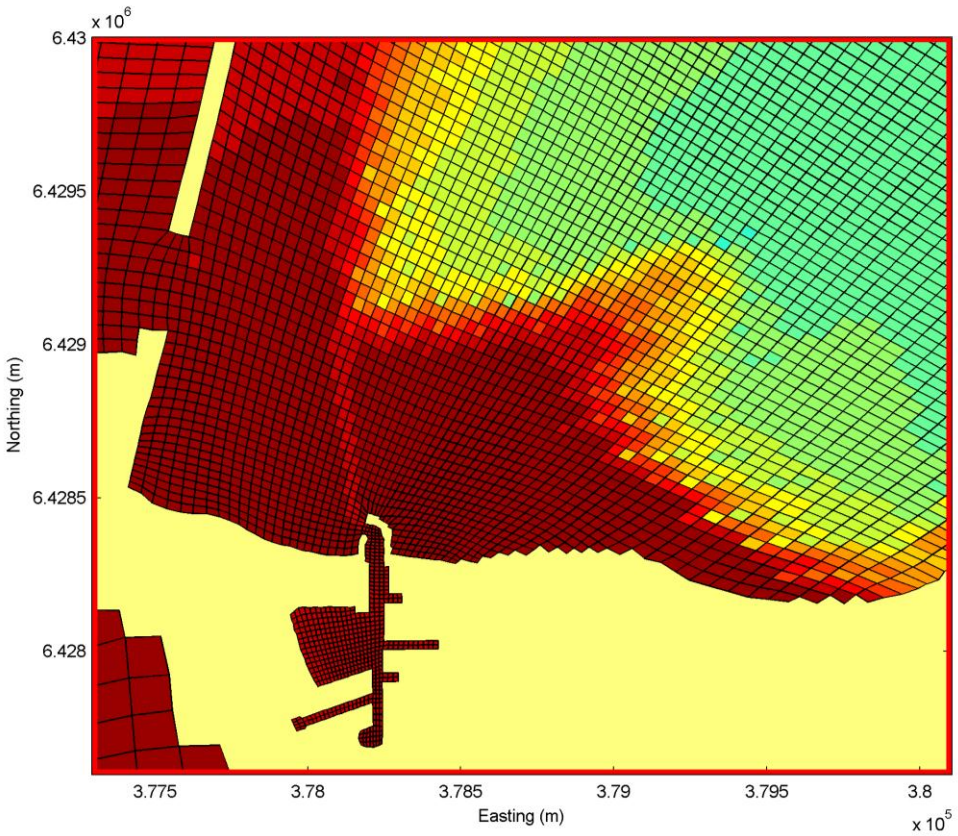

Figure 5-2 Computational grid and bathymetry in region of proposed development

The water column in the model was discretised into 6 layers, which followed the sigma grid (terrain following) format where each layer interface occurs at a constant proportion of the local water depth. The top and bottom layers were set to 10% of the local water depth, with the remaining interior layers set to 20% of the local water depth.

5.2.2 Model Forcing and Boundary Conditions

5.2.2.1 Water Levels

During the initial set up and calibration phase of the project, tidal data was applied along the open boundary of the model from a large scale ocean model covering the south-west of Western Australia. This model included the major tidal constituents and was driven using constituents extracted from the TOPEX 7.2 global tidal database. Following initial comparison to the measured data, it was clear that the local oscillations in water level due to both higher and lower frequencies than pure tides were important in driving the circulation in and near Mangles Bay.

To overcome this, measured tidal data for Fremantle was obtained from the Department of Planning and Infrastructure (DPI). This data was filtered to remove very high frequency "noise" at frequencies related to very local effects, then applied along the open ocean boundary as a constant. Testing of the application of various lags along the western model boundary showed that the response within Mangles Bay, and particularly near the causeway, was relatively insensitive to phase variation along the boundary.

A very important component of the measured time-series was the gradual effect of varying atmospheric pressure on the mean water level in the region. It was clear that the mean water level varied at frequencies consistent with the expected flushing time of the proposed development, and was therefore an important consideration in the modelling. Figure 5-3 shows an example of the water level time-series (for the summer/autumn period) applied at the open ocean boundaries. Note the variation in the mean water level (about 0.0 m) in the record, where a period of around 7 – 10 days is evident.

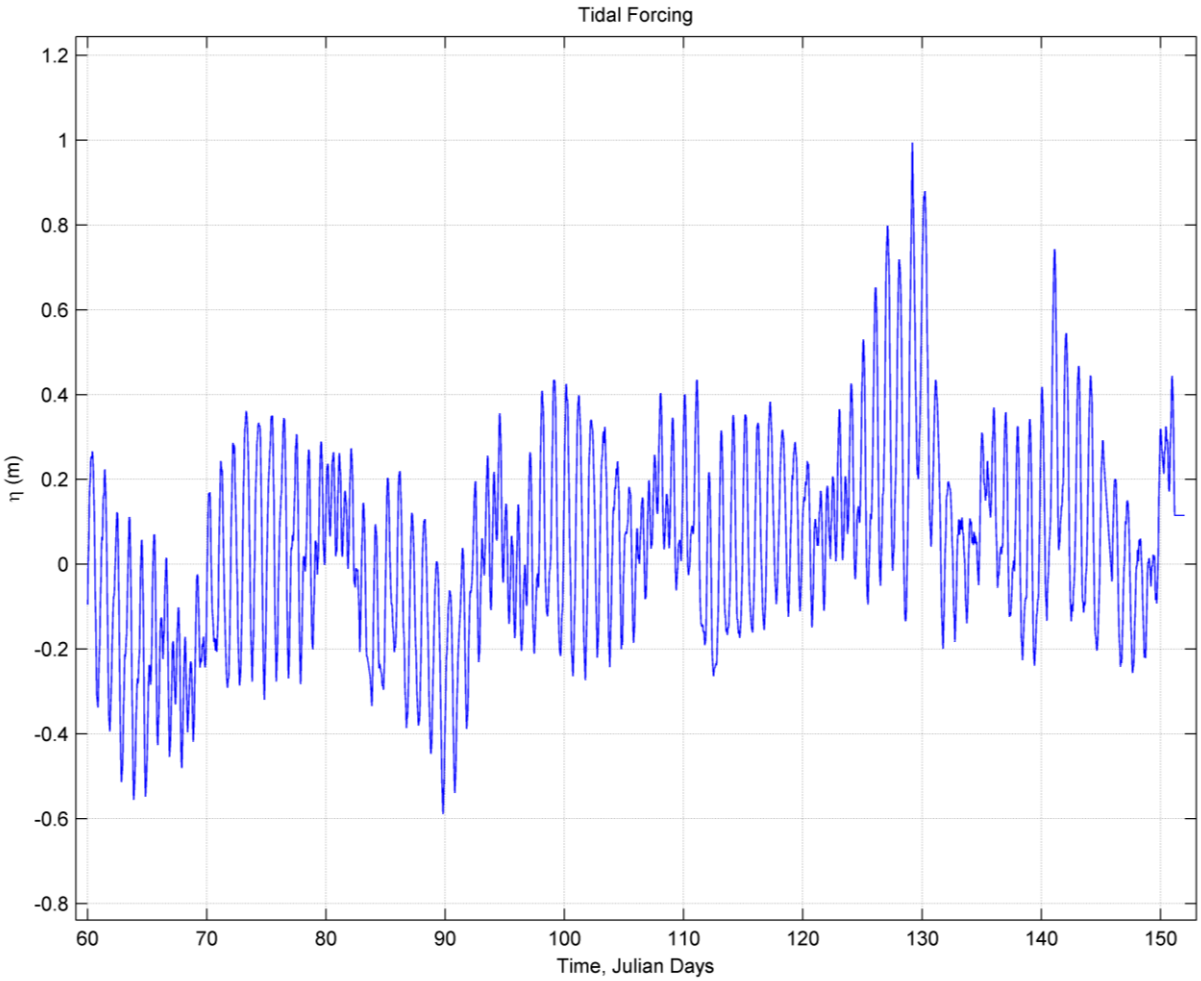

Figure 5-3 Time-series of water level measured at Fremantle during summer/autumn 2004 and applied at the model open boundary.

5.2.2.2 Wind

Forcing due to wind was input using hourly observations of wind from the BOM weather station at northern end of the Garden Island causeway. The wind field was applied as a constant over the domain. During the calibration process, the use of the Garden Island winds as a constant over the domain provided the best match to the measurements.

As identified by the comparison to wind measurements at the southern end of the causeway, The BOM wind station is in a relatively exposed location and a degree of sheltering from the

south-west and east is expected over Mangles Bay. . To investigate the influence of this, sensitivity analyses were undertaken using wind records based on the results of measurements undertaken near the site (see Section 7.3).

5.2.2.3 Atmospheric Forcing

Atmospheric fluxes were applied in the model and required input of relevant metrological information including air temperature, dew point temperature, relative humidity, atmospheric pressure, and incident solar radiation. All of this data except incident solar radiation was measured at the Garden Island BOM weather station and used for the study. Incident solar radiation data for Perth Airport were sourced from BOM for the study, being the closest available data that covered the required modelling periods.

5.2.2.4 Groundwater Inflows

Groundwater influx into the marina is an important input into the model, as it allows the influence of the relatively fresh water seepage on the hydrodynamics to be investigated. The excavated marina will intersect the existing groundwater table and some influx is expected to occur. This flow varies in both magnitude and quality throughout the year, and therefore the loading has a seasonal cycle. ERM were commissioned by Cedar Woods to prepare a groundwater model of the area that included the influence of the marina on local water levels. The predicted flow into the marina for the seasons assessed is summarised in Table 5-1.

Table 5-1 Predicted groundwater flow data for modelled cases

	Flow into the marina
Season	(m^3/day)
Summer	270
Autumn	620
Winter	940

The salinity of the inflowing groundwater was set to 10 pss, based on information also provided by ERM. The temperature of the groundwater inflow was given a seasonal variation based on local water temperature.

Groundwater was fed into the model along the edges of the marina, and not applied over the local coastline. This allowed the effects on the marina to be clearly investigated in isolation of other influences.

The nutrient concentrations that were applied in the tracer modelling are outlined in Section 8.

5.2.2.5 Temperature and Salinity

The open boundary of the model required boundary conditions that were representative of the annual ocean temperature and salinity variations within Perth coastal waters. Temperature and salinity conditions within Perth coastal waters generally follow a seasonal cycle with

highest temperatures and salinities in summer and lowest in winter (DEP, 1996). Time-series of water temperature and salinity measured during 1991 and 1992 at three locations within Perth coastal waters were presented in the Southern Metropolitan Coastal Waters Study (SMCWS; DEP, 1996). Plots of the data extracted from the SMCWS are presented in Figure 5-4. The plots reveal that the mean water temperature over the three locations ranged between 16º and 24 ºC and the mean salinity ranged between 34.5 and 36.5 pss.

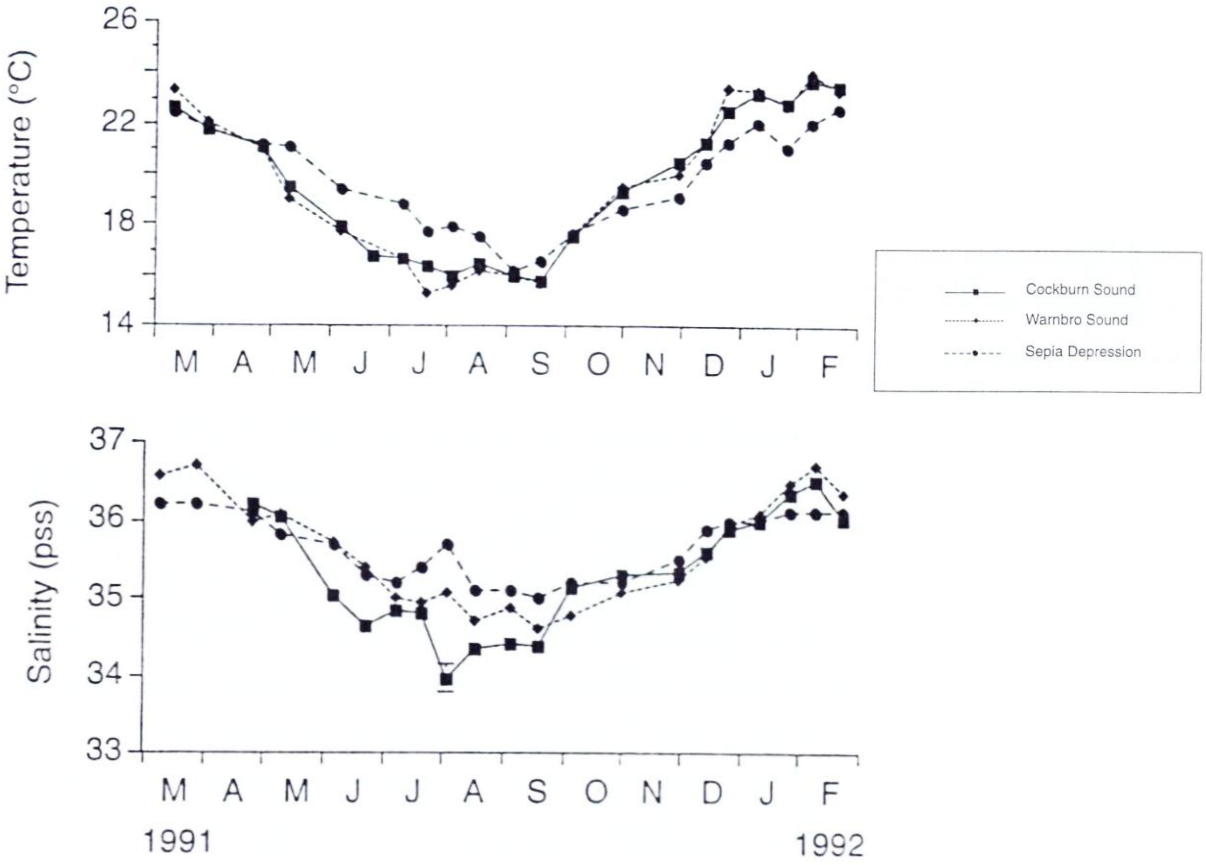

Figure 5-4: Annual patterns of water temperature and salinity measured at three locations in the Perth Coastal Waters Region during 1991 and 1992 (DEP, 1996).

The mean of the data over the three locations was used to develop an annual time-series of temperature and salinity for application to the open boundary in the model, thus allowing an effective transition between the seasons in the model.

The models for each season were initialised with constant salinity and temperature fields set to according to the appropriate value from the annual time-series developed for the open boundary. Horizontal and vertical gradients then developed during the model warm-up and simulation period.

5.3 Model Validation

5.3.1 Comparison to fixed point ADCP measurements

Following the setup of the model and initial trialling, a series of simulations were undertaken using a variety of forcing data. These simulations focussed primarily on determining the best approach to take with specifying the water level and wind boundary conditions in order to get the best comparison with the measurements. The first ADCP deployment when the instrument was at the Mangles Bay location from February 10 to March 11, 2011 was used for comparison.

The outcome of these trial simulations was that applying the un-modified Garden Island wind record across the domain together with the measured water levels at Fremantle at the offshore boundaries produced the best match to the ADCP record. The use of the modified Garden Island wind record produced currents that were in general too weak in the dominant current directions, indicating that wind acting over the wider Cockburn Sound influenced circulation in Mangles Bay. An attempt to use tidal forcing data from a larger scale regional model failed to reproduce both the observed trend in water level and local current directions within Mangles Bay. This was not surprising given the findings of Rose (2001) who highlighted the strong role of long period water level forcing on regulating exchange through the Causeway.

The resulting comparison for the first deployment period is presented in Figure 5-5 (time-series) and Figure 5-6 (statistical comparison). Figure 5-5 shows the comparison of the elevation, current speed and current direction time-series, together with the measured wind (Garden Island) during this period. The modelled elevation is shown to be a good match to the measured data; however the shortcomings of using the Fremantle measurements are apparent in the small amplitude errors seen in the record. Note that the majority of the elevation error is likely to be due to the accuracy of the measured depth at the deployment sites.

The current speed and direction time-series show qualitatively that the model produces an adequate match to the trends in both speed and direction for the majority of the time. Several short term peaks have been either missed or are under-represented and these are possibly due to local wind variations in either speed or direction near the measurement site. The direction is particularly well represented for the majority of the period.

Several important features of the measured current record have been replicated by the model. The transition between the moderate easterly wind conditions to the strong summer seabreeze pattern has been captured well (see February 27 through to the end of the record, March 11). Also the anticlockwise rotation of the current direction during some of the higher tidal ranges (see February 18 and March 2 and 3 for example) has been captured at a time where the modelled current speeds are also very well matched.

Figure 5-6 presents a comparison of the statistical summary data from the measured and modelled records. The roses show the expected excellent agreement in terms of current direction and magnitude, with the comparative occurrence and cumulative occurrence graphs in the lower panels also highlighting the good match to the overall range of current conditions at the site.

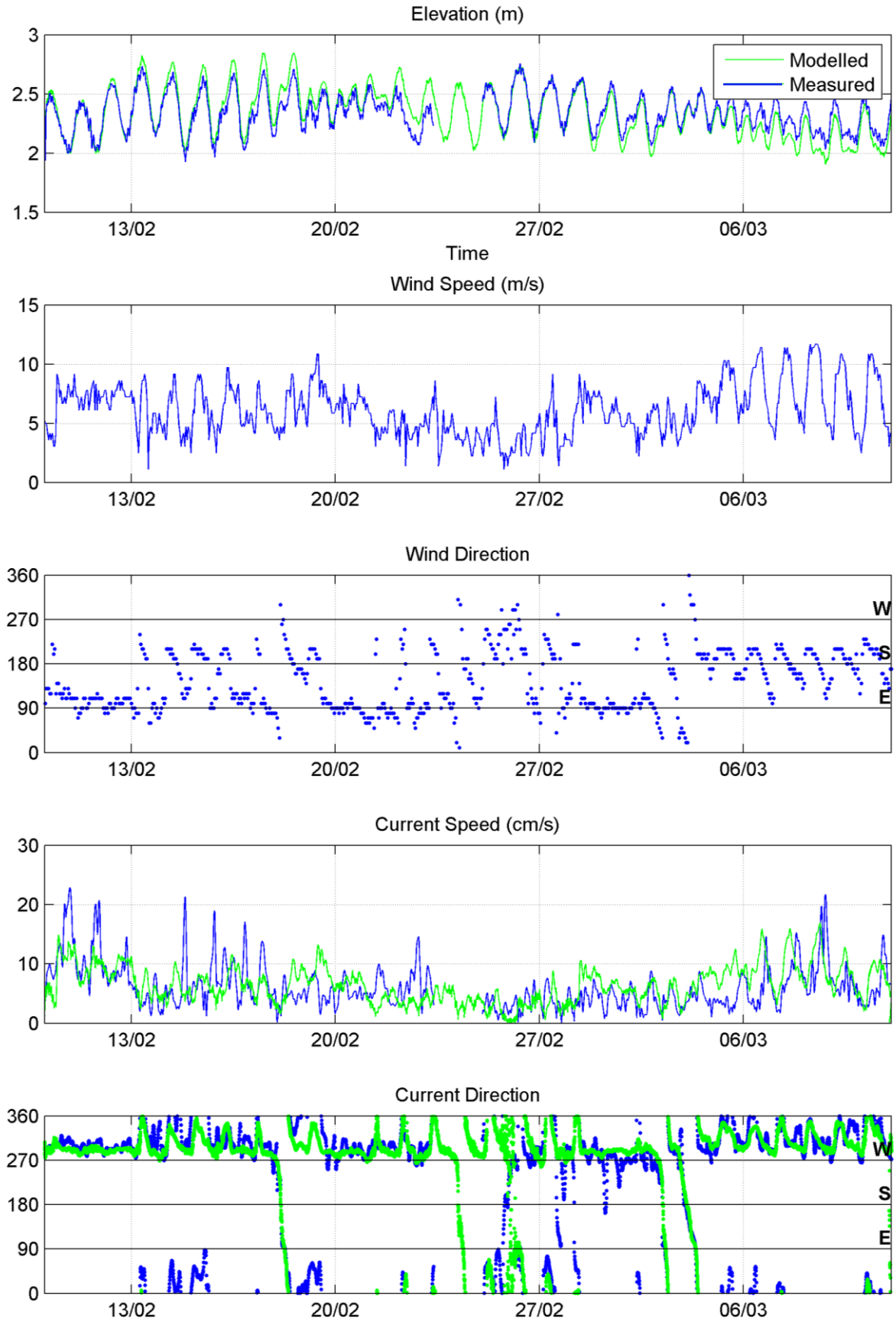

Figure 5-5 Time-series comparison of measured (blue) and modelled (green) elevation (top panel), current speed (4th panel) and current direction (bottom panel) for Deployment 1 (February 10 to March 11, 2011). Measured wind data (BOM) also shown on the second and third panels.

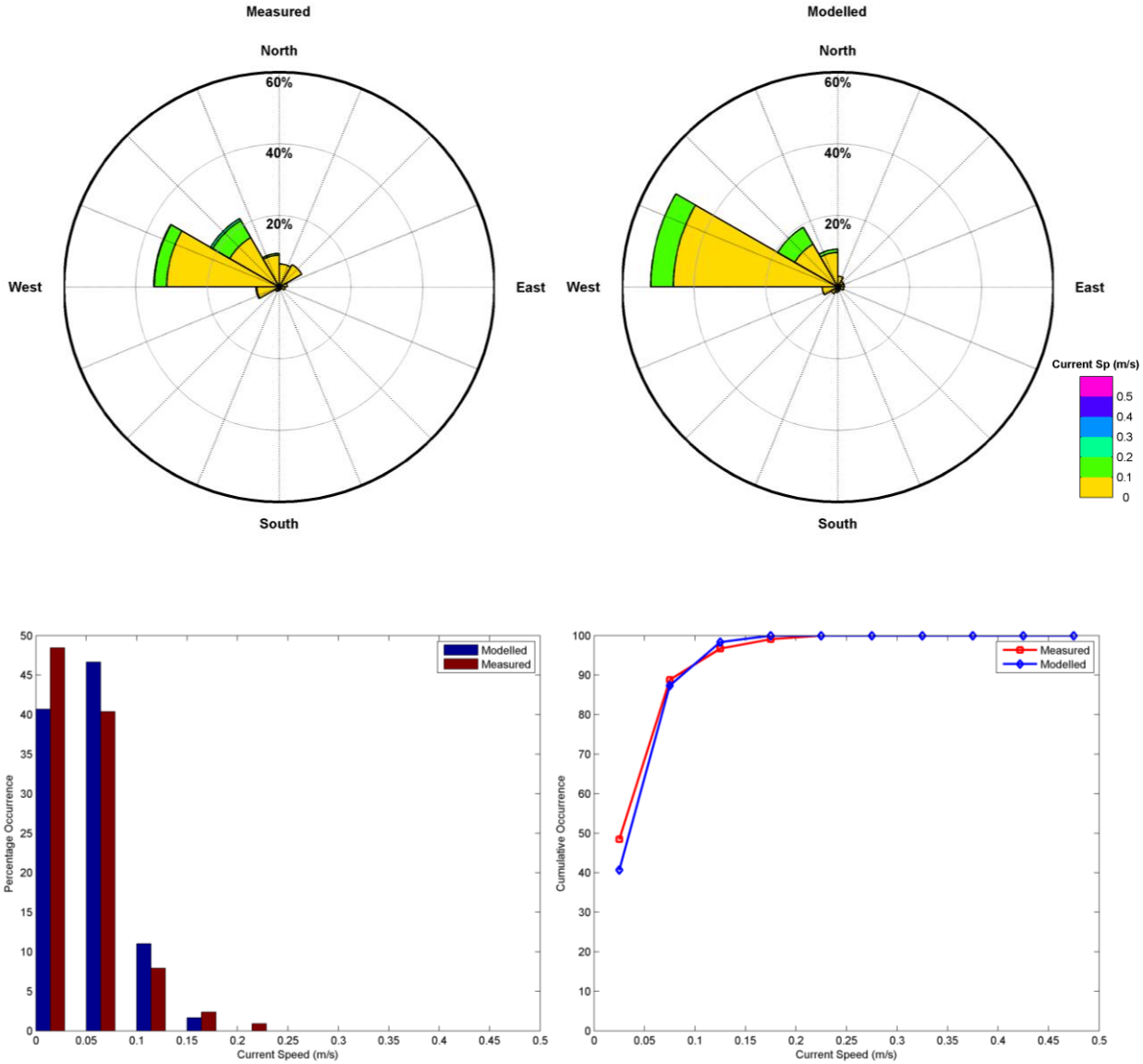

Figure 5-6 Comparison of measured and modelled current roses (top left and top right) and the percentage occurrence and cumulative occurrence for Deployment 1 (February 10 to March 11, 2011).

The comparison for the second deployment period is presented in Figure 5-7 (time-series) and Figure 5-8 (statistical comparison). Again, the elevation, current speed and current direction comparisons are presented with the measured wind data at Garden Island during this period. It is immediately clear that the time-series comparison at this location is not as good as that achieved at the Mangles Bay location.

The field measurements show a very complicated current regime at this location, where the flow can persist as either an inflow or outflow for periods of several days, independent of the tide. This appears to be a general response to longer period sea level fluctuations, where flow in general was into Cockburn Sound, when the mean water level was decreasing, and out of Cockburn Sound, when the mean water level was increasing.

A similar phenomenon was observed by both Rose (2001) and Pattiaratchi (2002) during investigations of the flows through the northern Causeway entrance. This highlights the importance of including longer period and larger scale water level oscillations, as the gross exchange through the Causeway appears to be driven in almost equal measures by tidal and longer period fluctuations of similar amplitude.

The lack of suitable boundary condition that included these long period variations presents an obvious weakness in the model setup. However it is important to note that while the true time comparison of measured and modelled data shows significant disparity at times (for example predicted tidal flood and ebb flow versus persistent inflow), the model produced a current regime that exhibited consistent directional and speed regimes when compared to the measurements (Figure 5-8).

The model was also able to produce periods where outflow persisted through multiple spring tidal cycles during a period where the gradual rate of increase in mean water level was well represented (see the period from March 14 to March 17). It is also shown that the model is able to represent the varying direction of rotation as the flow turns from inflow to outflow – sometimes the current vectors rotate in a clockwise fashion, and other times in an anti-clockwise fashion. Similar high frequency responses are also seen in the modelled record.

Given the model comparison to the Mangles Bay location, which exhibited a much stronger correlation with the prevailing wind conditions, and the findings of Pattiaratchi (2001) who also found that currents in northern Mangles Bay were strongly correlated with the wind at Garden Island, it is expected that the conditions at the Causeway are localised. Nevertheless, the ability of the model to demonstrate some of the main features of this complex flow, albeit at differing times to the measurements, suggests that the flow conditions near the marina entrance are suitably represented by the model for the study purposes.

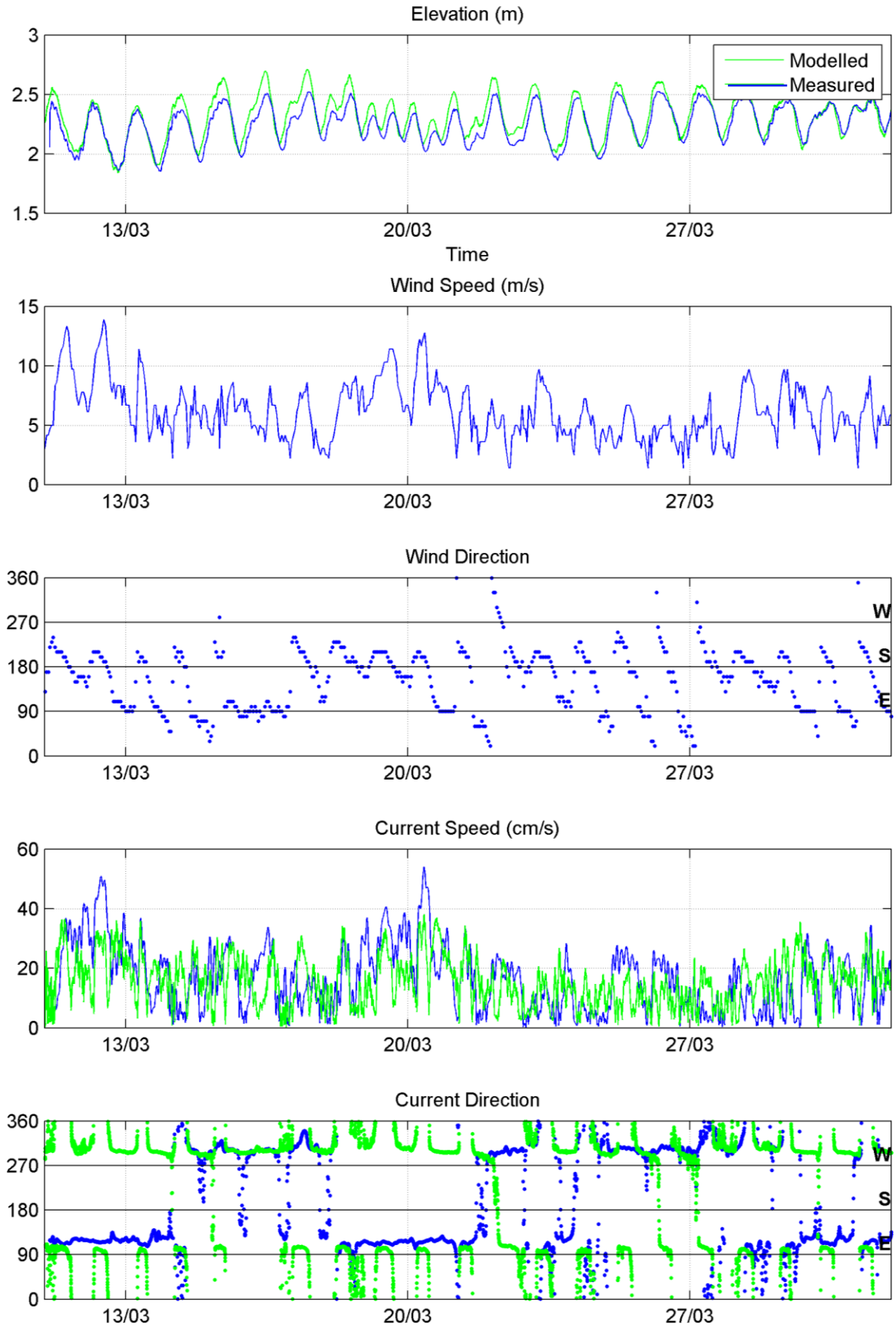

Figure 5-7 Time-series comparison of measured (blue) and modelled (green) elevation (top panel), current speed (4th panel) and current direction (bottom panel) for Deployment 2 (March 11 to April 7, 2011). Measured wind data (BOM) also shown on the second and third panels.

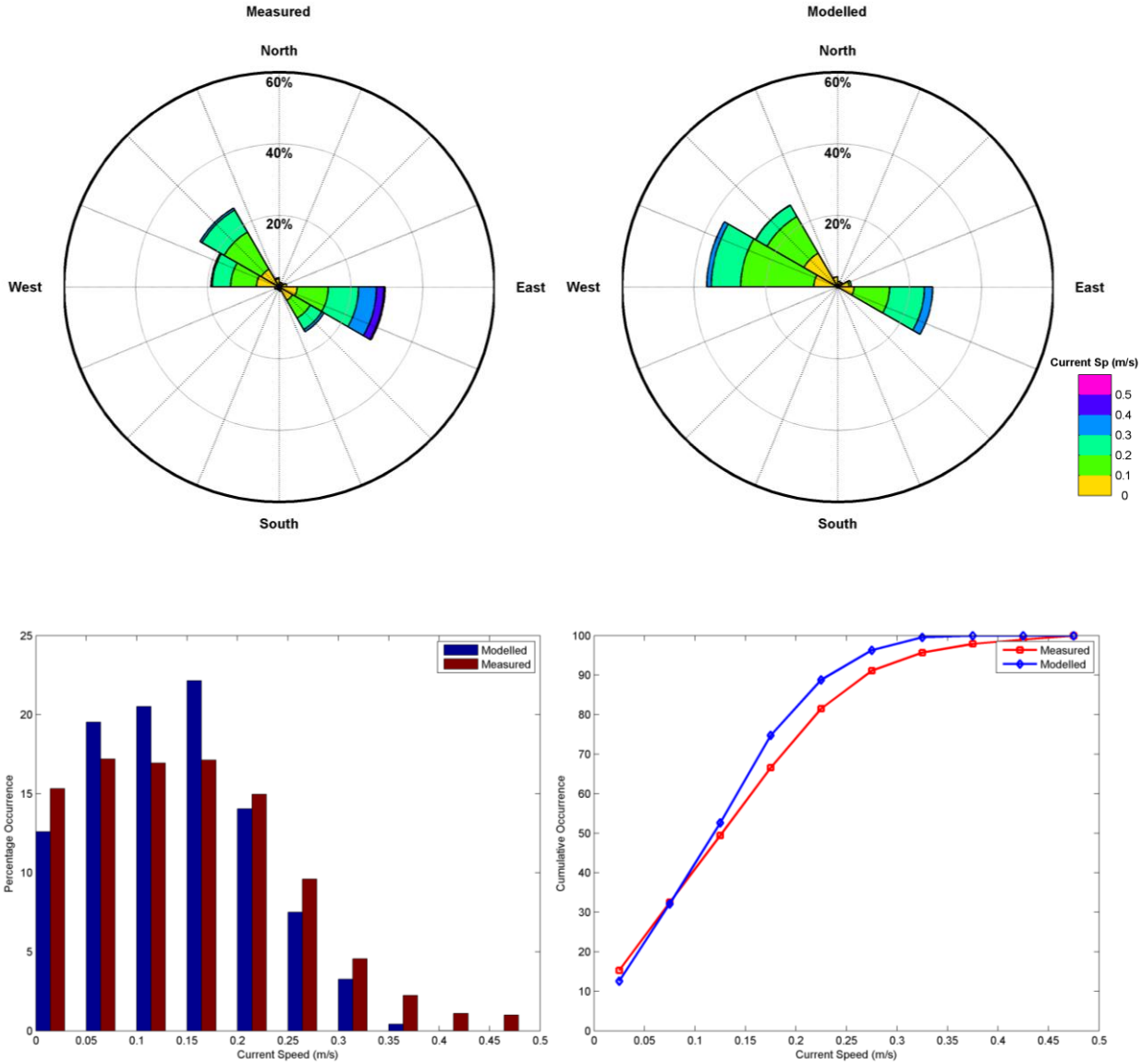

Figure 5-8 Comparison of measured and modelled current roses (top left and top right) and the percentage occurrence and cumulative occurrence for Deployment 2 (March 11 to April 7, 2011).

A quantitative analysis of the model skill at replicating the water temperature was conducted through the use of the Index of Agreement (IOA), presented in Willmott (1981) and the Mean Absolute Error (MAE), which is discussed in Willmott (1982) and Willmott and Matsuura (2005).

The MAE is simply the average of the absolute values of the difference between the observed and modelled value. The higher the MAE, the lower the quality of agreement between the data sets. The Index of Agreement (IOA) is determined by:

$$\mathrm{IOA} = 1 - \frac{\sum |X_{\mathrm{model}} - X_{\mathrm{obs}}|^2}{\sum \left(|X_{\mathrm{model}} - \overline{X_{\mathrm{obs}}}| + |X_{\mathrm{obs}} - \overline{X_{\mathrm{obs}}}| \right)^2}$$

In this equation, *X* represents the variable being compared and $\overline{X}$ the time mean of that variable. A perfect agreement can be said to exist between the model and field observations if the index gives a measure of one, and complete disagreement will produce an index measure of zero (Willmott, 1981). While it is difficult to find guidelines for what values of the IOA might represent a good agreement, Willmott *et al* (1985) suggests that values meaningfully larger than 0.5 represent good model performance. Clearly, the higher the IOA and the lower the MAE, the better the model performance.

The results of the IOA and MAE analysis for both of the deployment periods are given in Table 5-2. The results reflect the observations made above in that the overall match during Deployment 1 was of a higher quality than Deployment 2, with the directional comparison weakest at the causeway site during Deployment 2. However, IOA for each of the records was above 0.5 and as discussed above, the overall representation of the range of conditions at the sites is consistent with the measured ranges.

Overall the model provides a suitable basis for use in the assessment of the flushing performance of the proposed marina, given that the modelled conditions in the near-shore zone where the marina meets Mangles Bay will be similar to those expected in the field.

Table 5-2 Summary of quantitative model skill assessment

	Water level (m)	**Current Speed (m/s)**	**Current Direction (degrees TN)**
Deployment Period 1			
Index of Agreement (IOA)	0.87	0.66	0.94
Mean Absolute Error	0.08	0.03	34
Deployment Period 2			
Index of Agreement (IOA)	0.94	0.58	0.69
Mean Absolute Error	0.07	0.09	93

5.3.2 Comparison to drogue measurements

In addition to the fixed point comparisons undertaken above, the drogue measurements undertaken on the four days in February, March and April (see Section 3.2) were used to assess the performance of the model. The modelled current fields for each of these days were used to advect a numerical drogue or drifter over the same period of time that the measurements were undertaken. This allows the drogue track to be directly compared, providing an indication of the quality of the model performance in a lagrangian (moving with the flow) sense.

The result of the comparison for each of the days is presented in Figure 5-9. The Day 1 tracks were very well represented, with the orientation of the flow direction replicated and the magnitudes of the displacement only slightly underestimated. Some minor drift between the measured and modelled directions is likely due to either wind drift acting directly on the drogue or due to the coarse nature of the bathymetry in the model when compared with the real environment.

The Day 2 comparisons were again quite good with the exception of release 2, where the model predicted very little movement while the drogue was observed to drift towards the east. The comparisons were also reasonably good on Days 3 and 4, with the exception of the third release on Day 3 where the currents through the causeway have been over-predicted and for the second release on Day 4 where the flow detail near the causeway barrier has not been replicated.

Overall the comparison is good, and in general the flow directions in the areas were well resolved, despite the issues observed in the fixed point comparison for the Causeway site.

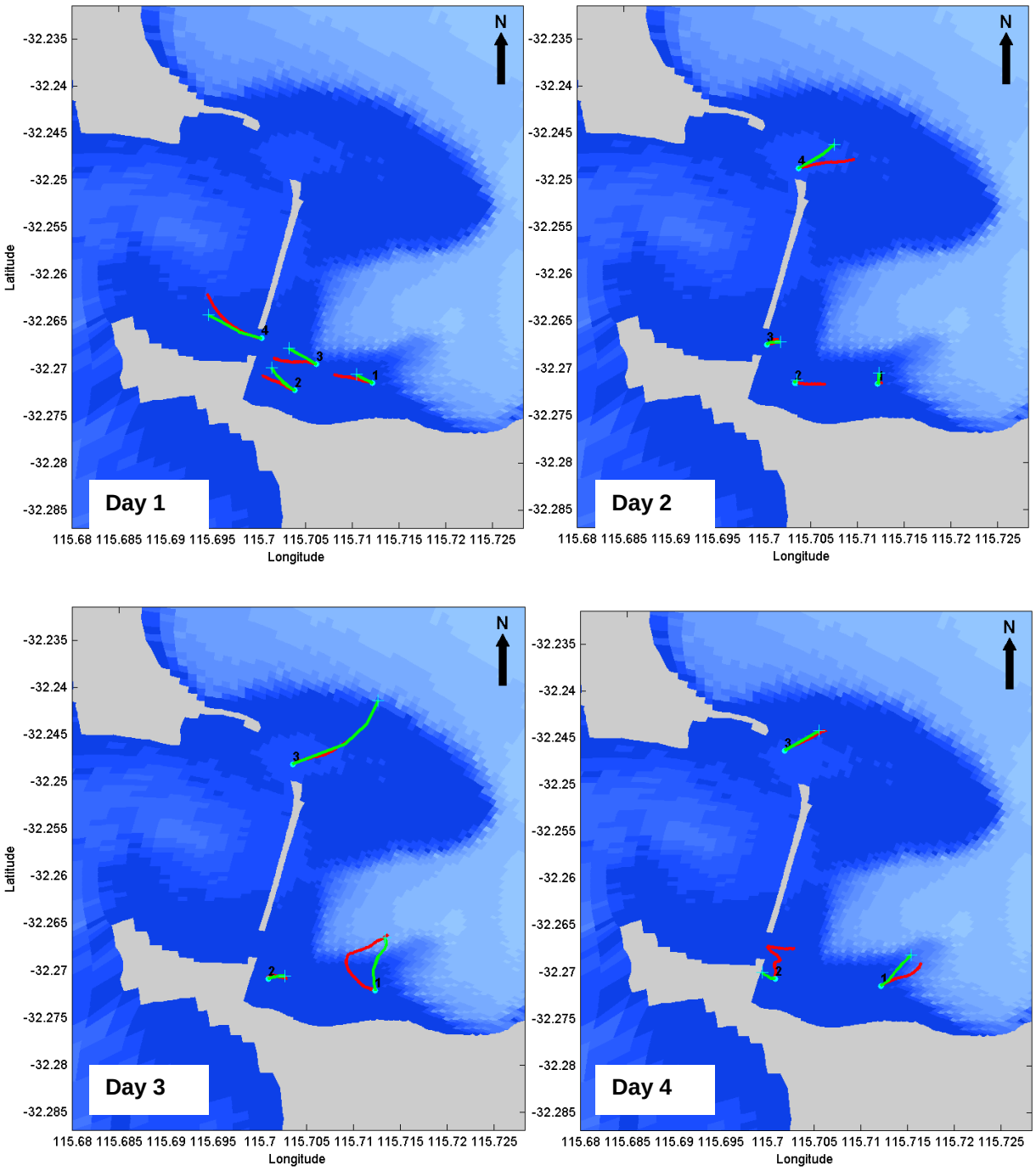

Figure 5-9 Comparison of measured (red) to modelled (green) drogue releases for Day 1 (February 10, 2011 – top left), Day 2 (February 25, 2011 – top right), Day 3 (March 11, 2011 – bottom left) and Day 4 (April 7, 2011 – bottom left).

5.4 Typical Circulation Patterns

Figure 5-10 shows examples of the near-surface current vectors in the south-western region of Mangles Bay. The region of strong currents to the east of the Causeway is shown to be highly localised and confined to the openings and the relatively shallow area immediately adjacent. Current speeds are shown to reach around 0.35 m/s through both openings, consistent with the historical measurements of Pattiaratchi (2002). Calculated current speeds are significantly weaker adjacent to the proposed marina entrance and more variable in direction as indicated by the field measurements.

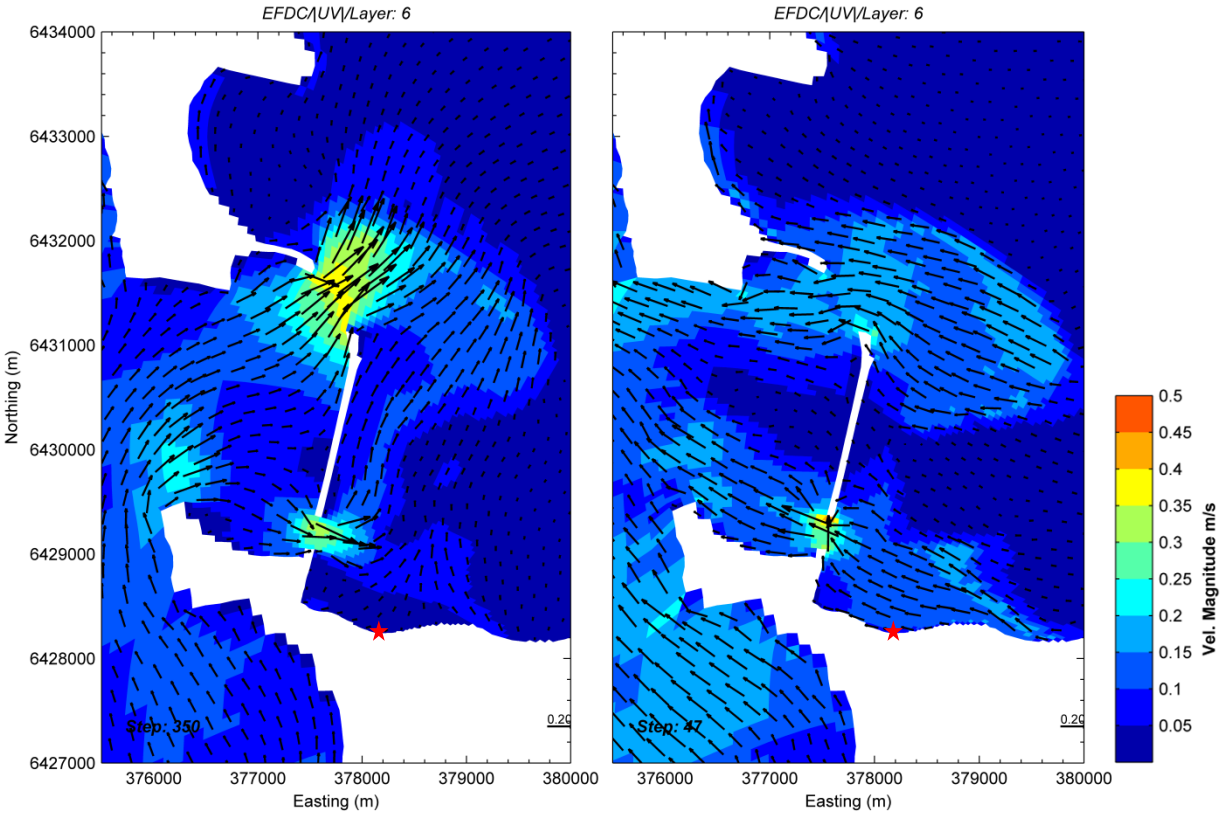

Figure 5-10 Typical current patterns in south-western Mangles Bay during inflow (left) and outflow (right) conditions. The location of the proposed marina entrance is indicated by the red star. The colour scale reflects the relative current speed as per the scale, while the vector arrows point to where the current flow is going.

6 WAVE MODEL

6.1 Introduction

To represent the wave-induced effects on settlement and resuspension of dredged sediment released during dredging of the approach channel, a wave model has been established using the Simulating Waves Nearshore (SWAN) model. The SWAN model was developed to simulate spatially-varying wave conditions over a wide domain, including the Cockburn Sound and Mangles Bay regions. The large size of the wave model domain was required to ensure adequate representation of wave evolution in the regional waters by propagation from offshore.

The model requirements included the competing requirements of both a high spatial resolution, to appropriately represent local variations, and efficient computation over long run-times, to cover the duration of the proposed dredge operation. The need to resolve a large section of complex coastline in the area at different resolutions, combined with the long simulation periods was met by developing and applying the unstructured mesh version of SWAN.

The SWAN model was run by hindcasting spatial wave parameters over the model domain for the period of 1st of January 2003 to the 30th of June 2006, inclusive. This database provided a robust sample from which inter-annual variability could be analysed. The model results have been validated against the available measured wave data, as described below.

6.2 Model Description

The SWAN model is a spectral phase-averaging wave model developed by the Delft University of Technology (Holthuijsen et al, 2001). SWAN is a numerical model for simulating realistic estimates of wave parameters in coastal areas for given wind, bottom and current conditions. The model is a third generation model based on the energy balance equation.

SWAN includes algorithms for the following wave propagation processes: propagation through geographic space, refraction due to bottom and current variations, shoaling due to bottom and current variations, blocking and reflections by opposing currents, transmission through or blockage by obstacles. The model also accounts for the dissipation effects due to white-capping, bottom friction and wave breaking as well as non-linear wave-wave interactions. SWAN is fully spectral (in all directions and frequencies) and computes the evolution of wind waves in coastal regions with shallow water depths and ambient currents.

6.3 Computational Grid and Bathymetry

The computational grid for the SWAN model was set up using the unstructured mesh option. Unstructured meshes, which have varying cell resolutions, provide a much better representation of complex boundaries such as coastlines and areas around islands than do conventional regular grids. The biggest advantage of unstructured meshes is that they

provide the opportunity to concentrate mesh resolution in areas of interest and regions of strong bathymetric variations, to a degree not possible using a regular or curvilinear grid. There is no need for nesting and an unstructured mesh will in general resolve the model area with superior accuracy and with significantly fewer grid points when compared to regular or curvilinear grids. Although the CPU cost per iteration is relatively higher than cases with structured grids, this effect is more than offset by the reduction in the number of grid points.

Selecting appropriate areal extents for the model domain was an important aspect in ensuring that wave propagation to the nearshore region of Mangles Bay was accurately predicted in the model. Capturing wave generation within Cockburn Sound, and diffraction of longer period swells around the edge of Garden Island, would only be possible if the Sound was accurately resolved and the offshore extent was set at a minimum of 30 km from the coast.

The mesh resolution was adjusted in the model to maximise computational efficiency. Generally, the mesh should have higher resolution in areas where the bathymetry or evolution of the waves change rapidly and lower resolution in areas where the physics or depth changes less rapidly. The model resolution in the nearshore zone was also optimised, through a number of trial runs performed using low and high resolution models, to ensure that the model was producing accurate predictions whilst maintaining a high level of run-time efficiency. The final model employed for this study is presented graphically in Figure 6-1.

The bathymetry for the SWAN model was taken from the C-MAP digitized chart database acquired in 2007, the same data set as that used in the hydrodynamic modelling. As indicated in Figure 6-1, the nearshore bathymetry is characterised by a steep slope offshore from below 400 m to approximately 80 m 20km west of Rottnest. It then gradually slopes to 35 m depth near the western edge of Rottnest, with the gradient continuing to 10 m depth to the west of Garden Island.

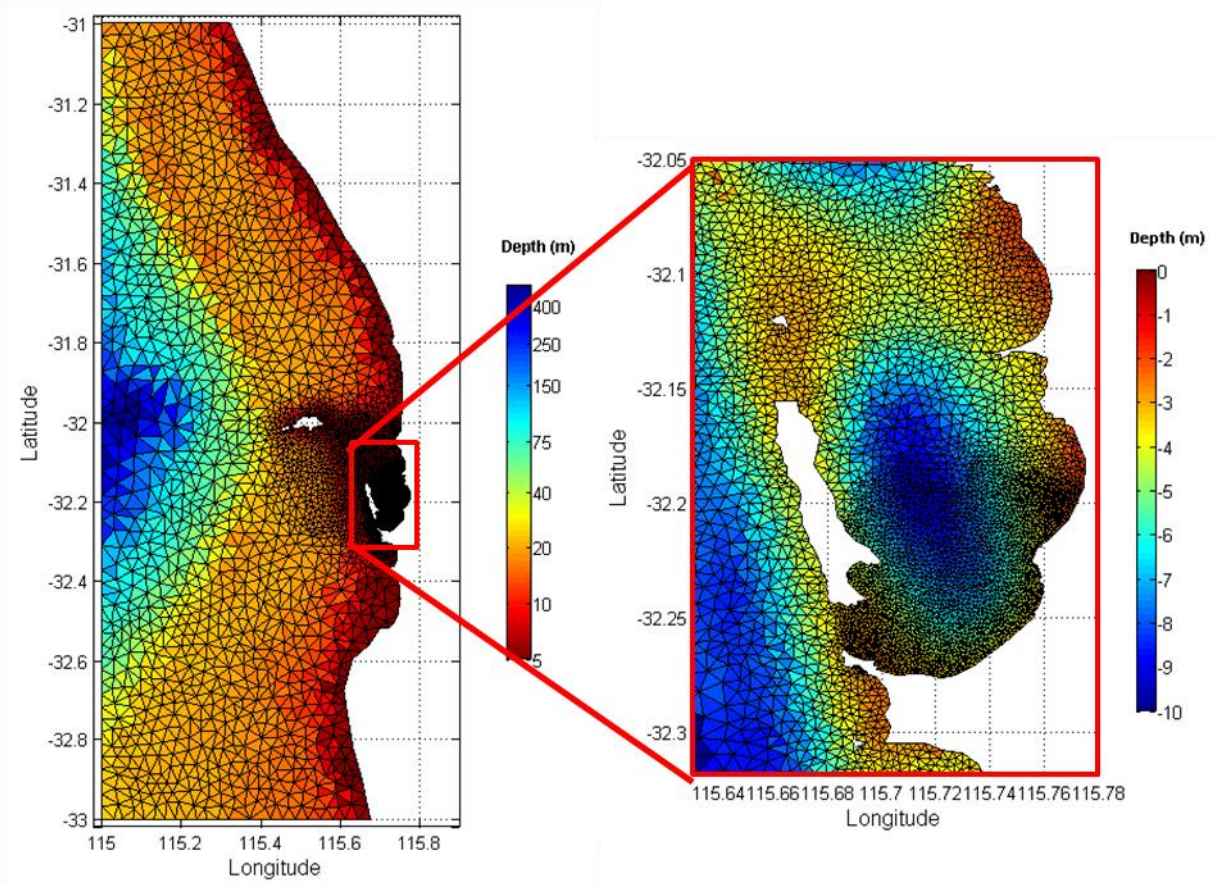

Figure 6-1 SWAN model Bathymetry over the computational mesh. The mesh spans the coast from Lancelin in the North to Preston Beach in the south and offshore to a depth of approximately 450 m. Depths are shown with reference to MSL (please note different scales).

6.4 Model Forcing and Boundary Conditions

6.4.1 Water Levels

Water levels affect the propagation of higher energy swells to the coast and the shoaling of waves in shallow areas. Water elevations over time were derived a tidal prediction using available constituents from the Warnbro Sound location and applied spatially over the entire domain.

6.4.2 Waves

The active offshore boundaries were on the west, north and east of the model domain. The land boundary on the south of the grid absorbs all incoming wave energy. A parametric spectral input (offshore boundary condition) was generated using a standard JONSWAP spectrum. The wave parameters that govern the spectral shape of the JONSWAP spectrum applied at the open boundary are significant wave height (H_s), peak wave period (T_p), peak wave direction (Dir) and the directional spreading of waves (i.e. how 'focussed' the swell conditions are).

The offshore boundary condition was defined by using deep-water wave parameters obtained from the National Center for Environmental Prediction (NCEP/NOAA) WAVEWATCH III (WW3) global wave model. Hindcast wave data is available on a 3 hour time step over a global ocean grid over the range 77°S to 77°N with a longitude x latitude resolution of 1.25° x 1°.

The wave parameters H_s, T_p and Dir were extracted from the WW3 hindcast dataset for the point 32° S; 115° E, the closest and most relevant point to the open boundaries. Care was taken to test the boundaries to avoid the propagation of any errors into the area of interest.

6.4.3 Wind

The same wind dataset as used in the hydrodynamic modelling was adopted for the SWAN assessment. Again these single point-source winds were spatially implemented across the model domain as they represented a good approximation of the total area as described in Section 2.

6.5 Model Parameters

The physical processes selected for the simulations were: white-capping, depth-induced wave-breaking, bottom friction and triad wave-wave interactions. The process of white-capping in the SWAN model is represented by the pulse-based model of Hasselmann (1974), reformulated in terms of wave number to be applicable in finite water depth (Komen *et al*, 1984). The default SWAN parameterisation of depth-induced wave breaking was used with a constant breaking factor of 0.73 (Eldeberky *et al*, 1996b).

Bottom friction was activated using the Madsen model (Madsen *et al* 1988). This formulation is similar to that of Hasselmann *et al* (1968), but in this case the bottom friction factor is a function of the bottom roughness length scale and the wave conditions. The bottom roughness length scale was set to 0.05 m. For modelling the triad wave-wave interaction, SWAN uses the Lumped Triad Approximation (Eldeberky, 1996a) in each spectral direction. Quadruplet wave-wave interaction was also included.

Model output was written on an hourly time-step for the entire computational grid that was later post-processed to obtain wave parameters at the validation sites and to provide suitable input for the sediment fate model.

6.6 Model Scenario

The wave model was run for the conditions required for the sediment fate analysis, which was winter of 2003. Model output was stored hourly for input to the sediment fate model, DREDGEMAP.

7 FLUSHING ANALYSIS

7.1 Background

Flushing is a measure of the rate of renewal of waters within a region. A water body that is efficiently flushed experiences a turnover in water that results in local water quality very near to that of the adjacent source water (in this case the water of Mangles Bay and the Causeway area). Assuming that source water quality meets environmental and aesthetic standards, efficient flushing generally indicates that the adjacent water body will also meet those standards.

The primary mechanisms by which a marina or canal development flushes are generally a combination of the following:

- Tidal driven exchange, where the rise and fall of the tide brings new water into the semi-enclosed water body and then allows mixed waters to be ejected from the entrance. Tidal flushing tends to operate from the entrance to the remote parts of the water body, and the relative length of the water body with respect to the tidal excursion is the main determinant of flushing effectiveness.
- Other water level variations, which can be both longer period than the tide (eg coastally trapped waves, atmospheric pressure induced variations) or shorter (eg localised seiching, long period resonance).
- Wind driven exchange, where the action of the wind on the local water surface can drive currents. Depending on the conditions, two layered flows can be set up where the surface currents and bottom currents are in opposite directions. At other times, vertical mixing due to wind energy input can either promote mixing by dilution over the depth or enhance horizontal dispersion, or retard mixing by increasing the hydrodynamic viscosity of the water column and thus damping other exchange processes.
- Density driven exchange, which is generally due to the effect of night time cooling, where the upper layer of the water column cools more rapidly than the waters below, and a convective flow can develop or due to groundwater inflows setting up density gradients within the enclosed water body. At times of weak winds, these processes can lead to very efficient exchange as the gradients in density (and therefore pressure) are subject to less erosion. In larger water bodies, density driven exchange can result from the effect of evaporation creating salinity and therefore density gradients over time.

All of the above factors have been considered in the modelling process, with a large range of conditions modelled to provide predictions when one or more of the above processes may be important.

The flushing performance of the marina for a series of cases was determined by seeding the water area corresponding to the marina with a conservative dye (concentration only changes by dilution and dispersion) in the model (Figure 7-1). The initial dye concentration was set to 100, representing 100% of an arbitrary contaminant. The flushing time was assessed as the

time it takes for the concentration at a series of locations within the development to reduce to 1/e, or approximately 37% of the original concentration. This is known as the e-folding time and is a timescale that allows bulk flushing performance to be compared between regions of water subject to similar contaminant input conditions.

Many marinas and harbours within Western Australia have e-folding times of up to 7 days, with some exhibiting longer flushing times (14 days or greater) under certain conditions.

7.2 Simulation Scenarios

Simulations were conducted to represent the three identified hydrodynamic regimes in Cockburn Sound/Mangles Bay; being summer, autumn and winter. In this way a wide range of typical environmental conditions at the site was covered. The selection of typical or representative conditions for each regime involved an analysis of more than 10 years of wind data measured at Garden Island by the Bureau of Meteorology. This is the closest, recent, long-term wind record that was available for the study.

The representative periods were chosen based on a statistical assessment of the wind magnitudes to select years consistent with mean conditions. The selected periods were also defined based on achieving a good match with the overall directional roses for that season. A summary of the selected periods is provided in Table 7-1.

Table 7-1: Summary of selected representative periods and the wind statistics for these periods. Bracketed values represent the statistics for that season for all years in the dataset.

Season/regime	Selected Period	Mean Wind Speed (m/s)	75th percentile Wind Speed (m/s)	95th percentile Wind Speed (m/s)
Summer	1/12/05 – 28/02/06	7.2 (7.2)	9.3 (9.3)	12.5 (12.5)
Autumn	1/03/04 – 29/05/04	5.4 (5.4)	8.4 (7.8)	12.3 (11.7)
Winter	1/06/03 – 29/08/03	6.6 (6.3)	9.9 (9.3)	14.3 (13.7)

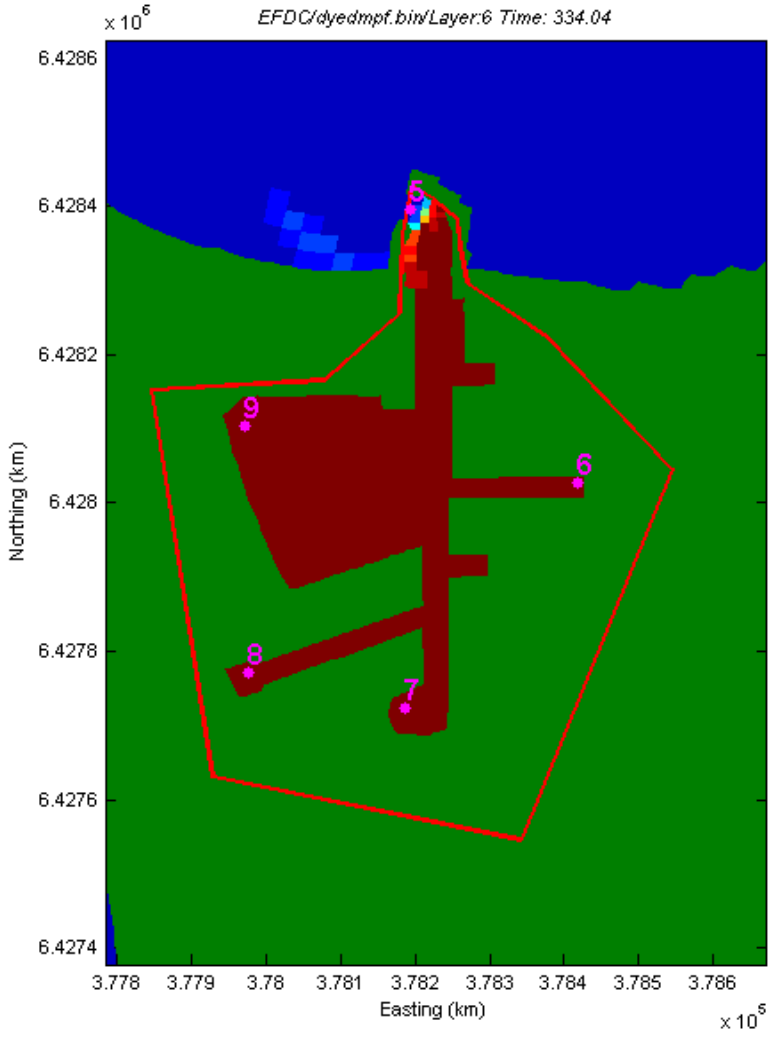

Figure 7-1 Initial tracer concentration within the marina precinct. The locations of the 5 assessment points are shown (points 5, 6, 7, 8 and 9). The red boundary shows the Marina precinct defined in the model.

Table 7-2 Flushing analysis locations (see Figure 7-1 for locations).

Analysis Point Number	Site Name
5	Entrance
6	East Canal
7	South Canal
8	West Canal
9	Marina

Simulations of each season were completed for the marina development case over a period of 60 days. As the flushing time depends on the prevailing conditions, during each of the seasonal simulation periods a range of model flushing tests were completed over differing tidal and wind conditions, as summarised in Table 7-3.

Table 7-3 Flushing scenarios undertaken for existing and developed cases

Season	Scenario	Start Date	Conditions
Summer	1	01-Dec-2005	**Tides** Moderate tides rising to spring range of 0.8 m then dropping to 0.2 m on neaps after 7 days **Winds** Strong seabreeze cycle, SW dominated with weak easterlies Mean wind speed 6.6 m/s
	2	16-Dec-2005	**Tides** Moderate tides rising to spring range of 0.6 m then dropping to 0.2 m on neaps after 7 days **Winds** SW dominated with seabreeze pattern and stronger winds at end of period Mean wind speed 6.9 m/s
	3	31-Dec-2005	**Tides** Spring tides with a range 0.9 m falling to neaps after 5 days **Winds** Strong seabreezes to start followed by weaker and variable direction winds Mean wind speed 7 m/s
	4	15-Jan-2006	**Tides** Moderate tides with range of 0.6 m progressing to neaps with a generally falling mean water level **Winds** Weak winds at beginning before strong consistent seabreeze pattern Mean wind speed 7.7 m/s
	5	08-Dec-2005	**Tides** Neap tides at the start rising to 0.8 m range after 7 days **Winds** Persistent SW winds through most of the period with some seabreeze events Mean wind speed 6.1 m/s
	6	23-Dec-2005	**Tides** Neap tides at the start rising to 1.0 m range after 8 days **Winds** Early SW dominance then very strong winds after 9 days before a variable strength seabreeze cycle Mean wind speed 7.4 m/s

Season	Scenario	Start Date	Conditions
	7	07-Jan-2006	**Tides** Neap tides at the start quickly rising to 0.6 m range for next 10 days **Winds** Consistent seabreeze before sustained easterlies and weaker winds. Mean wind speed 7.1 m/s
Autumn	1	01-Mar-2004	**Tides** 0.5 m range at start, falling to neaps after 7 days **Winds** Moderate to strong seabreeze cycle then weakening winds. Mean wind speed 7.1 m/s
	2	16-Mar-2004	**Tides** 0.5 to 0.6 m range throughout most of the period **Winds** Moderate seabreeze to variable and strong SW winds later in the period Mean wind speed 6.6 m/s
	3	31-Mar-2004	**Tides** 0.4 m range at the start rising to 0.6 m **Winds** Generally weaker winds for most of the period with some light seabreezes Mean wind speed 5.1 m/s
	4	15-Apr-2004	**Tides** 0.4 m range at the start rising to 0.6 m **Winds** Weak seabreezes then sustained NW for a period followed by persistent easterlies Mean wind speed 5 m/s
	5	08-Mar-2004	**Tides** Neap tides at the start progressing to 0.6 m after 7 days **Winds** Clear seabreeze pattern throughout with some scattered easterly events Mean wind speed 5.5 m/s

Season	Scenario	Start Date	Conditions
	6	23-Mar-2004	**Tides** 0.4 m range at the start increasing to 0.6 m after 7 days **Winds** Strong wind events with a periodicity of around 5 days, mostly from the SW with some N winds Mean wind speed 7.1 m/s
	7	07-Apr-2004	**Tides** 0.6 m at the start reducing to 0.2 m after 10 days **Winds** Weak and variable winds from NW to SW mainly Mean wind speed 4.6 m/s
Winter	1	01-Jun-2003	**Tides** Spring tides with range of 0.6 m at start, reducing to neaps with range of 0.2 m with generally falling mean water level **Winds** Episodic strong winds from variable directions Mean wind speed 5.2 m/s
	2	16-Jun-2003	**Tides** Moderate range of 0.7 m at start on a rising mean water level. **Winds** Weak and persistent easterlies for first 8 days, then shifting to W to NW during storms Mean wind speed 6.8 m/s
	3	01-Jul-2003	**Tides** Moderate range of 0.7 m at start with neaps after 6 days **Winds** Episodic W to NW storms Mean wind speed 7 m/s
	4	16-Jul-2003	**Tides** Generally low 0.2 to 0.3 m range for first 10 days, rising to springs thereafter **Winds** Weak easterlies to start then strong storm from SW after 7 days Mean wind speed 5.7 m/s

Season	Scenario	Start Date	Conditions
	5	08-Jun-2003	**Tides** Neap tides with rang of 0.2 m to start rising to 0.8 m springs after 7 days **Winds** Variable then prolonged period of weak easterly winds Mean wind speed 4.4 m/s
	6	23-Jun-2003	**Tides** Neap tides to start with a generally falling mean water level, reaching 0.6 m range after 7 days **Winds** Relatively strong W to NW dominated winds for the most part Mean wind speed 8 m/s
	7	08-Jul-2003	**Tides** 0.3 m neap tides at the start increasing to 0.9 m range after 6 days over a generally falling mean water level **Winds** Strong NW winds over the first 3 days then variable including weak easterlies after 8 days Mean wind speed 6.5 m/s

A further set of simulations for the summer cases were completed to assess the sensitivity of the results to the potential wind sheltering that may occur within southern Mangles Bay. These simulations were conducted for the same periods as those described in the table above, however the wind speeds from the south-west and the east were factored according to the relationships derived through the measurements discussed in Section 3.3. The results of these simulations have been compared with the non-modified summer cases and are also discussed in the following section.

7.3 Results

Flushing times were determined by the time between initialisation and when the proportional concentration at a number of key locations (Figure 7-1, Table 7-2) within the Marina area fell below the e-folding level of 37%. The flushing time was calculated for both the surface and the bottom layers of the water column. In general there was very little difference over the depth; however at times for some sites a difference of 1.3 days was found. The concentration of the bottom waters generally reached the e-folding level slightly before the surface waters were considered flushed. The results are summarised in Table 5-2.

Flushing typically proceeds from near the entrance towards the areas furthest away from the entrance and therefore source water. The longest flushing times are predicted to occur for the West Canal (Site 8), which is the most remote location from the marina entrance (furthest point of this canal is approximately 820 m from the entrance).

Figure 7-2 shows an example time-series of the dye tracer concentration at the analysis sites for one of the winter scenarios (scenario 1). Each plot includes a time-series over a 15 day period for the surface and bottom layer in the model. Figure 7-3 shows an example of the spatial variation of dye concentration at several times through the period of the same scenario. Note that the concentration remains highest for longest further away from the marina entrance.

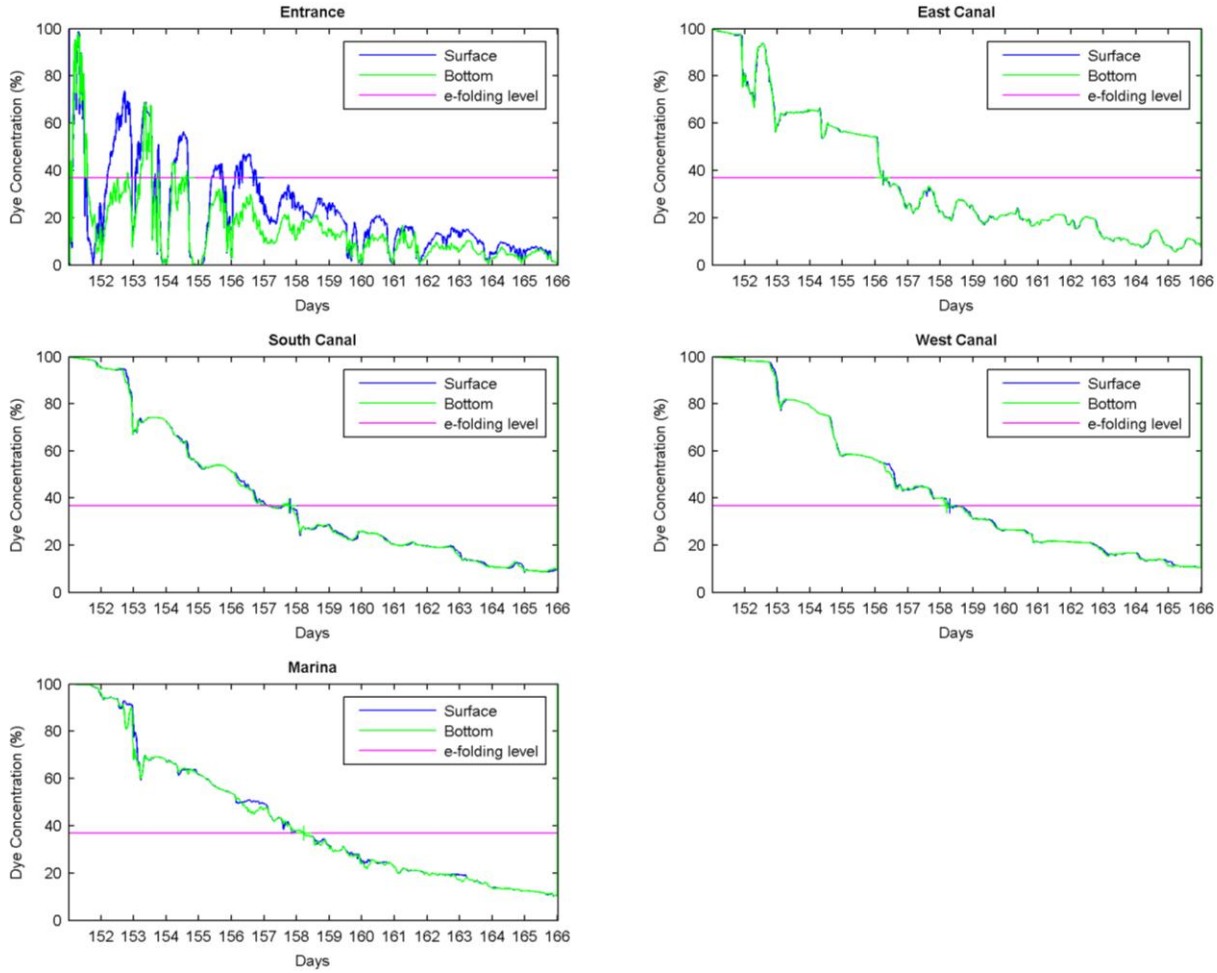

Figure 7-2 Example time-series of dye tracer concentration at 5 sites within the proposed development for winter, scenario 1. Note that the flushing time (time until the blue and green lines drop below the pink level) increases with distance away from the entrance. Also note that the entrance concentration fluctuates over a wide range with the tide.

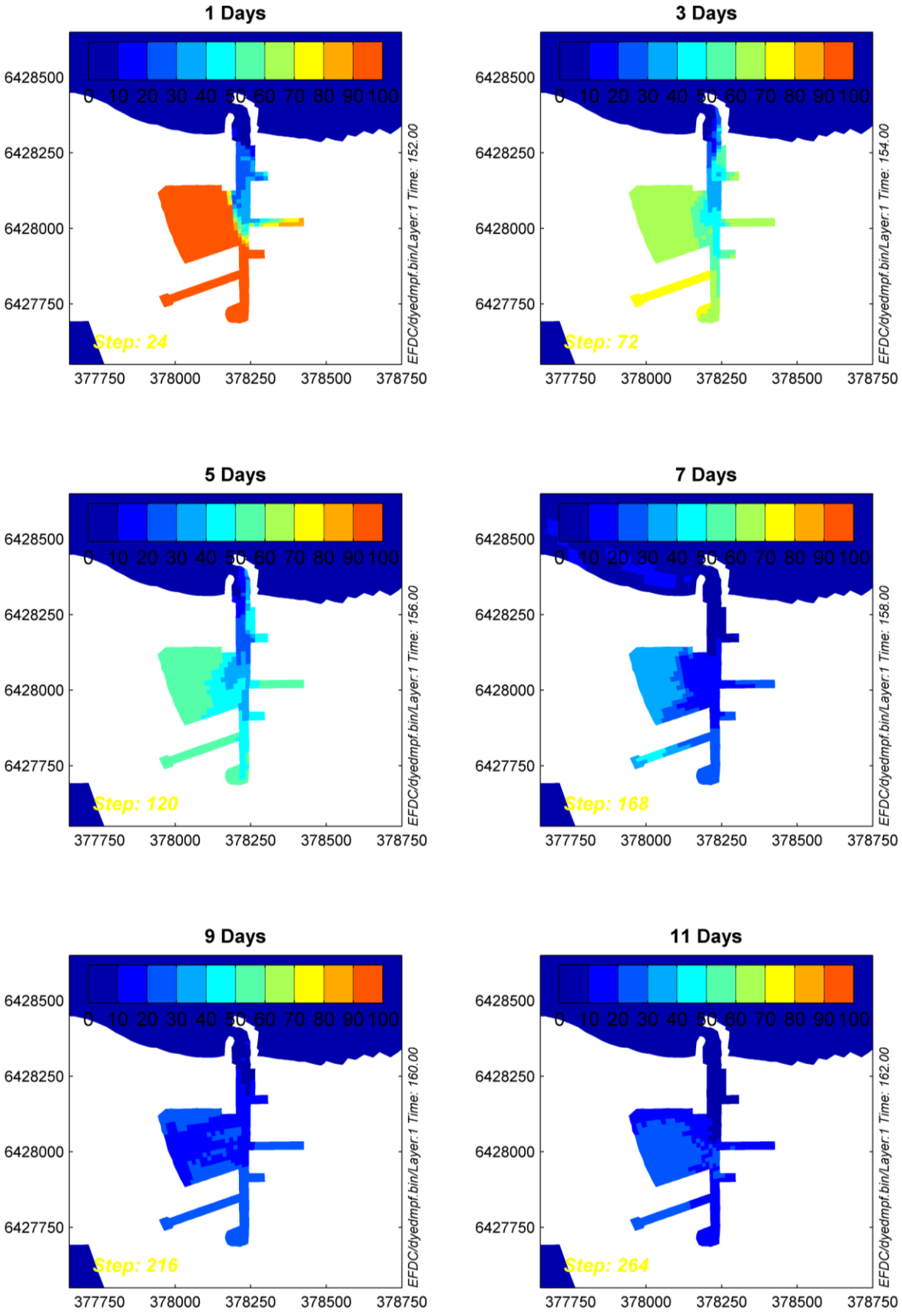

Figure 7-3 Snapshots of the surface layer dye concentration for winter scenario 1 at 1, 3, 5, 7, 9 and 11 days after the initialisation of the initial tracer distribution.

The shortest flushing time was predicted during one of the summer scenarios (4 days for the slowest flushing location; Scenario 4). However, quite rapid flushing times (< 7 days) were also predicted during some of the winter scenarios. Average (± standard deviations) of the maximum flushing times calculated for the back end of the canals overlapped for the seasons, indicating statistical similarity for summer (8.36 ± 2.21 days), autumn (9.91 ± 2.14) and winter (8.30 ± 2.30) cases (refer also to Figure 7-4). However, simulations for the autumn period produced a higher proportion of flushing times exceeding 10 days.

For all the simulations and all of the sites, the median flushing time is predicted to be 6.8 days, with a maximum for the modelled scenarios of 12.7 days. 83% of the flushing time predictions were 10 days or less and 55% of predictions were less than 7 days.

Table 7-4 Flushing times (days) for scenarios undertaken for existing and developed cases. The minimum and maximum flushing times relate to the range across the five analysis sites and the surface and bottom layers (a total of 10 samples in all).

Season	Scenario	Minimum Flushing Time (days)	Maximum Flushing Time (days)
Summer	1	4.0	7.6
	2	4.7	8.5
	3	6.9	10.6
	4	1.9	4.0
	5	6.9	10.5
	6	6.4	8.7
	7	3.2	8.6
		Approximate range	4 – 11 days
Autumn	1	6.8	12.7
	2	3.8	7.7
	3	2.8	10.0
	4	4.6	10.3
	5	6.8	11.5
	6	6.8	10.7
	7	3.7	6.5
		Approximate range	6 – 13 days
Winter	1	3.6	7.3
	2	4.7	11.4
	3	3.4	6.6
	4	4.3	6.4
	5	5.4	11.8
	6	5.3	7.1
	7	4.4	7.5
		Approximate range	6 – 12 days

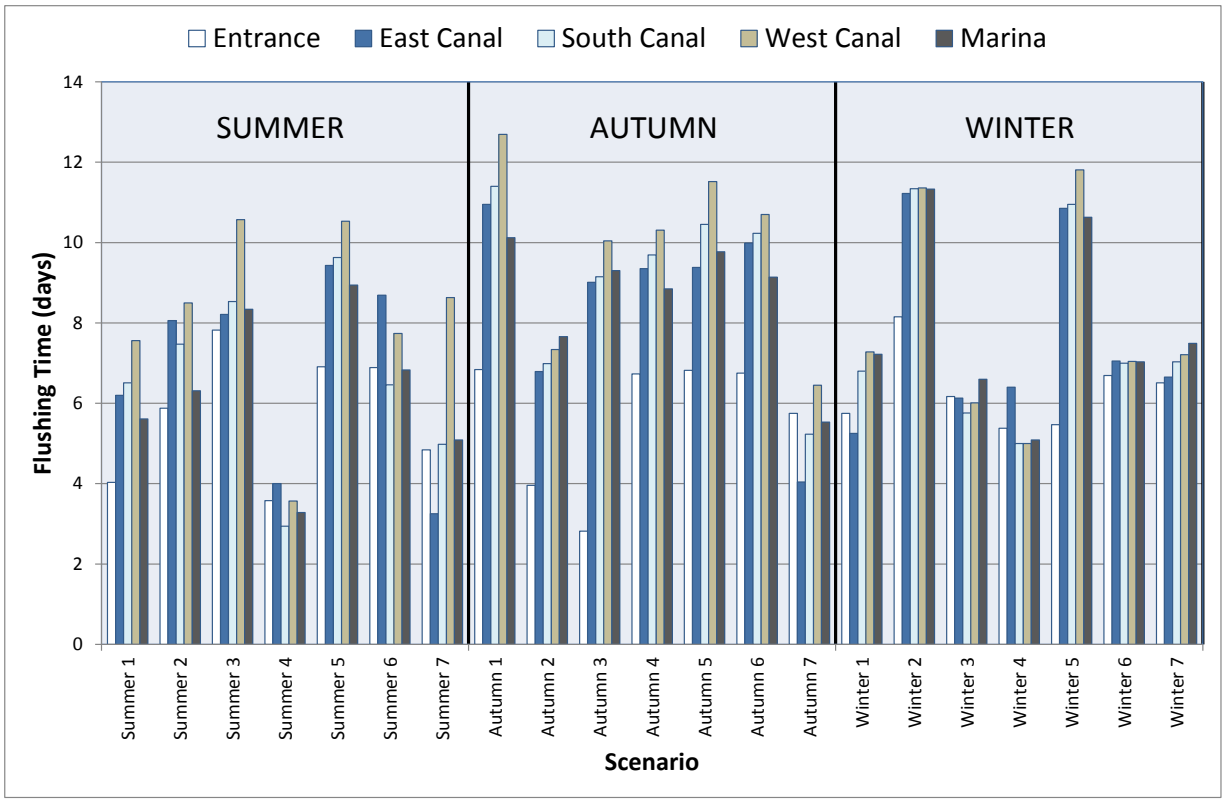

Figure 7-4 Summary of predicted flushing times at the 5 analysis sites across all scenarios modelled.

As noted above, a series of sensitivity tests were completed for the summer cases, applying the factored Garden Island wind record resulting from comparison of the Mangles Bay and Garden Island measurements. Simulations were run for the same 7 cases described above. Summer was selected due to this being the period where winds were most persistent from the directions where the speed variation was most pronounced.

The results showed that, in general, the simulations with the reduced winds generally led to a slightly lower (more rapid) flushing time (data points below the red line in Figure 7-5), by a factor of 10-15%. However, in some cases the flushing time increased (26% of the results), but the maximum flushing time for the summer cases reduced by 0.5 days (from 10.5 to 10) and the median flushing time also reduced (by 1.3 days).

This general reduction is likely to be due to the weaker winds generating less turbulence in the water column, a process that can act as a damping mechanism for the baroclinic flow (see Burling, 1999 for example). Night time cooling, which can create plunging cooler, denser water and groundwater influx are two processes that contribute to baroclinic exchange, which is typically most efficient in the absence of external energy inputs.

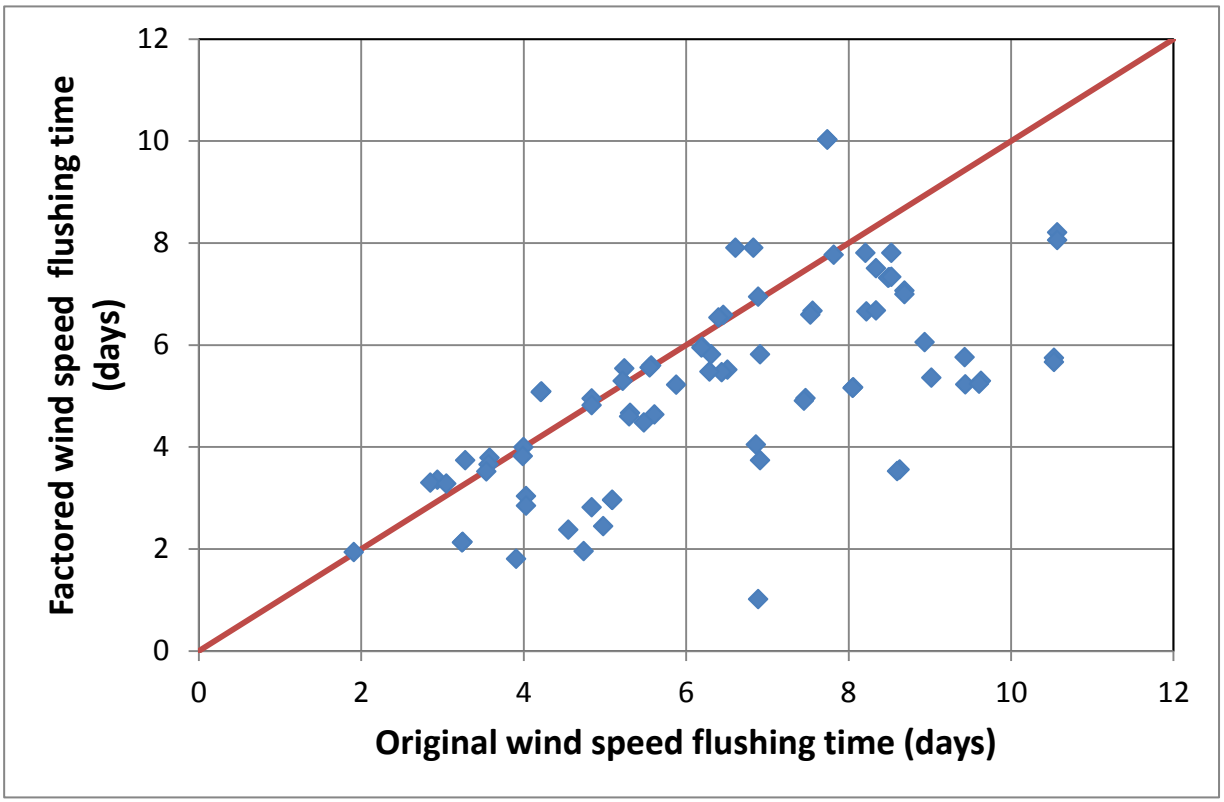

Figure 7-5 Comparison between the factored (Y axis) and original (X axis) flushing time results. The 1:1 parity line is also shown in red. Markers below the parity line indicated a flushing time that has reduced due to the factored wind speeds.

8 NUTRIENT TRACER MODELLING

8.1 Background

While the flushing analysis provides guideline values that can be compared against typical rules of thumb, modelling of the potential long term build-up of contaminants and nutrients provides a more realistic indication of the likely effects. For example, nitrogen and phosphorous provide the necessary building blocks for algal growth, and high availability under favourable meteorological conditions can lead to blooms. By assessing the variation from background values, marine ecologists can infer the likely nature and impact of any change in water quality.

For this study, a series of model tests were conducted to demonstrate the potential effect of the new marina on dissolved nitrogen (DIN) within the development and in the adjacent waters. The intersection of the water table created by the marina allows the infiltration of relatively fresh (compared to the ocean water in the marina) groundwater carrying nutrients and other dissolved substances. The lower flushing rate of the marina compared to adjacent and existing water areas creates the potential for the build-up of nutrient concentrations over time.

8.2 Methodology

Nitrogen and phosphorous were modelled as conservative tracers, a simple but effective approach that is typically used for short to medium term water quality modelling. Although release by sediments and decaying organic matter is ignored in this approach, the uptake by biological processes is also excluded and the results are generally suitable for initial water quality assessments and providing context to the likely effect of hydrodynamic flushing on water quality.

The primary source of nutrients to the southern area of Cockburn Sound is groundwater that percolates along the coastal margin. The groundwater flow varies in both magnitude and quality throughout the year, and therefore the loading has a seasonal cycle. ERM were commissioned by Cedar Woods to prepare a groundwater model of the area that included the influence of the marina on local water levels. This model also allowed the flux of groundwater and the DIN loading into the marina to be evaluated. Table 8-1 shows the modelled ground water flow data, as provided by ERM. Nutrient concentrations for the model were determined by ERM from the average seasonal values from a range of bore samples for coastal station along the Mangles Bay foreshore.

Flow rates are highest during the winter months and lowest during spring/summer. Conversely, nutrient concentrations are typically highest in winter/spring and lower in the other months. Overall, the nutrient load (in terms of total mass per day) is expected to be highest in winter, being 7 times the mass flux expected in summer.

Table 8-1 Groundwater flow (total for marina), concentration and nutrient load data for modelled cases

	Groundwater Inputs		
	Flow	**DIN**	**DIN-load**
Season:	(m^3/day)	(mg/l)	(kg/day)
Summer	270	0.37	0.1
Autumn	620	0.33	0.2
Winter	940	0.78	0.7

A constant background concentration value of 6 µg/l (0.006 mg/l) was assumed, which was based on data provided by Oceanica, and the flux of DIN from the local groundwater system was applied along the marina edges. Groundwater flux was not applied to the adjacent coastline, to allow the potential build up within the marina to be clearly modelled. The selected background values takes into consideration the relatively rapid flushing of the near coastal areas where the measurements were available.

Model simulations were completed for each of the three seasons considered over a 58 day period that included a 28 day warm-up period. Statistical analysis and result presentation was completed for the final 30 days of each simulation.

8.3 Results

Time-series of DIN concentrations were extracted from each of the simulations at a set of 5 output points that covered the interior of the proposed marina (points 5 to 9 on Figure 7-1). Figure 8-1 presents the time-series of DIN concentrations at these locations points for each of the modelled scenarios over the 30-day analysis period.

The time-series plots show an overall seasonal variation in the predicted DIN concentrations within the marina, with smaller amplitude variations occurring due to the variable flushing rate. As expected, there is a general increase in the predicted DIN concentration as points are further away from the entrance. Importantly, the results show that the flushing is expected to be sufficiently effective to prevent the gradual build-up of concentrations over time, with a clear rise and fall in levels as flushing efficiency is weaker then stronger. This suggests that the risk of adverse escalations is relatively low, based on the assumptions made and the input data provided for this study.

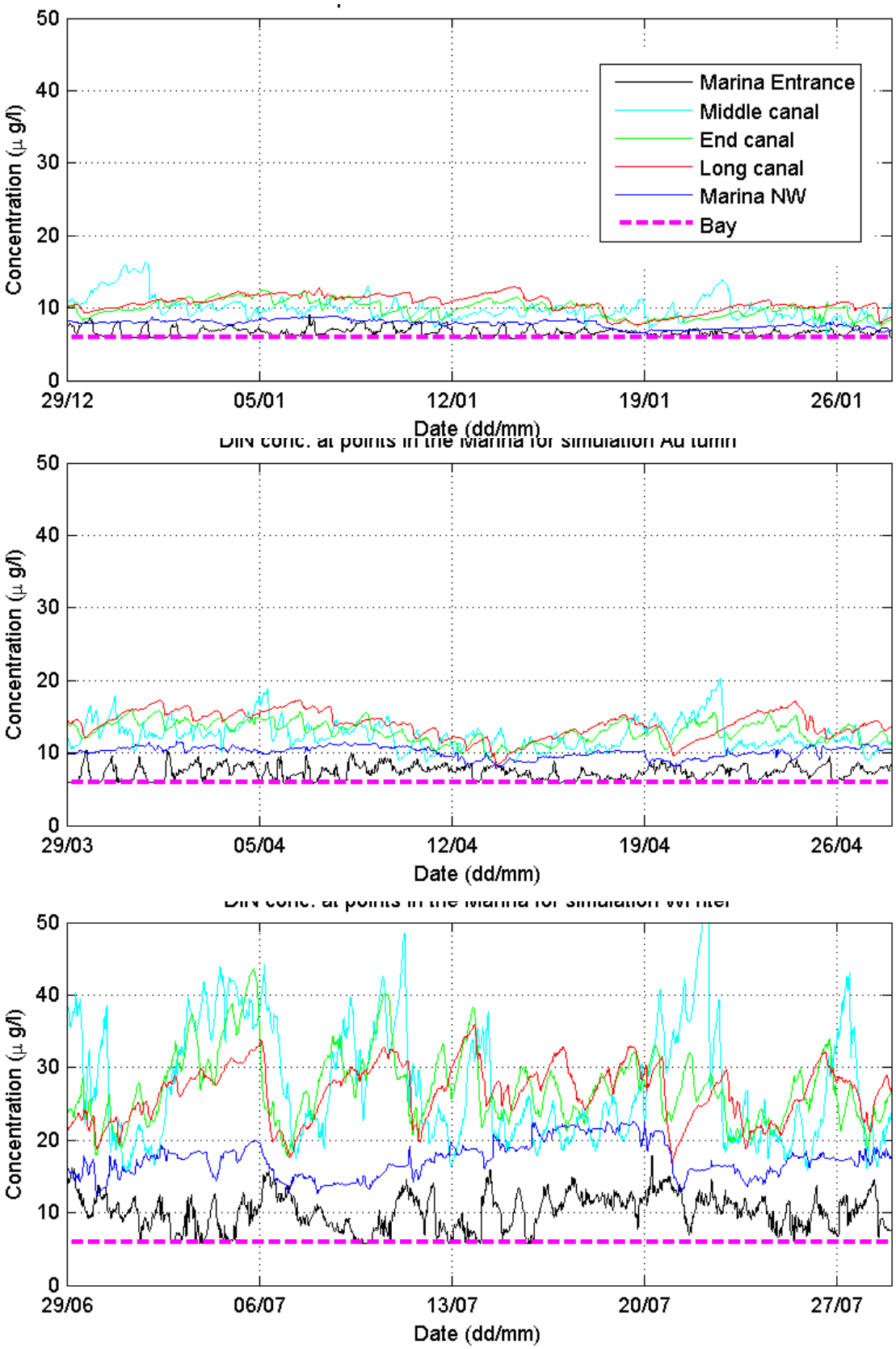

Figure 8-1 Predicted DIN concentrations at sites within the marina for the 30-day analysis period for each seasonal case (summer, autumn and winter, arranged vertically from the top). The background concentration (6 µg/l) is shown by the pink dotted line.

The time series results from each of the seasonal simulations were analysed to define the individual, and comparative median, 80th percentile and 98% percentile of the data. These statistical thresholds are typical of those applied as low risk trigger values (eg ANZECC, 2000) or environmental criteria (eg EPA, 2005). For each run, five sites within the marina were considered (see Figure 7-1), with the average and maximum of the outcomes across the sites presented in Table 8-2.

Table 8-2 Predicted average and maximum median, 80th and 98th percentile DIN concentrations over all marina output points for each scenario. Maximum modelled value for each scenario through the analysis period also shown. Note that the results are presented in µg/l and the background value applied in the modelling was 6 µg/l.

	Average of 5 marina points			Maximum of 5 marina points			Modelled Maximum
Scenario	**Median**	**80th**	**98th**	**Median**	**80th**	**98th**	
Summer	9	12	21	11	15	30	41
Autumn	11	12	14	14	15	18	21
Winter	20	26	34	25	33	44	55

The results show that the DIN concentration is expected to be highest during winter when the loading is highest, with concentrations generally being up to 4 times background. During autumn and summer, the DIN concentration is expected to be generally less than twice the background concentration, based on the values applied in these scenarios. Peak concentrations are predicted to reach 55 µg/l at times. However, these peaks are quickly resolved by increased flushing efficiency as conditions change.

Outside of the marina, there was very little effect on local water DIN concentrations predicted, predominantly due to the efficient flushing of the area by the causeway through flow and the typically prevailing southerly winds.

9 SEDIMENT FATE MODEL

9.1 Introduction

The proposed Mangles Bay Marina development will include an access channel that extends approximately 700m offshore from the entrance to the proposed marina. A key issue for the project is the potential impacts on the ecology of Cockburn Sound from suspended sediment plumes generated by dredging of the access channel. Dredge dispersion modelling has been conducted to determine the potential magnitude and persistence of suspended sediment plumes generated by dredging within the Mangles Bay and wider Cockburn Sound area. The following Section outlines the setup of the model, the methodology used and the model results in terms of total suspended sediment concentrations (TSSC).

9.2 Model Description

Modelling of the dispersion of suspended sediment resulting from the various dredging and disposal operations has been undertaken using an advanced sediment fate model – SSFATE, operating within the ASA DREDGEMAP system. This model computes the advection, dispersion, differential sinking, settlement and resuspension of sediment particles. The model can be used to represent inputs from a wide range of suspension sources, producing predictions of sediment fate both over the short-term (minutes to days following a discharge source) and longer term (days to years following a discharge source).

DREDGEMAP allows the three-dimensional predictions of suspended sediment concentrations and seabed sedimentation to be assessed against allowable exposure thresholds. Sedimentation thresholds often relate to burial depths or rates, while suspended sediment concentration (SSC) thresholds are usually more complicated, involving tiered exposure duration and intensities. As a result, assessing the project generated sediment distributions against these thresholds in both 3D space and time is a computationally intensive task. A variety of SSC threshold formulations have recently been applied in Western Australian coastal waters and at present there is no general guideline.

SSFATE (Suspended Sediment FATE) is a computer model originally developed jointly by the U.S. Army Corps of Engineers Engineer Research and Development Center and Applied Science Associates (ASA) to estimate suspended sediment concentrations generated in the water column and deposition patterns generated due to dredging operations in a current-dominated environment, such as a river (Johnson *et al.* 2000, Swanson et. al. 2000, 2004). ASA has significantly enhanced the capability of SSFATE to allow the prediction of sediment fate in marine and coastal environments, where wave forcing becomes important for reworking the distribution of sediments (Swanson *et al.* 2007).

SSFATE is formulated to simulate far-field effects (~25 m or larger scale) in which the mean transport and turbulence associated with ambient currents are dominant over the initial turbulence generated at the discharge point. A five class particle-based model predicts the transport and dispersion of the suspended material. The classes include the 0 to 130 micron range of sediment sizes that typically result in plumes. Heavier sediments tend to settle very rapidly and are not relevant over the larger time and space scales of interest here. Table 9-1 shows the material classes used in SSFATE.

Table 9-1 Material size classes used in SSFATE

Material Class	Particle Size Range
Clay	*< 7 microns*
Fine Silt	*8 to 35 microns*
Coarse Silt	*35 to 74 microns*
Fine Sand	*74 to 130 microns*
Coarse Sand	*> 130 microns*

Particle advection is calculated using interpolated currents obtained from the hydrodynamic model, integrated over time. Particle diffusion is assumed to follow a random walk process. The Lagrangian approach of calculating transport through a grid-less space removes limitations of grid resolution, artefacts due to grid boundaries and also maintains a high degree of mass conservation.

Following release into the model space, the sediment cloud is transformed according to the following processes:

- Advection in the background three-dimensional current field.
- Diffusion by a random walk model with the mass diffusion rate specified ideally from measurements at the site. As particles represent an ensemble of real particles, each particle in the model has an associated Gaussian distribution, governed by particle age and the mass diffusion properties of the surrounding water.
- Settlement or sinking of the sediment due to buoyancy forces. Settlement rates are determined from the particle class sizes and include allowance for flocculation and other concentration dependent behaviour, following the model of Teeter (2001).
- Deposition of the sediment. Deposition is determined using a model that couples the deposition across particle classes (Teeter, 2001). The likelihood and rate of deposition depends on the shear stress at the bed. High shear inhibits deposition, and in some cases excludes it all together, with sediment remaining in suspension. The model allows for partial deposition of individual particles according to a practical deposition rate, thereby allowing the bulk sediment mass to be represented by fewer particles.
- Potential resuspension of material, governed by exceedence of required shear stress at the seabed due to the combined action of waves and currents. Different thresholds are applied for resuspension depending upon the duration of sedimentation, based on empirical studies that have demonstrated that newly settled sediments will have higher water content and are more easily resuspended by lower shear stresses (Swanson et al 2007). The resuspension flux calculation also accounts for armouring of fine particles within the interstitial spaces of larger particles. Thus, the model can indicate whether deposits will stabilise or continue to erode over time given the shear forces that occur at the site. Resuspended material is released back into the water column to be affected by all of the processes defined above.

SSFATE formulations and proof of performance have been documented in a series of USACE Dredging Operations and Environmental Research (DOER) Program technical notes (Johnson et al. 2000; Swanson *et al.* 2000), and published in the peer-reviewed literature (Anderson *et al.* 2001, Swanson *et al.,* 2004; Swanson *et al.,* 2007). SSFATE has been applied and validated by APASA against observations of sedimentation and suspended sediments at multiple locations in Australia, notably Cockburn Sound for Fremantle Ports and Mermaid Sound for the Pluto dredging project.

9.3 Dredging Project Description and Model Operational Assumptions

9.3.1 Summary of Proposed Dredging Operation

The proposed access channel will extend approximately 700m offshore from the entrance to the marina development; the channel design width is 30 m with additional width for stable batters and the design depth is -3.24 mCD (-4 mAHD). The dredge footprint modelled was as outlined in Taylor Burrell Barnett Town Planning and Design, Drawing 10/033/005B (11/04/2011) – Workshop Outcomes Concept Plan. Figure 9-1 shows the dredge footprint for the proposed access channel with the relevant sediment sampling sites overlain.

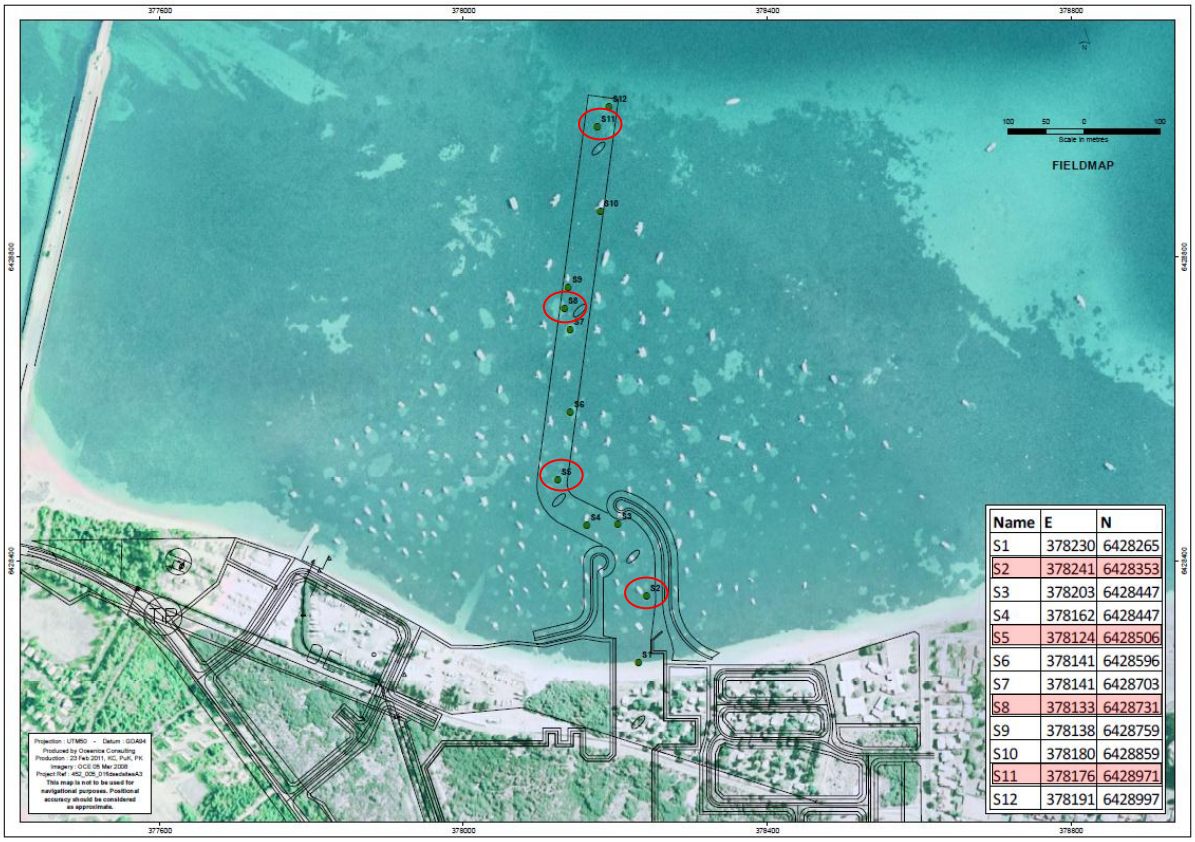

Figure 9-1 Dredge footprint for the proposed access channel (Source: Oceanica). Sediment sampling sites which were used in DREDGEMAP are shown circled in red.

The total volume of material to be removed is approximately 40,000 m^3 using a small cutter suction dredge (CSD) (JFA, 2010). Dredged material will be pumped to onshore settling basins via a floating pipeline and water from the settling basins will be managed through

infiltration, with no tail water released directly into Mangles Bay. Dredging works will commence from the offshore end of the access channel and progress towards the site of the proposed marina development (JFA, 2010).

It is proposed that the dredging will start in early June and run through to early August covering 9 weeks within the winter period. The dredge will operate 6 days each week (Monday to Saturday), working 12 hours per day during daylight hours (nominally 6am – 6 pm). Note that the expected dredging duration assumes minimal downtime for blockages or due to sea state related work stoppages (JFA, 2010). Based on the time required to remove the volume of material a production rate of 62.5 m^3/hr has been assumed for the modelling.

9.3.2 Sediment Characteristics

The sediment characteristics applied in the model were based on the results of sediment sampling conducted along the channel alignment by Oceanica. There were 12 sampling locations along the channel alignment. The samples were laboratory tested by Microanalysis Australia for particle size distribution (PSD) to get an indication of the proportions of each sediment class present in the material to be dredged. Laser diffraction analysis was conducted on the samples from four sites which provided sufficient data distinguish between clay, fine silt and coarse silt. Therefore the sediment samples from these 4 sites at 2 to 3 depths through the dredge zone were used to characterise the dredge sediment for modelling. The sampling locations are presented in Figure 9-1. The PSDs of each of these four sites were used as input into DREDGEMAP.

Table 9-2 presents a summary of the PSD percentages for each of the sediment samples at the 4 sites in terms of the DREDGEMAP sediment classes. Figure 9-2 displays a bar chart of the sediment sample data for each of the sediment classes and Figure 9-3 displays a bar chart of the sediment sample data excluding the course sand proportion so that the proportions of the other classes can be clearly seen. The sediment sample PSD along the channel alignment indicated that the material to be dredged is generally course sand with on average 9% fines (<75 µm). The PSD are relatively consistent along the channel and with depth, however furthest offshore site (11) presented a higher proportion of fines than the other sites particularly in the top and middle samples.

No rock was encountered during the sampling program and it is expected that no cutting will be required during the dredging program.

Table 9-2: Summary of sediment sample PSD (%) with reference to the DREDGEMAP sediment classes. Top, Middle and Bottom define the vertical sampling relative to the local dredge depth, where Bottom refers to the lowest elevation of the expected cut.

	DREDGEMAP Classes (Microns)				
	Clay	**Fine Silt**	**Coarse Silt**	**Fine Sand**	**Coarse Sand**
Sample Location	*0-7*	*7-35*	*35-74*	*74-130*	*>130*
'S2 Top'	1.6	4.8	1.9	2.7	89.0
'S2 Middle'	1.9	3.5	1.0	3.4	90.2
'S5 Top'	1.6	4.6	2.5	1.6	89.7
'S5 Middle'	0.8	1.7	0.8	1.2	95.4
'S5 Bottom'	0.5	1.7	0.9	0.4	96.6
'S8 R2 Top'	2.1	5.1	2.6	2.6	87.6
'S8 R2 Middle'	1.3	2.7	1.0	1.0	94.0
'S8 R2 Bottom'	0.9	2.0	1.1	0.2	95.7
'S11 Top'	6.8	11.4	6.5	8.9	66.2
'S11 Middle'	5.4	7.9	5.4	7.4	73.9
'S11 Bottom'	1.4	2.3	1.7	0.1	94.5

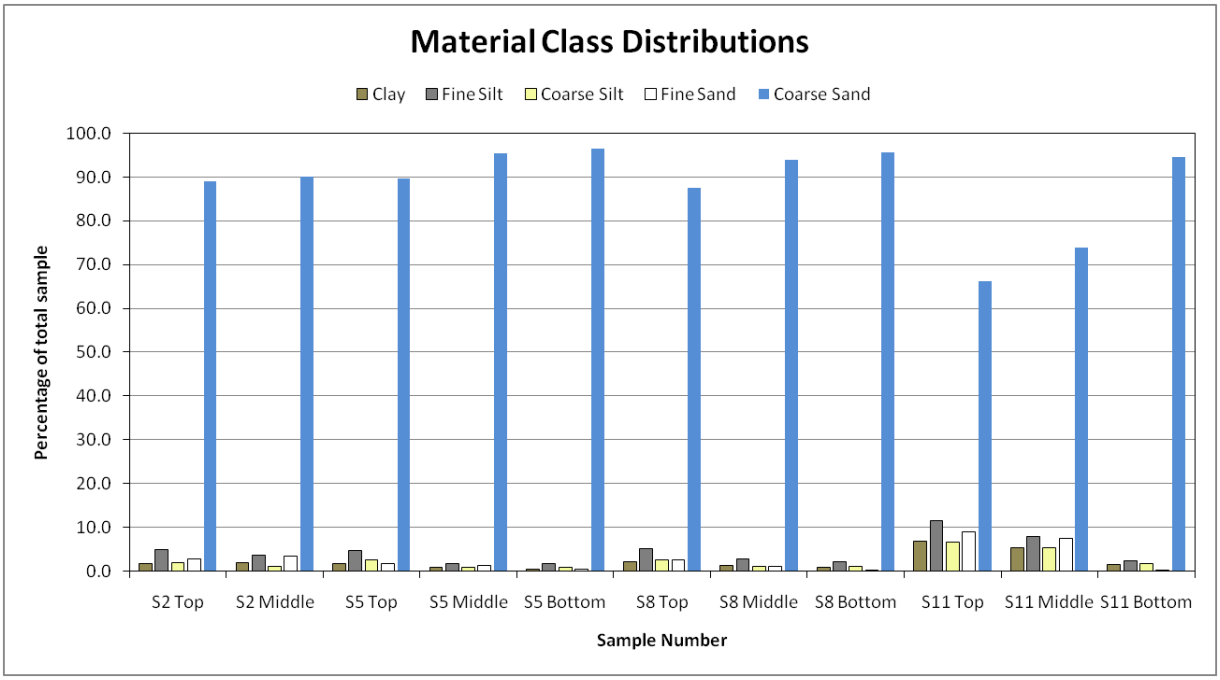

Figure 9-2: Sediment sample material class distributions.

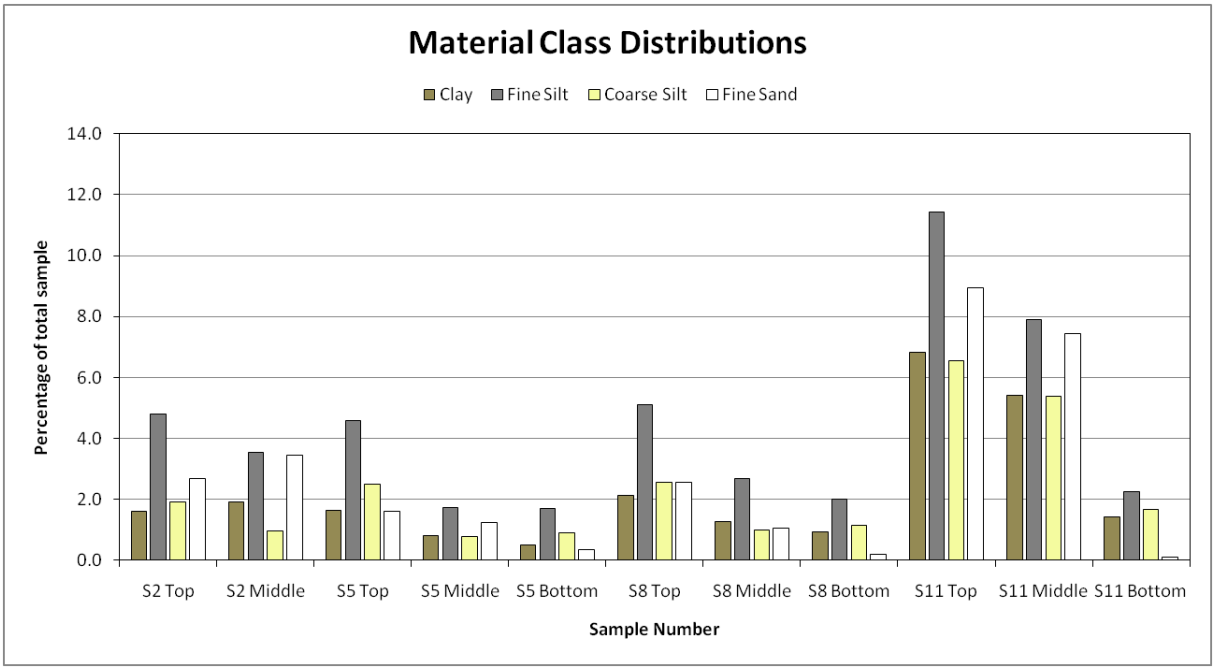

Figure 9-3: Sediment sample material class distribution excluding coarse sand.

9.3.3 Model Sediment Sources

To accurately represent the dredge operations in DREDGEMAP a range of information was provided for the proposed dredging operations including methodology, material types, volumes and production/flow rates. The following section outlines how the provided information was used to represent the dredging operation in the model and any assumptions that were made to supplement the provided information.

It is evident from the proposed dredging methodology that there will be only one source of suspended sediment plume from the direct suspension of material at the cutter head during dredging. In DREDGEMAP each suspected sediment source is defined by its source strength, movement of the source in time, the vertical distribution of sediment that it generates in the water column and the sediment grain-size distribution of the material to be dredged. This section outlines the source parameters that were used in the model to represent the suspended sediment source from the cutter head of the CSD.

9.3.3.1 Source Strength

There is a reasonable amount of literature pertaining to the generation rate of suspended sediment during CSD operations. The volume of material suspended during the CSD dredging is proportional to the production rate. Results from field measurement and empirical models have been presented in Hayes and Wu (2001) and Anchor Environmental (2003). A broad range of source rates have been found, generally being less than 0.5% of the gross production rate (USACE, 2008). In fact, Hayes and Wu quote a maximum source rate of 0.51% from approximately 400 observations, with most rates less than 0.3%. The largest observed rates were apparently from the dredging of very fine sediment with high water content, typical of riverine or sedimentary estuarine conditions, rather than open coastal environments.

Anchor Environmental (2003) quote additional data to Hayes and Wu (2001), citing an average source rate of 0.77% of gross production based on the collected data set. However, the use of a mean in this instance appears to be biased by a select few large values. The median value is closer to 0.3% overall, and inspection of the relevant sediment characteristics shows that the value for sediment that is mainly sand is less than 0.1%. A recent validation model study undertaken for a project in Cockburn Sound found that 0.3% was a suitable input for a large CSD (Fitzpatrick et al, 2008).

For this study, a conservative source rate of 0.5% of the gross production rate has been adopted for the CSD operations.

9.3.3.2 Source Vertical Distribution

Typically in CSD operations material is observed to concentrate in the lower water column, with only small concentrations reaching the surface (Swanson *et. al*. 2004). A vertical distribution closer to the seabed is expected due to the practice of pumping the dredged material away from the dredging site during dredging. Figure 9-4 shows a typical distribution of suspended sediment at a CSD operation. The majority of the source is located near the seabed, with a majority within the first 3 m above the bottom and lower concentrations extending up towards the surface. Table 9-3 shows the assumed vertical distribution for the CSD source.

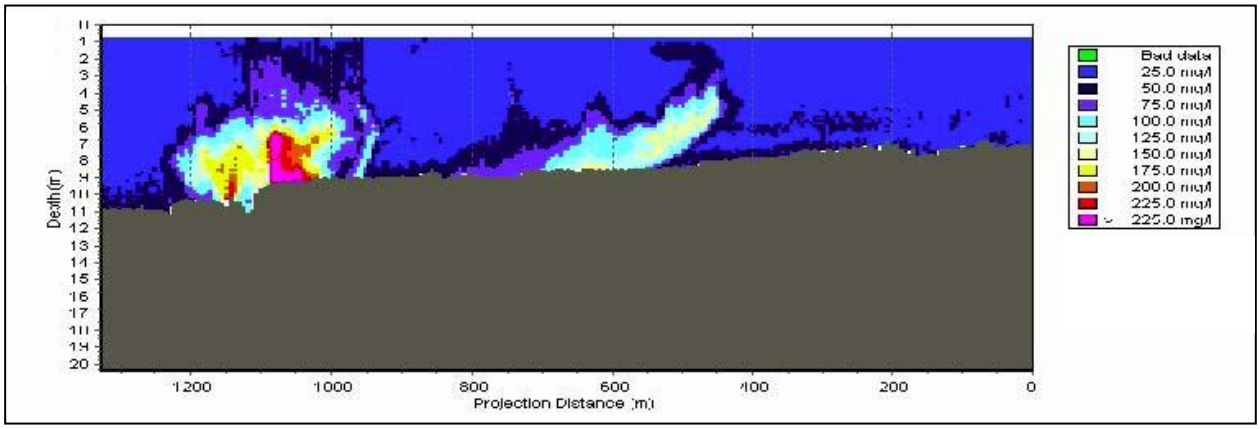

Figure 9-4: Example cross-section of a dredge generated sediment plume showing sediment concentrations measured by ADCP. Plumes were generated by discharge of material cut by a CSD and pumped through a hydraulic trunkline (reprinted from Swanson et al 2004).

Table 9-3: Initial vertical distribution of sediments in the water column for CSD.

Elevation above seabed (m)	% of sediments
4	5
3	15
2	20
1.5	40
1	20

Recent validation work undertaken by APASA within Cockburn Sound has confirmed the assumed distribution as a good basis for the initial source distribution. A series of sensitivity tests showed very little variation of the predicted extent or duration of the sediment plumes with varied initial vertical distributions. This is due to the extremely rapid settling of the majority of the sediment fraction (coarse sand).

9.3.3.3 Source Sediment Size Distribution

The material size characteristics were taken from the sediment sampling and laboratory testing conducted for the 4 sites along the channel alignment. The channel was broken into four sections for modelling with the PSD for each zone based on the mean of the vertical samples at each of the 4 sampling sites. As the CSD will not be cutting no modification of the PSD curves was undertaken to "simulate" the potential for generation of additional fine material due to the cutting and grinding process. Given that there is little basis for defining what may eventuate without field measurement, and allowing for the possibly conservative effects of laboratory PSD analyses, it was concluded that the most appropriate basis for modelling was to use the laboratory derived PSD curves without modification.

Table 9-4 presents the PSD that were used in the model for the cutter head source for each of the four channel sections, using the DREDGEMAP sediment classes. The size composition of the material is dominated by coarse sand with small proportions of fine sand, silt and clay sized particles.

Table 9-4: Particle size distributions for a range of chainages along the proposed channel for sediments suspended by the cutterhead, based on particle size distributions from the sediment sampling.

Classification	Size range (µm)	Ch 0-100 % of total	Ch 100-300 % of total	Ch 300-550 % of total	Ch 550-700 % of total
Clay	0-7	2	1	1	5
Fine silt	7-35	4	3	3	7
Coarse silt	35-74	1	1	2	5
Fine sand	74-130	3	1	1	5
Coarse sand	>130	90	94	93	78

9.3.3.4 Dredge Movement in Time

As noted previously the dredging works will commence from the offshore end of the access channel and progress towards the site of the proposed marina development. For the modelling the channel was broken down into 4 sections based on the sediment variability and volume. A volume for each area was approximated based on the bathymetry in each section and the channel dimensions. In this way the modelled dredge progression is realistic with the dredge remaining longer in the shallower areas, which require a larger volume to be removed.

9.3.3.5 Typical observed concentrations

Anchor Environmental (2003) presents a range of TSSC data from measurements near hydraulic cutterhead dredges. Generally the elevation in TSSC attributable to the CSD operations is less than 100 mg/l in the nearfield, with a median value of around 15 mg/l. Concentrations would be expected to reduce rapidly away from the source.

These values represent very site specific and operational specific values. They serve as a general guide when considering the validity, and perhaps conservatism, of the results of this study.

9.3.4 Sediment Fate Scenarios

One sediment fate scenario was modelled for the proposed dredging operations. The scenario assumes that dredging will begin at the start of June and run for 9 weeks until the beginning of August, assuming the expected production rates are achieved. The dredge will operate 6 days a week (Monday to Saturday), 12 hours a day (6am to 6pm).

The selection of typical conditions for a representative winter regime involved an analysis of 7 years of wind data at Garden Island. This is the closest, recent long term wind record that was available for the study. The selected year was chosen based on a statistical assessment of the wind magnitudes to select a year consistent with mean conditions. The selected time period was also defined based on achieving a good match with the overall directional roses for that season. A summary of the selected period is provided in Table 9-5.

Table 9-5: Summary of selected representative period and the wind statistics for the winter season of 2003. Bracketed values represent the statistics for that season for all years in the dataset.

Scenario	Selected Period	Mean Wind Speed (m/s)	75th percentile Wind Speed (m/s)	95th percentile Wind Speed (m/s)
Winter	2/06/03 – 3/08/03	6.6 (6.3)	9.9 (9.3)	14.3 (13.7)

The scenario was forced using hydrodynamic and wave model data from the modes developed for this study, and presented in previous sections.

9.4 Results

The results of the 3D sediment fate model were output hourly over the model domain, for the duration of the 9 week dredging program.

Post-processing was undertaken to derive maximum TSSC through the water column, which were used to predict the extent of the visible plume and compare against given threshold values. The following sections present a description of the general plume movement, the likely extent of the visible plume and an assessment of the predicted TSSC against given threshold values. Note that all quoted TSSC refer to the excess generated by dredging, and do not include the naturally occurring sediment concentration/turbidity. All threshold values relate to this above background measure of effect.

9.4.1 General Plume Movement

Figure 9-5 shows a set of hourly snap shots of maximum TSSC over a 6 hour period on 21st June 2003, approximately 3 weeks into the dredging operations. In general, only a small area of the domain is covered by the plume at any hourly time step. This is expected given that the bulk of the dredged material is coarse sand which settles rapidly to the seabed.

Dredged sediment that has previously settled to the seabed towards the northern end of the dredge channel is predicted to be resuspended during this time period. Peak concentrations up to 20 mg/l, highlighted by the orange areas, are expected up to 30 m from the dredge channel. The plume is initially predicted to drift slightly towards the east then from 6 pm until 10 pm, the general pattern of plume movement is towards the west out through the southern entrance of the Causeway, as the easterly winds strengthen to around 20 knots.

A 10 hour time series of maximum TSSC plots at 2 hour intervals between 12 pm and 10 pm on 18/07/2003 is presented in Figure 9-6. The CSD is operating in the southern (inshore) end of the channel (first four snap shots) and is predicted to generate a small plume during this time. Peak concentrations outside of the dredge channel are again predicted to be relatively low (≤ 5mg/l) due to the bulk of the material being coarse sand. The general pattern of plume movement is towards the west, drifting with the ebbing tide and easterly winds.

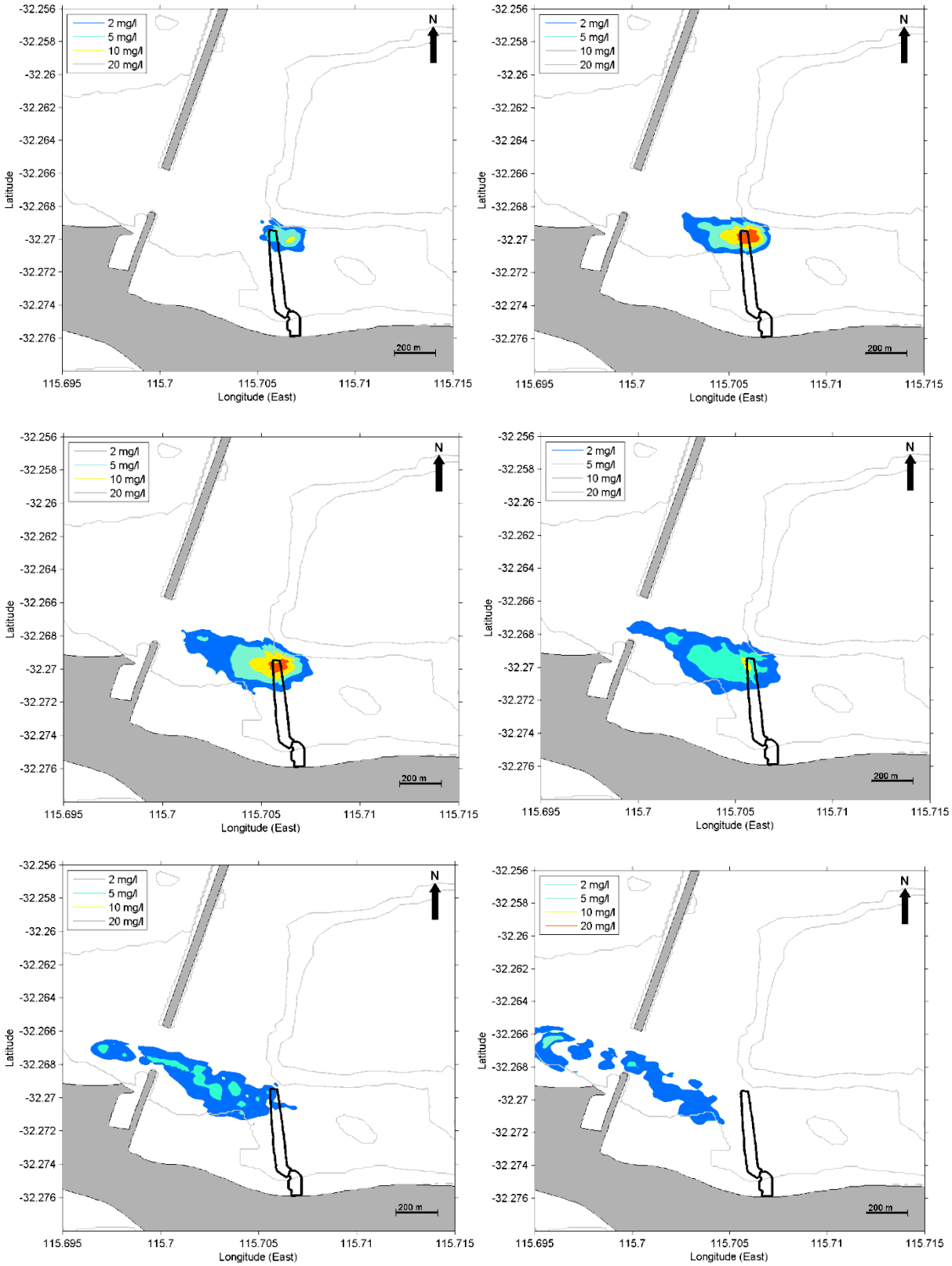

Figure 9-5: 6 hour time-series of maximum TSSC every hour from 5pm (top left) to 11pm (bottom right) on 21/06/2003.

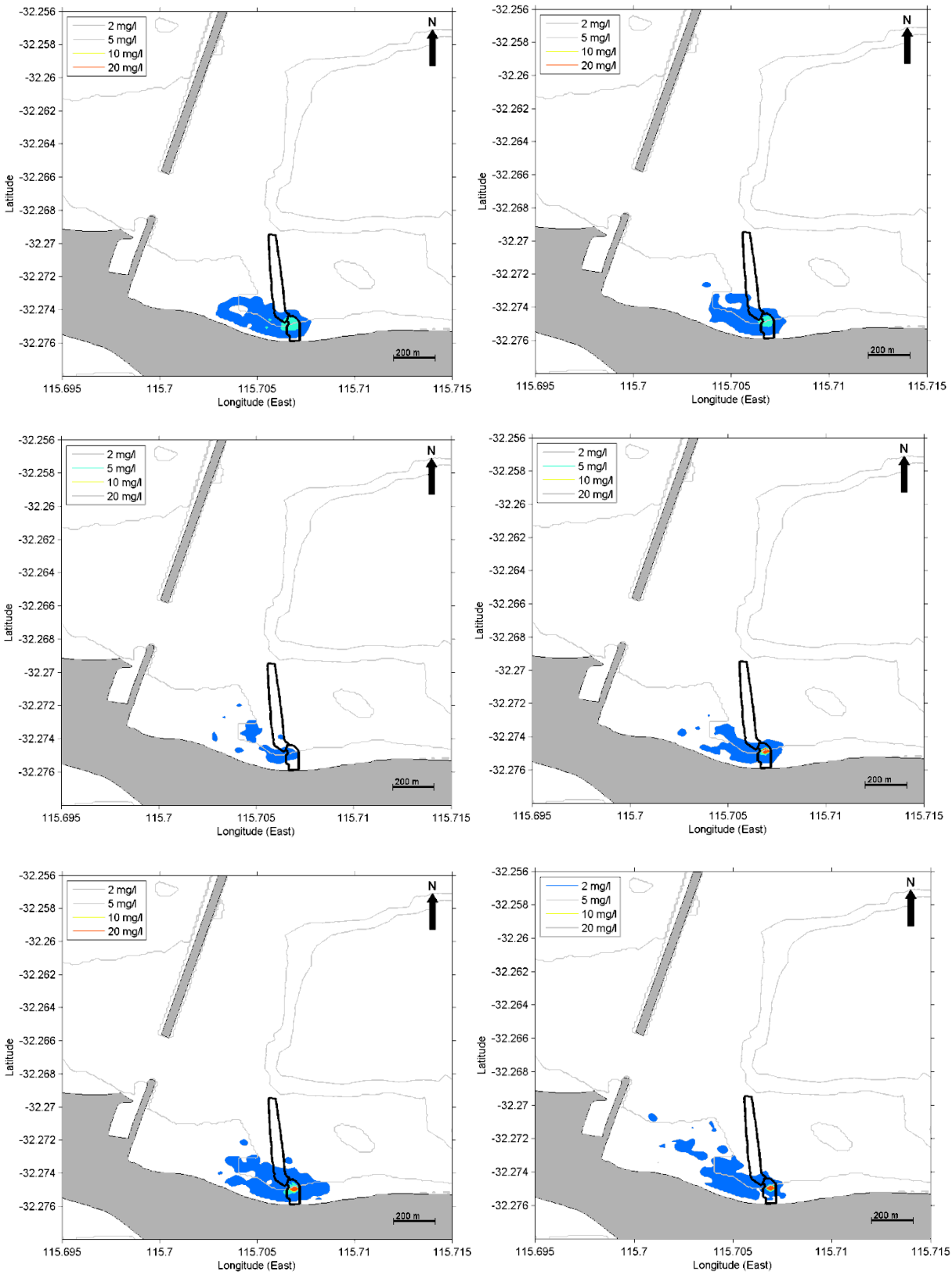

Figure 9-6: 10 hour time-series of maximum TSSC every 2 hours from 12pm (top left) to 10pm (bottom right) on 18/07/2003.

9.4.2 Extent of Visible Plume

The extent of the visible plume in these relatively clear waters is expected to be where the combined TSSC of the dredge-generated plume and background suspended sediment concentration is above approximately 4 mg/l. Previous studies (DEP, 1996) have identified background TSSC values for Perth Coastal Waters of the order of 2 - 3 mg/l; hence a dredge-generated TSSC threshold of 2 mg/l was plotted as the extent of the visible plume.

The predicted extent of the visible plume is presented by the 99th percentile TSSC plot in Figure 9-7. The 99th percentile has been used to indicate the potential extent of the visible plume based on the EPA's Draft Environmental Assessment Guidelines for Marine Dredging Proposals (EPA, 2010). It should be noted that the 99th percentile plot does not shows where the visible plume may be seen at one moment in time, it represents the summation of rarely occurring conditions over the entire dredging program. The region where a visible plume is expected to occur will generally be restricted to within the vicinity of the dredging channel, although a weakly concentrated plume may be visible up to 100-200 m away at times.

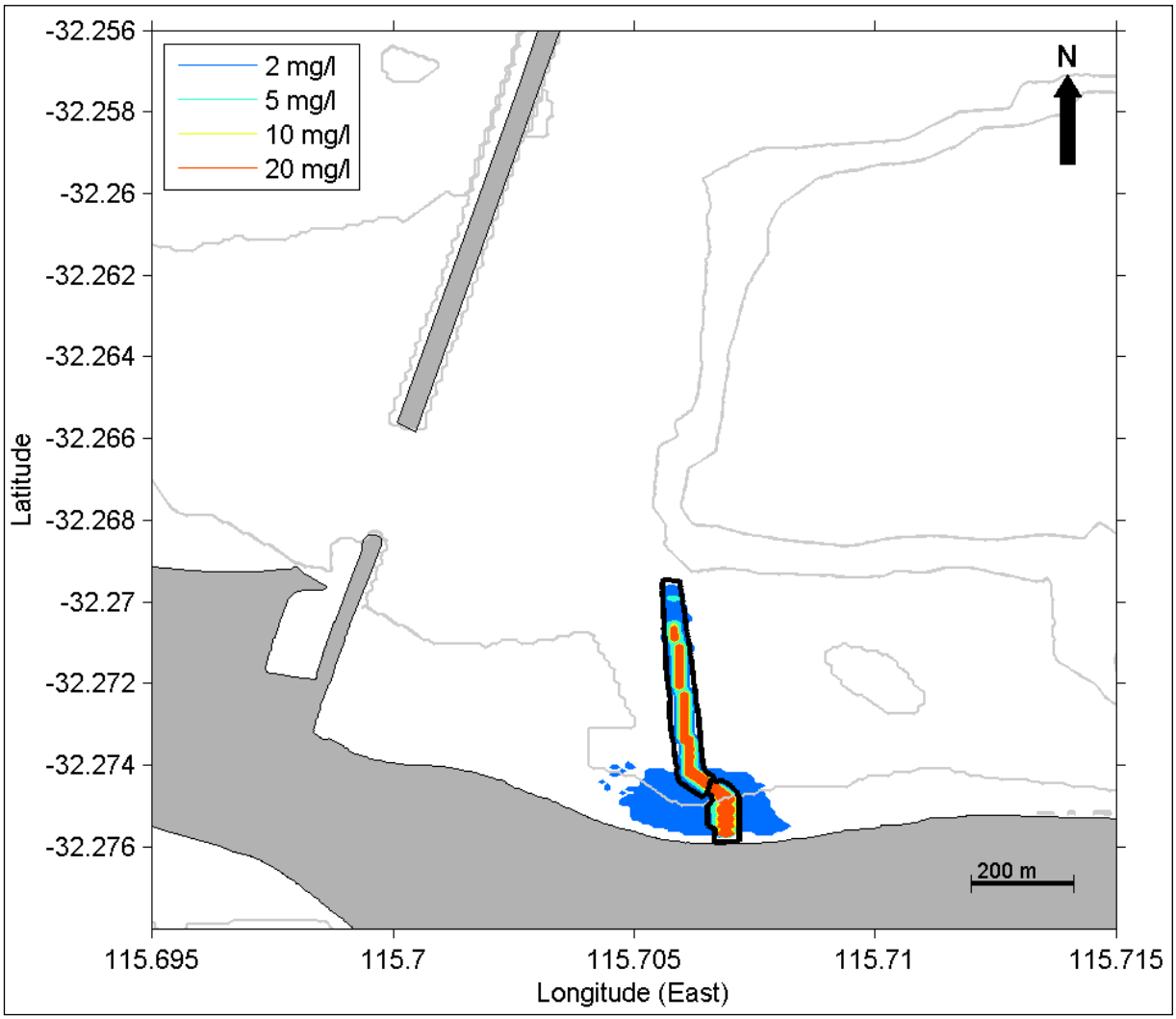

Figure 9-7: Potential extent of the visible plume based on the 99th percentile TSSC. Note the TSSC plume will not cover the entire area shown in the 99th percentile map at one moment in time. This represents the summation of rarely occurring conditions over the entire dredging program.

9.4.3 Statistical Summary

The predicted dredge generated elevations in TSSC were assessed against threshold values of 5, 10 and 20 mg/l for the 50th, 80th and 95th percentiles throughout the dredging operation, as specified by Oceanica. The 2 mg/l contour has also been included in the threshold analysis based on it being the approximate visible plume threshold when combined with typical background TSSC concentrations for the region. The presented percentile maps should be interpreted as showing contours where the TSSC are predicted to be below the levels shown for X% of the time during the dredging operation.

The 50th and 80th percentile plots of maximum TSSC showed no exceedence of the 2 mg/l threshold, meaning that for up to 80% of the time, TSSC generated by the dredging works are not expected to exceed 2 mg/l over the model domain. Therefore these plots have not been included in this report.

The 95th percentile maximum TSSC map is presented in Figure 9-8. The plot shows that the TSSC plume is not predicted to persist for long periods of time (<5% of the time) over the majority of the dredging area. Some persistence of the plume is evident at the southern end of the access channel, however the persistent TSSC are predicted to be less than 10 mg/l.

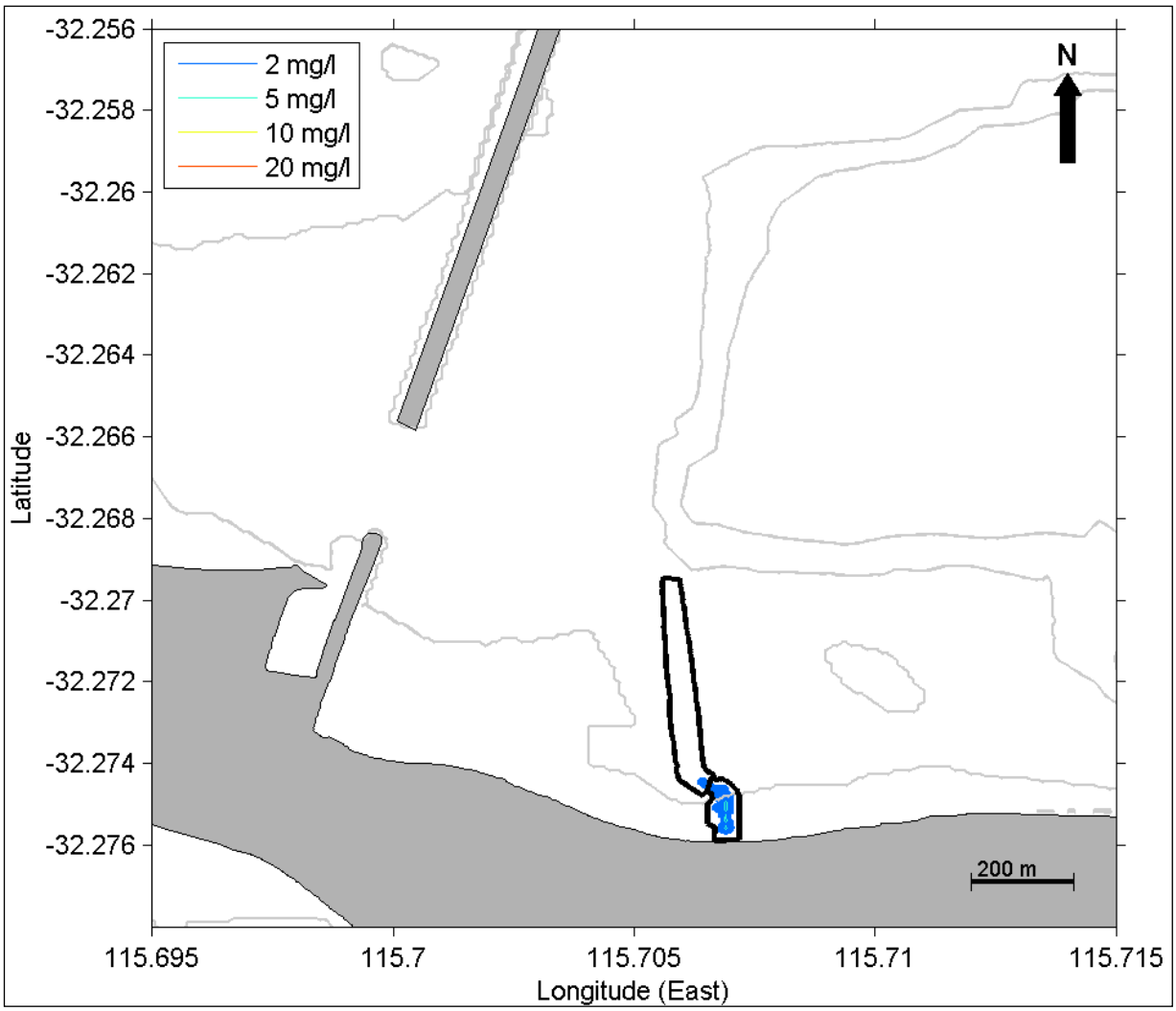

Figure 9-8: 95th percentile maximum TSSC over the dredging operation.

10 CONCLUSIONS

A detailed marine modelling study has been completed. The following main conclusions have been made relating to the flushing, nutrient and sediment modelling components of the project:

FLUSHING PERFORMANCE

- Flushing will rely primarily on tidal exchange and wind-induced circulation. Due to the relatively small tidal range and the design of the proposed marina, having smaller canals branching off a main canal that will have one entrance channel, only incomplete flushing will occur over any tidal cycle. Increased flushing would be expected when strong winds are aligned with the proposed canal system;
- Overall flushing times would be most rapid during certain summer conditions, when strong winds align with the proposed development. Rapid flushing should also occur during winter storm conditions.
- Flushing will be fastest near the entrance to the main channel and decrease with distance from the entrance. Minimum flushing times near the entrance in any simulation was 1.9 days. Maximum flushing times calculated for the back end of the longest secondary canal (the western canal) was 12.7 days.
- A wide range of flushing times can be expected for any given location, depending upon the prevailing tide and wind conditions. The range of maximum flushing rates, calculated at the back of the canals in the simulations, varied from 4 days to 13 days.
- Average maximum flushing times calculated at the back end of the canals were statistically similar for simulations using example wind conditions for summer (8.36 $\pm$ 2.21 days), autumn (9.91 $\pm$ 2.14) and winter (8.30 $\pm$ 2.30).
- The median flushing time for all locations throughout the canals, for all seasons, is estimated at 6.8 days and 83% of the flushing time predictions were 10 days or less, while 55% of predictions were less than 7 days.
- Only small differences in flushing times should occur between the surface and the bottom waters at a given location, with the surface waters flushing fastest.83% of the flushing time predictions were 10 days or less and 55% of predictions were less than 7 days.
- Sensitivity testing using a factored wind record representing the observed sheltering that occurs in southern Mangles Bay suggested that the lower winds will generally lead to a 10 – 15% reduction in flushing time (more rapid).

NUTRIENT MODELLING

- Dissolved Inorganic Nitrogen (DIN) concentrations within the development are expected to be highest during winter when the loading is highest, with concentrations generally being up to 4 times background.

- During autumn and summer, the DIN concentration is expected to be generally less than twice the background concentration, based on the values applied in this study.
- Peak concentrations of DIN are predicted to reach 55 µg/l at times however these peaks are quickly resolved by increased flushing efficiency as conditions change.
- Outside of the marina, there was very little effect on local water DIN concentrations predicted.
- Flushing is expected to be sufficiently effective to prevent the gradual build-up of concentrations over time. This suggests that the risk of adverse escalations is relatively low, based on the assumptions made and the input data provided for this study.

SEDIMENT FATE MODELLING

- The region where a visible plume is expected to occur will generally be restricted to within the vicinity of the dredging channel, although a weakly concentrated plume may be visible up to 100-200 m away at times.
- The 50^{th} and 80^{th} percentile plots of maximum TSSC showed no exceedence of the 2 mg/l threshold, meaning that for up to 80% of the time, TSSC generated by the dredging works are not expected to exceed 2 mg/l over the model domain. This is primarily due to the fact that the majority of the material to be dredged is coarse sand and that the dredging methodology is relatively clean.
- A significant TSSC plume is not predicted to persist for long periods of time (<5% of the time) over the majority of the dredging area. Some persistence of the plume is predicted at the southern end of the access channel where the dredging is most intense, however the persistent TSSC are predicted to be less than 10 mg/l.

11 REFERENCES

Anchor Environmental (2003). Literature review of effects of resuspended sediments due to dredging operations. Prepared for Los Angeles Contaminated Sediments Task Force, Los Angeles, California. June 2003.

ANZECC (2000), Australian and New Zealand Guide lines for Fresh and Marine Water Quality, Australian and New Zealand Environment and Conservation Council, National Water Quality Management Strategy Paper No. 4.

Burling, MC, Ivey GN and Pattiaratchi, CB (1999), Convectively driven exchange in a shallow coastal embayment, Continental Shelf Research, 19, 1599-1616.

Coastline Surveys Limited (1999), Marine Aggregate Mining: Benthic & Surface Plume Study Final Report, To: United States Department Of The Interior Minerals Management Service & Plume Research Group, July 1999

CSMW (2005) Results from CSMW Task 2, Natural and Anthropogenic Turbidity, report of the Coastal Sediment Management Workgroup, Government of California, http://www.dbw.ca.gov/CSMW/PDF/Results_From_CSMW_Task2.pdf

D'Adamo N (1992), Hydrodynamics and recommendations for further studies in Cockburn Sound and adjacent waters, EPA TS41

DEP (1996), Southern Metropolitan Coastal Waters Study (1991-1994). Report 17, Department of Environmental protection.

DOER (2000). Description of the SSFATE Numerical Modelling System. Technical Note ERDC TN-DOER-E10. April 2000

Eldeberky, Y. and J.A. Battjes, (1996), Spectral modelling of wave breaking: Application to Boussinesq equations, J. Geophys. Res., 101, No. C1, 1253-1264.

Eldeberky, Y. and J.A. Battjes, (1996), Spectral modelling of wave breaking: Application to Boussinesq equations, J. Geophys. Res., 101, No. C1, 1253-1264.

Fitzpatrick, N, Burling, M, Bailey, M, Modelling the marine environmental impacts of dredge operations in Cockburn Sound, WA, proceedings of Coasts and Ports 2009.

Galperin, B, Kantha L, Hassid S and Rosati, A, (1988). A Quasi-equilibrium Turbulent Energy Model for Geophysical Flows, Journal of the Atmospheric Sciences, Vol 45, No. 1, American Meteorological Society.

Hamrick, J M (1992) A Three-Dimensional Environmental Fluid Dynamics Computer Code: Theoretical and Computational Aspects. The College of William and Mary, Virginia Institute of Marine Science, Special Report 317.

Hamrick, J M, (1992b) Estuarine environmental impact assessment using a three-dimensional circulation and transport model. Estuarine and Coastal Modeling, Proc. of the 2nd International Conf., M. L. Spaulding et al, Eds., ASCE, New York, 292-303.

Hamrick, J M, and Wu, T S (1997) Computational design and optimization of the EFDC surface water hydrodynamic and eutrophication model. Next Generation Environmental Models and Computational Methods. G. Delich and M. F. Wheeler, Eds., SIAM, Philadelphia, 143-156.

Hamrick, J M, Kuo A Y, and Shen J (1995) Mixing and dilution of the Surrey Nuclear Power Plant cooling water discharge into the James River. a report to Virginia Power Company, The College of William and Mary, Virginia Institute of Marine Science, Gloucester Point, VA.

Hasselmann, K., (1974), On the spectral dissipation of ocean waves due to whitecapping, Bound.-layer Meteor., 6, 1-2, 107-127.

Hasselmann, K., (1974), On the spectral dissipation of ocean waves due to whitecapping, Bound.-layer Meteor., 6, 1-2, 107-127.

Hayes, D. & Wu, P. 2001 “Simple approach to TSS source strength estimates” Western Dredging Association Proceedings. WEDA XXI, Houston, TX, June 25027, 2001.

Holthuijsen, L.H., N. Booij, R. Ris, J.H. Andorka Gal and J.C.M. de Jong, (1997), A verification of the third-generation wave model "SWAN" along the southern North Sea coast, Proceedings 3rd International Symposium on Ocean Wave Measurement and Analysis, WAVES '97, ASCE, 49-63.

Holthuijsen, L.H., N. Booij, R. Ris, J.H. Andorka Gal and J.C.M. de Jong, (1997), A verification of the third-generation wave model "SWAN" along the southern North Sea coast, Proceedings 3rd International Symposium on Ocean Wave Measurement and Analysis, WAVES '97, ASCE, 49-63.

Ilich, K (2006), Origin of continental shelf seiches Fremantle Western Australia, unpublished thesis, School of Environmental Systems Engineering, The University of Western Australia.

JFA, 2010. *Mangles Bay Project Preliminary Assessment of Dredging of Channel.* Document Reference: R-199.06.01-1, September 2010, prepared for TABEC.

Johnson, B. H., Andersen, E., Isaji, T., Teeter, A. M., and Clarke, D. G. (2000). “Description of the SSFATE numerical modeling system,” *DOER Technical Notes Collection* (ERDC TN-DOER-E10), U.S. Army Engineer Research and Development Center, Vicksburg, MS. *www.wes.army.mil/el/dots/doer*

Kantha, L.H. & C.A. Clayson, 2000. Numerical models of ocean and oceanic processes. Academic Press, San Diego, CA, 940 pp.

Komen, G.J., S. Hasselmann, and K. Hasselmann, (1984), On the existence of a fully developed wind-sea spectrum, J. Phys. Oceanogr., 14, 1271-1285.

Komen, G.J., S. Hasselmann, and K. Hasselmann, (1984), On the existence of a fully developed wind-sea spectrum, J. Phys. Oceanogr., 14, 1271-1285.

Madsen, O.S., Y.-K. Poon and H.C. Graber, (1988), Spectral wave attenuation by bottom friction: Theory, Proc. 21 th Int. Conf. Coastal Engineering, ASCE, 492-504.

Madsen, O.S., Y.-K. Poon and H.C. Graber, (1988), Spectral wave attenuation by bottom friction: Theory, Proc. 21 th Int. Conf. Coastal Engineering, ASCE, 492-504.

Madsen, P.A. and O.R. Sorensen, (1993), Bound waves and triad interactions in shallow water, Ocean Engineering, 20, 4, 359-388.

Madsen, P.A. and O.R. Sorensen, (1993), Bound waves and triad interactions in shallow water, Ocean Engineering, 20, 4, 359-388.

Mellor, G L and Yamada, T (1982), Development of a Turbulence Closure Model for Geophysical Fluid Problems, Reviews of Geophysics and Space Physics, Vol 20, No 4, Pages 851-875, American Geophysical Union.

Molloy, E (2001), Seiching in Cockburn Sound, unpublished thesis, Department of Environmental Engineering, The University of Western Australia.

NEPA (2001), Kingston Container Terminal Environmental Impact Assessment, http://www.nepa.gov.jm/eias/Kingston_Container_Terminal/TOC.htm

Pattiaratchi, CB (2002), Field Measurements of Current Flows through Causeway and Mangles Bay, report prepared for Cockburn Sound Management Council, April 2002.

Rose, E (2001), The dynamics of flow between Cockburn Sound and Sepia Depression, unpublished thesis, Department of Environmental Engineering, The University of Western Australia.

Soulsby, R., 1997. Dynamics of marine sands: A manual for practical applications- Thomas Telford Publications, London, UK

Swanson, J., Isaji, T., & Galagan, C. (2007) “Modelling the ultimate transport and fate of dredge-induced suspended sediment transport and deposition” Presented at WODCON XVIII, 27 May - 1 June 2007, Orlando, FL, USA

Swanson, J., Isaji, T., Clarke, D. & Dickerson, C. (2004) Simulations of dredging and dredged material disposal operations in Chesapeake Bay, Maryland and Saint Andrew Bay, Florida. Proceedings of the 36th TAMU Dredging Seminar, WEDA XXIV, 6-9 July 2004, Orlando Fl.

Swanson, J., Isaji, T., Ward, M., Johnson, B.H., Teeter, A., & Clarke, D.G. (2000). “Demonstration of the SSFATE numerical modelling system”, DOER Technical Notes Collection (ERDC TN-DOER-E12, U.S. Army Engineer Research and Development Center, Vicksburg, MS. www.wes.army.mil/el/dots/doer

Teeter, A M (2001), Clay-silt sediment modelling using multiple grain classes. Part I:Settling and deposition, Coastal and Estuarine Fine Sediment Processes, pp 157-171, WH McAnally and AJ Mehta (Eds), Elsevier Science BV.

US Army Corps of Engineers (USACE), 2008. *Dredging Operations and Environmental Research Program - The Four Rs of Environmental Dredging: Resuspension, Release, Residual, and Risk.* Washington, DC

USAE Waterways Experiment Station (USAEWES, 1988), Environmental Effects of Dredging, Technical Notes, Sediment Resuspension by Selected Dredges, Vicksburg, Mississippi.

Willmott, CJ (1981), On the Validation of Models. *Physical Geography* 2**,** 184-194.

Willmott, CJ (1982), Some comments on the evaluation of model performance, Bulletin of the American Meteorological Society, pp 1309 – 1313.

Willmott, CJ and Matsuura, K, Advantages of the mean absolute error (MAE) over the root mean square error (RMSE) in assessing average model performance, Journal of Climate Research, Vol 30, pp 79 – 82.

Willmott, CJ, Ackleson, SG, Davis, RE, Feddema, JJ, Klink, KM, Legates, DR, O'Donnell, J and Rowe, C (1985), Statistics for the evaluation and comparison of models, Journal of Geophysical Research, Vol 90 C5, pp 8995 – 9005, September.

Wu, J (1980), Wind-stress coefficients over sea surface near neutral conditions – a revisit, Journal of Physical Oceanography, Volume 10, pp 727-740, May 1980.